To the Graduate Council:
I am submitting herewith a dissertation written by Okan Ciftci entitled "Distribution Congestion Management Using CVSR Devices." I have examined the final paper copy of this dissertation for form and content and recommend that it be accepted in partial fulfillment of the requirements for the degree of Doctor of Philosophy, with a major in Electrical Engineering.

Kevin Tomsovic, Major Professor

We have read this dissertation
and recommend its acceptance:

Kevin Tomsovic

Seddik M. Djouadi

Fangxing "Fran" Li

Mingzhou Jin

Accepted for the Council:

Carolyn R. Hodges

Vice Provost and Dean of the Graduate School

To the Graduate Council:
I am submitting herewith a dissertation written by Okan Ciftci entitled "Distribution Congestion Management Using CVSR Devices." I have examined the final electronic copy of this dissertation for form and content and recommend that it be accepted in partial fulfillment of the requirements for the degree of Doctor of Philosophy, with a major in Electrical Engineering.

Kevin Tomsovic, Major Professor

We have read this dissertation
and recommend its acceptance:

Kevin Tomsovic

Seddik M. Djouadi

Fangxing "Fran" Li

Mingzhou Jin

Accepted for the Council:

Carolyn R. Hodges

Vice Provost and Dean of the Graduate School

(Original signatures are on file with official student records.)

Distribution Congestion Management Using CVSR Devices

A Dissertation Presented for the

Doctor of Philosophy

Degree

The University of Tennessee, Knoxville

Okan Ciftci

August 2023

© by Okan Ciftci, 2023
All Rights Reserved.

To my family and my home country Turkiye.

Acknowledgements

First and foremost, I would like to extend my heartfelt gratitude to my advisor, Dr. Kevin Tomsovic, for his invaluable guidance, unwavering support, and endless patience throughout my PhD journey. I am truly grateful for his extensive knowledge and expertise, which have constantly inspired and propelled my research forward. Without his assistance and mentorship, this work would not have been possible. I am indebted to Kevin for his creative insights and comprehensive advice. Thank you for believing in me and for your unwavering dedication.

I would like to thank my committee members, Dr. Seddik M. Djouadi, Dr. Fangxing "Fran" Li and Dr. Mingzhou Jin. I would like to thank one of my proposal committee members, Dr. Rapinder S. Shawhney, who passed away last year. You were very joyful and helpful person, rest in peace. Also, I would like to special thank Dr. Djouadi for being supportive and student-friendly anytime I need.

I would like to thank my friends, Efe Tuncer, Abdurrahman Demir, and Ufuk Sen from Baton Rouge, LA; Safak Ceylan, Stephen Fatokun, Onur Kalender, and Emrullah Aydin from Knoxville, TN; Furkan Mol, Gamze Kartal, and Altan Brother from Austin, TX for their great friendship. I also want to thank Gokhan Ozkan even he didn't show up my graduation ceremony. I would like to express my gratitude to my college and ESL friend, Emre Gonultas. His role in my academic journey has been significant, particularly for introducing me to the Turkish Government Scholarship for Masters and PhD degrees. Without his timely advice and guidance, I might have never had the opportunity to pursue higher education and achieve my current

academic standing. In relation to this subject, I gratefully acknowledge Republic of Turkey Ministry of National Education for the financial support during my PhD.

I am incredibly grateful to my family, and it is impossible to express my gratitude towards them in just a few sentences. To my parents, Gulhan and Necati, and my brothers, Arif and Sadettin, I want to extend my heartfelt thanks for their steady support and constant encouragement throughout my career. Your belief in me and your continuous presence have been instrumental in my achievements. I would like to thank Kaptan family. To my beloved wife, Fatma, words cannot adequately express my gratitude for your unconditional love, support, and the joy you bring to my life. Your continuous faith in me has been a source of strength and motivation during this challenging journey. Lastly, I want to express my gratitude to my dear son, Alp. Even at your young age, your infectious cheerfulness and humor have brightened our home and provided me with additional motivation and strength. As you continue to grow, my wish for you is a life filled with happiness and success. Always, Be the best at whatever you do!

"When you go through a hard period,

When everything seems to oppose you,

... When you feel you cannot even bear one more minute,

NEVER GIVE UP!

Because it is the time and place that the course will divert!"

— Rumi, The Mevlânâ Jalāl ad-Dīn

Abstract

Power demand and supply must be in balance to maintain frequency and stable power flow in distribution and transmission networks. Power flow control is an important problem where flows must be held within equipment limits. Distribution systems may experience congestion during peak consumption hours. Such congestion can overload distribution lines and transformers, particularly, in dense urban areas. Similar to the power electronic devices in the transmission network, power flow control devices are available for the distribution systems. However, there are very few control units in the distribution systems. D-STATCOM, energy storage, phase-shifting transformers, distributed generation (DG) and switches can be used to control power flow in the distribution systems.

The continuously variable series reactor (CVSR) is a newly proposed device and is used in this study for its ability to control distribution power flow. Compared to other power flow control equipment, the CVSR device is a reliable, fast-acting unit, and most importantly, economically low cost. The CVSR can be used to regulate the reactance on the primary side of a transformer to control power distribution among transformers in order to relieve overloading in a meshed distribution grid. This approach can allow a distribution system to avoid or defer transformer upgrades. An optimization problem is formulated to identify location and settings to relieve overloads. To integrate and model the CVSR device in the distribution network, a method is developed and simulation is performed using MATLAB and OpenDSS. The results are verified with the benchmark results on OpenDSS software. As a

result, a few ohm reactance CVSR is shown to be adequate to relieve loading on the transformers in a practical system. In addition, it was found that a piecewise approximation works well for mitigating the overloads and optimal CVSR locations on realistic meshed networks. The IEEE 342-node low voltage networked test system (LVNTS) and a portion of the Consolidated Edison's partial meshed distribution system are used to evaluate performance. Future work includes optimal location of CVSR devices with consideration of dynamic conditions, integration of advanced optimization techniques, expansion to other test systems and identification of open-mains in the meshed grids.

Table of Contents

1 Introduction **1**

1.1 Introduction and Motivation 1

1.2 Relieving Transmission and Distribution Congestion 4

1.2.1 Power Flow Control Devices 4

1.2.2 Phase-Shifting Transformer 10

1.2.3 Other Methods 12

1.3 Optimal Congestion Relief 13

1.3.1 Cost of Impact of Transmission Congestion 15

1.4 Optimal Placement of Electrical Devices in Power Systems 18

1.4.1 Optimization Techniques for Optimal Location Problems in Power Systems 19

1.5 Network Distribution Systems 37

1.5.1 Two Parallel Transformers 39

1.5.2 IEEE 342-Node Low Voltage Networked Test System(LVNTS) 39

1.5.3 Consolidated Edison(ConEd) System 41

2 The Continuously Variable Series Reactor (CVSR) Model **45**

2.1 Characteristics of CVSR Device 45

2.2 History of CVSR Devices 46

2.3 Steady-State Model of CVSR Device 52

2.3.1 Reformulations of Reactance and Power Flow Equations . . . 52

2.4 Sensitivity Analysis with the CVSR Device 55

3 Application of the CVSR Device for Power Flow Control 59

3.1 Introduction 59

3.1.1 Two-Parallel Transformers 60

3.2 Optimization Model 61

3.2.1 Linear Formulation 63

3.2.2 Piecewise Linear Formulation 63

3.3 Case Studies 65

3.3.1 System Description and Simulation Setup 65

3.3.2 IEEE 342-LVTNS 65

3.3.3 ConEd System 74

4 Optimal Location of CVSR devices 78

4.1 Introduction 78

4.2 Optimization Model 79

4.2.1 Shortest Path Algorithm 80

4.2.2 Loading Based Algorithm 82

4.2.3 Transformer Sensitivity Based Algorithm 84

4.2.4 Piecewise Optimization Based Algorithm 85

4.3 Case Studies 87

4.3.1 System Description and Simulation Setup 87

4.3.2 Case 1: Base Load 88

4.3.3 Case 2: x1.39 Base Load for All Loading Busses 91

4.3.4 Case 3: Area-Based Load Increment 94

5 Conclusion and Future Work 113

5.1 Conclusion 113

5.2 Future Work 115

Vita **140**

List of Tables

1.1 Transmission Congestion Costs ($ millions) in the United States from 2016-2019 17

2.1 Parameters for Prototype and Full-Scale CVSR Device (1). 50

3.1 Power Flow Results of T-23 T-24 and T-32 with only One CVSR device 67

3.2 Linear Optimization Result Comparison with the Benchmark Results 71

3.3 Piecewise Optimization: 2,4 and 5-Segment Comparison when Transformers are limited to 1000 kVA 72

3.4 Piecewise Optimization: 2,4 and 5-Segment Comparison when Transformers are limited to 950 kVA 73

3.5 Simple Linear Optimization Result Validation when Transformers are limited to 960 kVA. 77

3.6 Piecewise Optimization Result Validation. 77

List of Figures

1.1 Basic Configuration of TCSC 9
1.2 TCSC Equivalent Circuit 9
1.3 Representation of the CVSR in a lossless line 9
1.4 Cost of FACTS Devices ($/kVAr) 11
1.5 Representation of the PST Between Two Systems 11
1.6 Connecting a Phase Shifting Transformer to the Network 11
1.7 Distribution Network with DG Implementation 14
1.8 Power Flow Paths Before and After Reconfiguration of a Radial Distribution Network. 14
1.9 Optimization Categories and Their Methods for the Optimal Location Problem 21
1.10 Simple Graph Theory and Its Adjacency Matrix 28
1.11 Radial Distribution System 38
1.12 Spot Low-Voltage Network 38
1.13 Secondary Grid Distribution System (2) 40
1.14 One-Line Diagram of Two-Feeder Distribution System 40
1.15 One-Line Diagram of the IEEE 342-Node LVNTS (3) 43
1.16 Small-Meshed Grids in Con-Ed System 44

2.1 Schematic of CVSR Device. (4) 49
2.2 Demonstration of the CVSR Device. 49
2.3 Three-Phase CVSR Prototype. (5) 51

2.4 Second Version of Five-Legged Three-Phase CVSR Prototype.(6) . . . 51
2.5 Relationship Between the Apparent Reactance and the DC Bias Current. 53
2.6 CVSR Device Connected to the Transformer. 53
2.7 Transformer Sensitivity Matrix. 56
2.8 Sensitivity Analysis in Plots. 58

3.1 Simple Diagram of Two Feeders Distribution System with CVSR devices 67
3.2 Power Flow of Transformers when the CVSR is Only Implemented to the Transformer-1 68
3.3 Interaction Between MATLAB and OpenDSS. 69
3.4 Linear Illustration of Power Flow on a Transformer with Reactance Increments. 69
3.5 Piecewise Linear Illustration of Power Flow on a Transformer with Reactance Increments. 71
3.6 Power Flow of Transformers at Load.90 Multiplied by 1.80. 75
3.7 Power Flow of Transformers at Load.90 Multiplied by 1.62. 75

4.1 Flowchart of Optimization Methods for CVSR Optimal Location Problem 81
4.2 Djkstra's Shortest Path Algorithm for Optimal Location of CVSR Devices 83
4.3 Flowchart of Loading Based Algorithm 83
4.4 Loading Based Method Illustration with Small and Large Loads around a Transformer 86
4.5 Impact of Increasing CVSR Devices on Transformer Sensitivity Matrix Elements 86
4.6 Effect of Increasing CVSR Devices on Transformer Sensitivity Matrix Creation Time 100
4.7 Distance Matrix of Transformer and Load Buses 101

4.8 Optimal Location of CVSR devices using by Dijkstra's Shortest Path Algorithm . . . 102
4.9 Optimal Location of CVSR devices using by Loading Based Algorithm 102
4.10 Optimal Location of CVSR devices using by Transformer Sensitivity Based Algorithm . . . 103
4.11 Optimal Location of CVSR devices using by Loading Based Algorithm 103
4.12 Optimal Location of CVSR devices using by Transformer Sensitivity Based Algorithm . . . 104
4.13 Optimal Location of CVSR devices using by Piecewise Optimization Based Algorithm . . . 104
4.14 Initial Power Flow with Overloaded Transformers and Relieved Transformers after the Optimization . . . 105
4.15 Power Flow Comparisons of Initial, Optimization and Benchmark(OpenDSS) Results . . . 105
4.16 Particular Area of Load Increment in the IEEE-342 LVTNS . . . 106
4.17 Optimal Location of Two CVSR Devices Using Loading Based Algorithm 106
4.18 Optimal Location of Four CVSR Devices Using Loading Based Algorithm 107
4.19 Optimal Location of Six CVSR Devices Using Loading Based Algorithm 107
4.20 Optimal Location of Two CVSR Devices Using Transformer Sensitivity Based Algorithm . . . 108
4.21 Optimal Location of Four CVSR Devices Using Transformer Sensitivity Based Algorithm . . . 108
4.22 Optimal Location of Six CVSR Devices Using Transformer Sensitivity Based Algorithm . . . 109
4.23 Optimal Location of Two CVSR Devices Using Piecewise Optimization Based Algorithm . . . 109
4.24 Scenario 1: Initial Power Flow with Overloaded Transformers and Relieved Transformers after the Piecewise Optimization . . . 110

4.25 Optimal Location of Four CVSR Devices Using Piecewise Optimization Based Algorithm 110
4.26 Scenario 2: Initial Power Flow with Overloaded Transformers and Relieved Transformers after the Piecewise Optimization 111
4.27 Optimal Location of Six CVSR Devices Using Piecewise Optimization Based Algorithm 111
4.28 Scenario 3: Initial Power Flow with Overloaded Transformers and Relieved Transformers after the Piecewise Optimization 112

Nomenclature

δ_{ij}	The angle between bus i and j.
$\overline{Y_1}$	Nodal admittance matrix on one turn.
$\overline{Y_{Prim}}$	Primitive matrix of the transformer.
$\overline{Y_W}$	Winding admittance matrix.
B'_{ij}	The susceptance between bus i and j with $X_{CV,k}$.
G'_{ij}	The conductance between bus i and j with $X_{CV,k}$.
P'_{ij}	The active power flow between bus i and j with $X_{CV,k}$.
P_{ij}	The active power flow between bus i and j.
P_k, Q_k	The active and reactive power flows on the transformers after the overloading, respectively.
Q'_{ij}	The reactive power flow between bus i and j with $X_{CV,k}$.
Q_{ij}	The reactive power flow between bus i and j.
r	Load-loss or resistance in percentage.
R_{ij}	The resistance between bus i and j.
$S^{\min}$, $S^{\max}$	The minimum and maximum values the apparent power, respectively.

$S_{f,k}$	The apparent power with the maximum value of reactance increment has applied to the transformer.
$S_{in,k}$	The value of initial apparent power.
S_k	The apparent power flows on the transformers after the overloading.
$T^{lin}_{sm,k}$	Linearized sensitivity matrix.
$T^{pw}_{sm,k,s}$	Transformer sensitivity matrix for each segment, s.
$T_{sm,k}$	The transformer sensitivity matrix.
V_i, V_j	The voltages at bus i and j, respectively.
V_i, V_j	Voltages at bus i and j, respectively.
x	Leakage reactance in percentage.
X'_{ij}	The reactance between bus i and j with $X_{CV,k}$.
X'_k	The reactance increment by the CVSR devices
$X^{\min}_{CV}$, $X^{\max}_{CV}$	Minimum and maximum values of CVSR reactance increments, respectively.
$X_{CV,k}$	The reactance increment by the each CVSR device denoted by k.
X_{ij}	The reactance between bus i and j.
Y'	The admittance matrix with $X_{CV,k}$.
Y'_{ij}	The admittance between bus i and j with $X_{CV,k}$.
Z_{sc}	Short circuit impedance.
$\mathrm{I}_{k,s}$	Binary variable.

K	Total number of the CVSR devices.
S_n	The number of linear segments of piecewise approximation.

Chapter 1

Introduction

1.1 Introduction and Motivation

Both transmission and distribution systems are getting more stressed and difficult to operate as distributed energy sources (DERs) and inverter-based renewable resources increase. Furthermore, uncertain power flows and greater line losses may make transmission system more insecure due to increased demand. More efficient usage and controlling of the current transmission system infrastructure is necessaryto obtain reliable and economic performance. Accordingly, various power flow control devices have been proposed to maintain reliability, security and stability. Currently, the power flow control units are available, include: flexible alternating current transmission systems (FACTS), tap-changing transformers, synchronous condensers, switched shunt capacitors and inductors, and thyristor-controlled series capacitors (TCSC). Latest studies on power flow controller based on the saturation of a magnetic core proves that such a controller is able to control the power flow by varying the reactance (7; 8).

The distribution grid has similar issues as transmission grids nowadays. Increased loads with uncertainty and DERs make distribution system more prone to overloads. Moreover, peak consumption hours during any season of the year can be difficult

for distribution system operators (DSOs), customers and energy suppliers because the distribution system have less monitoring to detect issues. Especially in densely loaded urban areas, such as, New York City, there is a high risk of disruptions. Transformers are one of the most important power element in the distribution system. In most cases, transformers can be overloaded by increased demand. Again, power flow control devices or increased equipment capacity must be deployed in these dense loading areas. Still, there are not much options to control power flow in distribution systems compared to the transmission systems. Some FACTS devices are equipped in distribution systems to control power flows (9; 10; 11; 12). Distribution Static Compensator (D-STATCOM) is used in (13) to control power flow in distribution lines. Interline power flow controller is presented in (14) for large scale photovoltaic power system. Addition to FACTS devices, other methods can be used to manage power flow in the distribution systems, namely, energy storage systems (ESSs), reconfiguration, and distributed generation (DG). Energy storage is one option to control power flow in the distribution systems (15; 16; 17). Since batteries are fast acting devices, they can supply power to the grid in seconds. DGs supply the additional power to the distribution system to compensate changes in the loading (18). Using the distribution network reconfiguration, load can be balanced, losses can be reduced, and reliability can be strengthened (19; 20).

Additionally, the cost of energy delivery has been an important topic in power systems. The cost of any equipment: generator, lines, cables, etc., are a primary part of the cost. The cost of high power devices and units such as generators and their equipment, transmission lines and any type of transformers in transmission and distribution systems are very expensive. Some of them cannot be replaced with another equipment or materials but can be upgraded to improve power system reliability, security and stability. Comparing to the cost of new transformers, lines, and so on, power flow controldevices are much cheaper to maintain the reliability and security of the network.

A continuously variable series reactor (CVSR) is a unique device which is a series line reactor that can be used for controlling power flow in meshed power system grids. The working principle of a CVSR is controlled saturation of a ferromagnetic core with the help of DC supply (21). CVSR technology is used in several papers in the literature (22; 1; 4). For example, a CVSR is applied in the transmission system to controleffective impedance of transmission line (22). Authors in (4) present time domain model based on CVSR device that was constructed for electromagnetic transient simulation. Similarly, transient behavior of CVSR is studied in (23) where simulation results shows the effectiveness of modelled CVSR. Lastly, simulations of a CVSR under fault conditions with CCVTs is studied and the interaction of the CVSR with CCVTs decrease the effect on distance protection compared to the CVSR itself (1).

Although several researchers have used FACTS or other devices in the distribution system to control power flow, solving the optimal power flow problem while focusing the transformer overloading remains a significant challenge. Additionally, improving the cost effective and reliable solutions to dense distribution areas continues as a problem. In this dissertation, we reformulate the power flow equations with a CVSR device(s), determine the CVSR device features, and investigate methods for integration of CVSR devices into distribution system transformers without overloading. The target application of CVSR device is power flow control in meshed electric power systems where CVSR device regulates the reactance of a transformer. To avoid overloading of transformers, a CVSR device can be used to regulate reactance on the primary side of transformer and hence control power flow through the transformer. Therefore, normal operation of the system can be sustained without equipment upgrades. Depending on the transformer capacity in kVA and loading conditions, the CVSR size and requirement can be determined. A few ohms variability is generally enough to significantly reduce loading.

1.2 Relieving Transmission and Distribution Congestion

Increasing load of electricity may cause a congestion in any power system. In a competitive market, supply availability and insufficient transmission capacity can contribute to the transmission congestion. Because of the transmission line congestion, violation of security limits, voltage stability issues and reliability problems may appear (24). Similar to the transmission system, the congestion may occur in the distribution system. Recent years, development and applications of DERs, active loads and electric vehicles are popular. Normally, demand response (DR) can be effective in some systems. Regardless of their potential advantages to the distribution systems, uncoordinated actions of DERs and other devices may cause unexpected congestion in the distribution network (25). Especially, renewable energy resources and some loads can result in additional uncertainty. Therefore, their behaviors and impacts to the distribution system cannot be ignored. Additionally, peak demands can cause the transformers to be overloaded. In the literature, relieving congestion in transmission and distribution systems has been studied by numerous researchers. Accordingly, we will review the literature in three different subsections, namely, power flow control devices (FACTS and CVSR devices), phase-shifting transformers and other methods(DGs, energy storage and reconfiguration).

1.2.1 Power Flow Control Devices

Simply, power flow control is an ability to change power flows to other transformer and lines throughout the grid. Controlling the impedance on transmission lines, injecting a controlled voltage with a line, and switching the breakers to reroute power to other lines or transformers are among their possibilities. Power flow control devices are usually power electronic devices. Before developments of the power electronic devices, transmission and distribution system operators(TSOs and DSOs) had only the ability

to influence power flows by using the switches, generation dispatches and curtailment and tap changing. These new devices are faster and can be operated more frequently than switching devices.

1.2.1.1 Flexible AC Transmission Systems(FACTS)

FACTS was introduced by Hingorani and Gyugyi in 1999 (26). FACTS enables power flow to be controlled and altered in an accurate, fast, and precise manner. Using FACTS can also decrease power quality issues in the power systems. The FACTS are the static device mainly placed in the AC transmission network to enhance maneuverability and develop power flow transfer capability. The FACTS devices' main duty is to relieve congestion, maintain power transfer capability of the transmission system, and control the power flow. The devices can control different electrical parameters, such as, voltage and power flow, in the system. Since the smaller installation cost, quick response with active power, controllability and reliability of the power system, the FACTS are preferred to use in the transmission systems (27). The devices consist of a couple of power electronics based devices, namely, unified power flow controller(UPFC), thristor controlled series compensator(TCSC) and static compensator(STATCOM). There are variety of FACTS devices in the literature.

1.2.1.1.1 A Unified Power Flow Controller (UPFC) A unified power flow controller(UPFC) concept was offered by Gyugyi in early 90s (28). This FACTS device aims for controlling in real time. It has ability to control voltage, phase angle and impedance. UPFC is attractive in power systems because its ability to control power flow bidirectionally. UPFC device has a combination of two aspects of two other FACTS devices: STATCOM and static synchronous compensator(SSSC). Thus, UPFC is a simple synchronous voltage source (SVS). Usually, it can exchange reactive and active power in the transmission network(29). UPFC features two voltage-sourced converters that use a thyristor-controlled power electronic device. Shunt and series

converters are both used in the UPFC. These two converters are coupled through a DC link where active power exchange happens. Both converters are functioned as AC to AC.

1.2.1.1.2 Thyristor Controlled Series Compensator (TCSC) TCSC has been applied in the real power systems for more than decades to control power flow(30). A TCSC is a controllable FACTS device which can control power flow with variable reactance of a transmission line that linking two areas. TCSC has two anti-parallel thyristors, bypass inductor and capacitors. The configuration of a TCSC is represented in Figure 1.1. Reactance of TCSC can be modified with the firing angle (λ) of the thyristor to maintain active power flow of the connected line within limits. Although, this device can be considered as a variable reactance added to the transmission line as shown in Figure 1.2.

Power flow control with the TCSC can increase or decrease the impedance of overall transmission lines by supplying an inductance or capacitance accordingly(31). This model depicts the TCSC by a variable reactance, X_{TCSC}. The TCSC reactance can be calculated as follows:

$$X_{TCSC} = X_C // X_L(\alpha) = \frac{X_C X_L(\alpha)}{X_C + X_L(\alpha)} \tag{1.1}$$

where

$$X_L(\alpha) = X_L^{\max}\left[\frac{\pi}{\pi - 2\alpha - \sin 2\alpha}\right] \tag{1.2}$$

$$X_L^{\max} = L\omega \tag{1.3}$$

$$X_C = \frac{1}{C\omega} \tag{1.4}$$

X_C is capacitance reactance. $X_L(\alpha)$ is inductive reactance which depends on the firing angle (α) of the thyristors. X_{Lmax} is the maximum of inductive reactance that can be reached. Thus, final version of X_{TCSC} can be calculated in eq.(1.5) using equations (1.1 - 1.4) as follows belows:

$$X_{TCSC} = \frac{X_C X_L(\alpha)}{X_C + X_L(\alpha)} \tag{1.5}$$

The working limits of the TCSC should be between a specific range to neglect overcompensation. (31)

$$-0.8X_{line}^{ij} \leq X_{TCSC}^{ij} \leq 0.2X_{line}^{ij} \tag{1.6}$$

1.2.1.1.3 Static Compensator (STATCOM) The static compensator (STATCOM) is a form of a shunt FACTS controller based on a voltage supplied converter (VSC). STATCOM's controlled output voltage supplies the necessary reactive power amount to compensate any connected system bus. STATCOM has a controller, a shunt transformer, a dc capacitor, a VSC, and a magnetic circuit. Compared to the static VAR compensation (SVC), STATCOM controller can inject real power from any battery storage or large capacitor. Additionally, they do not need large inductance or capacitance to supply capacitive or inductive reactive power to transmission systems in contrast to the SVC. There is also a specific STATCOM controller for distribution system which is called D-STATCOM. D-STATCOM is simply a controlled current source in shunt connected to the distribution line. It can exchange reactive and real power as any other STATCOM (32).

In the literature, D-STATCOM has been studied for variety of aspects including dynamic control techniques of the D-STATCOM (13; 33; 34). Analysis of D-STATCOM under unbalanced voltage condition is observed in (35) to improve distribution balance. Optimal location of D-STATCOM is used to minimize losses and

total harmonic distortion for a radial distribution system (36). Also, power quality improvement using the D-STATCOM controlled by Fuzzy-PI is studied in (34).

1.2.1.2 Continuously Variable Series Reactor (CVSR)

The continuously variable series reactor (CVSR) is a newly proposed power electronic device similar to the FACTS device. Usage of the CVSR device in a power line is illustrated in Figure 1.3. The CVSR can continuously manage its output reactance by changing the saturation of a magnetic core, comparable to a series FACTS controller TCSC. By regulating the output reactance, it can control the overall impedance of the transmission line. As a result, the CVSR device can control the power flow in a meshed network (7; 21; 22; 37).

The investment cost for the CVSR device is around to be $10kVAr (21). Figure 1.4 shows the cost of similar rated of FACTS devices in % per kVAr. Cost comparison between similar FACTS devices and CVSR device has been made in (22) where the data shows CVSR device is far cheaper than the similar range of the FACTS devices. Since the cost of the CVSR is about %10 of the price of a equivalent rated FACTS device (like TCSC and UPFC), multiple CVSRs could be invested into to make transmission system more flexible. As with other power flow control devices, the CVSR device can improve the utilization of the existing power system network to avoid building new transmission lines or installing new transformers. With managing power flow, the CVSR device can lower total operating cost. Moreover, it gives flexibility to the system to provide corrective action in case of contingencies.

The total susceptance of a CVSR integrated into a lossless transmission line becomes as shown in Eq. 1.7:

$$B'_{line} = -\frac{1}{x_{line} + x_{CVSR}} = -(B_{line} + B_{CVSR}) \tag{1.7}$$

where

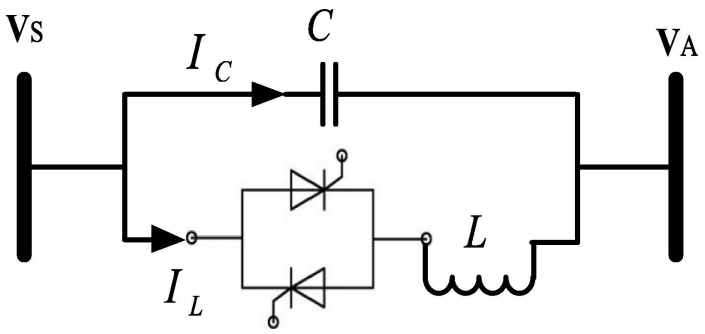


Figure 1.1: Basic Configuration of TCSC

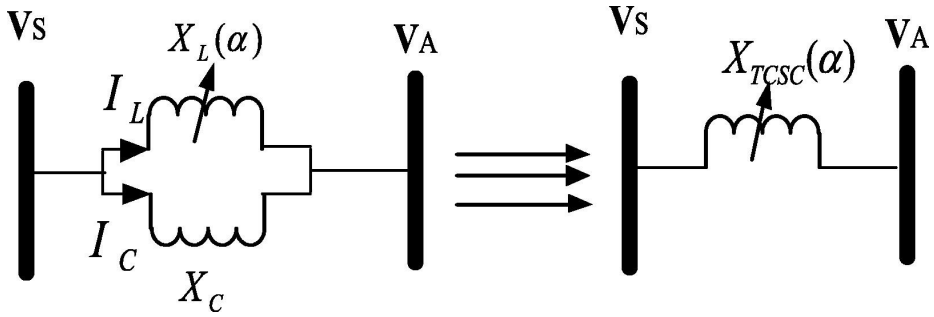


Figure 1.2: TCSC Equivalent Circuit



Figure 1.3: Representation of the CVSR in a lossless line

$$B_{line} = \frac{1}{x_{line}} \tag{1.8}$$

$$B_{CVSR} = -\frac{x_{CVSR}}{x_{line}(x_{line} + x_{CVSR})} \tag{1.9}$$

1.2.2 Phase-Shifting Transformer

Transformers are a vital component of the energy delivery chain. Phase-shifting transformers (PSTs) are used to control power flow in the power systems. When electricity passes from end to the other, voltage drop and shift phase-angle occurs between the source and the load. Thus, PSTs can be used to manage power flow between two systems by inserting a PST into one of the branches if parallel paths exist. The flow of active power from system 1 to system 2 requires an advanced phase-shifting angle. Figure 1.5 shows an example circuit with a PST and two systems (38).

Phase shifting transformers increase active power flow in the power system. Active power flow formulation is given in following equation:

$$P = \frac{|E_1||E_2|}{X_L} \sin(\delta) \tag{1.10}$$

where E_1 is sending voltage, E_2 is receiving voltage, δ is power angle and X_L is line reactance. Thevenin's equivalents of PST is shown in Figure 1.6. Accordingly, we can rewrite the active power flow formulation 1.10 below:

$$P = \frac{E_1 E_2 \sin\ , (\delta + \phi)}{(X_L + X_{PST})} \tag{1.11}$$

where ϕ is an angle of PST to shift phase to negative or positive value and X_{PST} is a PST's leakage reactance.

In the literature, PSTs are used in variety of applications(39; 40; 41; 42; 43). PSTs can be beneficial for couple cases, including one of them is preventing overloading on transmission lines (40). Moreover, different scenarios of power congestion are studied to perform power flow control with PSTs in (41). (42) focuses on the load alleviation

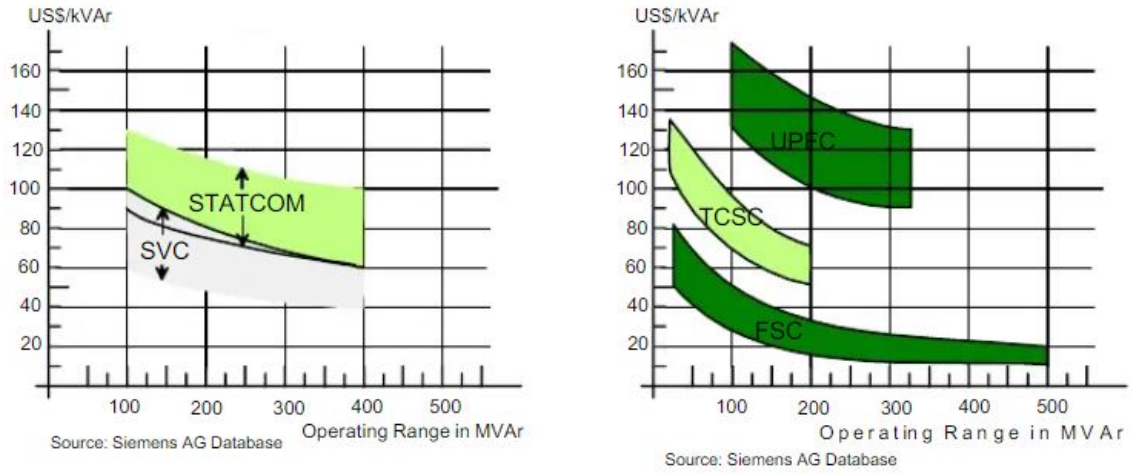


Figure 1.4: Cost of FACTS Devices ($/kVAr)

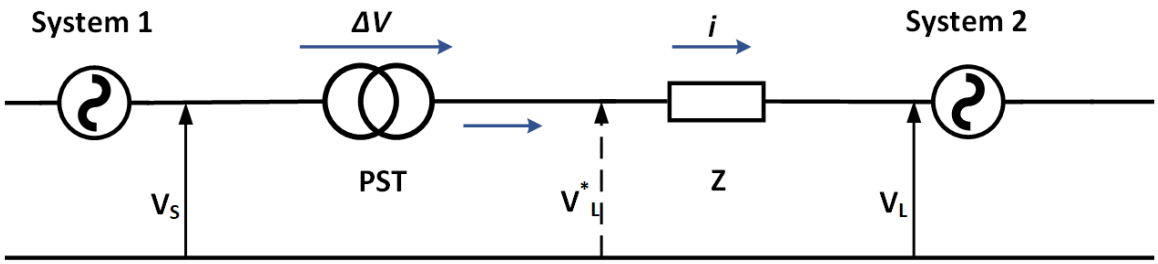


Figure 1.5: Representation of the PST Between Two Systems

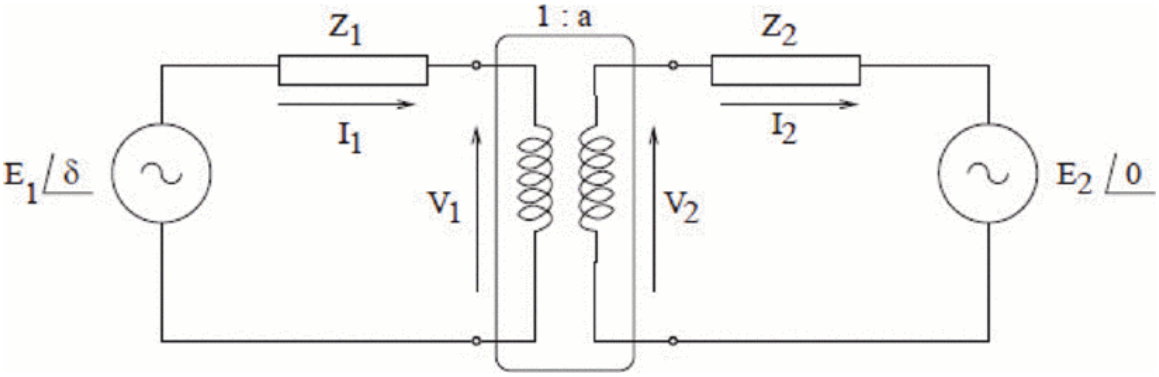


Figure 1.6: Connecting a Phase Shifting Transformer to the Network

with PST by changing phase angle to control power flow in transmission system. In (43), they manage congestion by PST using fuzzy logic control.

1.2.3 Other Methods

1.2.3.1 Distributed Generation

Power systems have traditionally relied on large power plants that supplied electricity over long distances over large transmission and distribution networks. Distributed generators(DGs) are rising as a practicable alternative to conventional power generation due to the cost of new power plants and environmental concerns that they cause. When supplying power with DGs,network upgrades can be eliminated (44). Since renewable energy sources, such as, solar and wind are environment friendly, renewable energy based DGs becomes more popular, especially in distribution networks. Yet, these DGs have disadvantages with their uncertainties. An example of distribution network with DG is illustrated in Figure 1.7.

Usually, the DG energy source in the literature is presumed to supply a constant output voltage (44; 45). DG can also be used to control power grid three-phase unbalance load (46). Generally, DGs are applied in distribution systems(45; 46; 47) except some can be used in transmission network(48; 49).

1.2.3.2 Energy Storage

Modern electric distribution grids include many applications that can utilize energy storage systems(ESSs). They can give such benefits to the power systems as reliability of the power service, smart load management, power flow control and power quality services. (15; 16; 17). For example, power flow is controlled by integrating truck mounted mobile energy resources to improve the resiliency of the system (50). Since batteries are fast acting devices, they can supply power to the grid in seconds. An experimental study (24) was conducted to evaluate the potential use of battery storage to further increase transmission capability of thermally limited paths. During a

contingency event, a battery is located at a congestion area to supply back-up energy to relieve thermal overload, which would then increase the transmission limit. In the early stages of a contingency occurrence, the battery provides power support for 15-to-20 minutes in order to prevent loading on affected components exceeding the emergency rating.

1.2.3.3 Network Reconfiguration

With the remote control ability of some switches, online reconfiguration can be an important distribution automation. In the power systems, network can be reconfigured for two reasons, namely, to reduce the power loss and to relieve the congestion in the network(51). Figure 1.8 shows the flow directions in a radial distribution network before and after reconfiguration.

The reconfiguration of radial distribution networks enable one to balance the load, reduce power loss, and improve reliability by changing the state of sectionalizing and tie switches(20). Researchers have proposed some methods to relieve congestion in the network with reconfiguration. For the load balance problem. In (51), Baran proposes network reconfiguration using a mixed integer programming (MIP). In (52), they propose a stochastic optimal power flow method for network reconfiguration design which relieves congestion. In (53), they formulate a simplified power flow model with mixed integer quadratic programming (MIQP) to obtain optimal reconfiguration. The transmission lines can be overloaded with excessive power flow when contingencies occur. To relieve transmission contingency, an AC power flow based mathematical formulation of network reconfiguration is proposed in (54).

1.3 Optimal Congestion Relief

The power industry is changing to a modern system with more automation, control and optimization approaches. Moreover, the power system becomes more a competitive market. Besides, the operating environment of the transmission

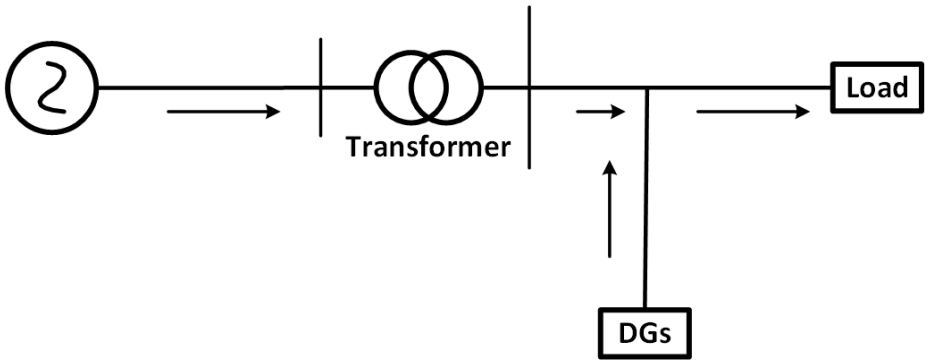
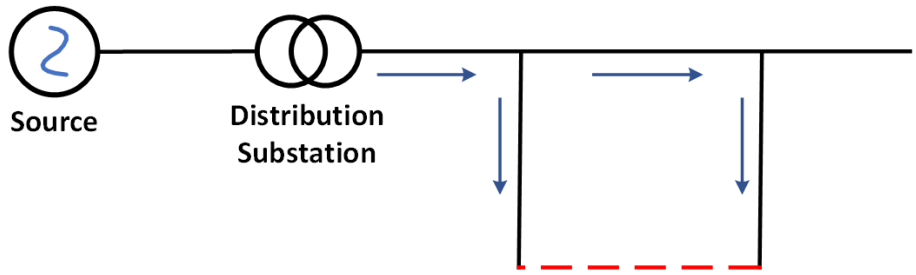
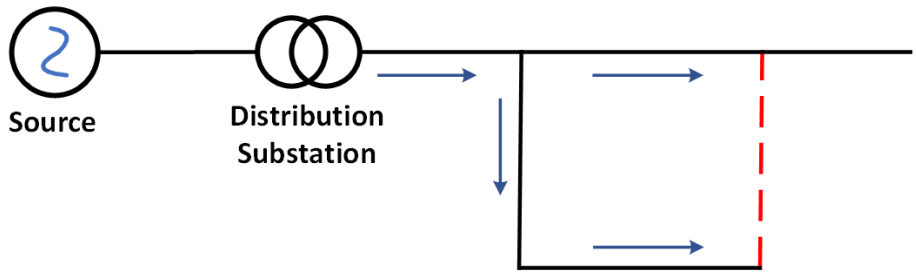


Figure 1.7: Distribution Network with DG Implementation



(a) Before Configuration



(b) After Configuration

Figure 1.8: Power Flow Paths Before and After Reconfiguration of a Radial Distribution Network.

system is growing with the more complexity since the competition in the market, environmental impacts to the power system, loading in the distribution system side and DERs increase. Eventually, power system congestion would be inevitable. Congestion management should be carried out immediately to prevent or relieve congested systems. Congestion management is divided into two main groups, namely technical and non-technical methods, according to Yusoff et al.(55). In this work, we focus on the technical methods. Power flow control devices are the ones with technical approaches. Optimization methods are used to control congested power systems. Whenever the power flow control devices are applied into the power system, optimization methods are needed to perform optimal location, optimal sizing etc.

In the literature, optimization is applied to the power flow control devices and other methods. The FACTS devices are used with optimization methods in (56) to perform optimal location and sizing. The mixed integer nonlinear programming (MINLP) was formulated to find optimal location of TCSCs in deregulated power system while maximizing the social welfare (57). Optimal network reconfiguration for congestion management based on genetic algorithm is proposed in (58). The article (59) presents optimal placement of DGs for congestion management purposes. Similar to (57), they formulate the problem on maximizing the social welfare and minimizing generator cost. An optimization method based on sensitivity is presented that enables the determination of the cost of congestion, the location of an UPFC, and its rating (60). Stochastic planning and scheduling of ESSs for managing congestions in power system where uncertainties of solar and wind units exist. Problem is formulated as a nonlinear programming, then solved with particle swarm optimization technique (61).

1.3.1 Cost of Impact of Transmission Congestion

It is inevitable that additional congestion costs will be incurred in order to solve the congestion problem. Since the power demand for the transmission capacity exceeds

the transmission capacity limits, the units with the low price must reduce their generation capacity and high priced generation units increase their capacity, thereby increasing the electricity cost. Congestion pricing concerns how much congestion costs, while congestion cost allocation concerns how the costs are shared equitably among market participants (62).

Congestion issue is a global problem for the countries while congestion costs continue. In the United States, among the Regional Transmission Companies (RTOs) and Independent System Operators (ISOs) that serve around 58% of U.S. electricity customers, transmission congestion costs significantly increased from 2016 through 2018 (63). Table 1.1 shows the transmission congestion costs in $ millions for six RTOs among the United States from 2016 to 2019. These RTOs covers the 58% of total electricity customer among the US. From 2016 to 2018, congestion costs increased by 34%. Although for some RTOs, congestion costs of 2019 fell down to 2016 levels which is around 30% scaled down. Meaning, the congestion relief techniques or devices like the FACTS, DGs worked and/or event of natural disasters are reduced. California Independent System Operator (CAISO) is not given in this table. However the data of CAISO is obtained by the DOE personal communications and given in the electric transmission congestion study in 2020 (64). Data shows that CAISO congestion costs surpassed $500 million during the years 2012-2014. Then, the costs were decreased below $500 million between 2015 and 2017 and increased again over $500 million in 2018 similar before 2014. According to the report(65), costs associated with managing congestion in the German electricity grid have reached a record high of 1.4 billion Euros in 2017 while the total congestion cost for 2023 is expected to be increased to 4 billion Euros.

As a result, reports shows that congestion relief methods should be implemented in the power systems to reduce cost of the power system congestion.

Table 1.1: Transmission Congestion Costs ($ millions) in the United States from 2016-2019

RTO	2016	2017	2018	2019
ERCOT	497	976	1,260	1100
ISO-NE	39	41	65	33
MISO	1400	1500	1400	900
NYISO	529	481	596	462
PJM	1024	698	1310	583
SPP	280	500	450	457
Total	3769	4196	5080	3535

1.4 Optimal Placement of Electrical Devices in Power Systems

Power electrical or electronic devices are used in the power systems to address any faults, corrections and changes to maintain network stability, reliability, security, power balance and efficiency. Integration of these devices needs to be evaluated for optimal size and location. The optimal sizing and location is very common problem in the power systems for decades. Studies have demonstrated that an inappropriate electrical device placement may increase total power losses, voltage deviation, exploitation costs, average interruption duration of the system, and may also impact voltage stability, and network reliability. Therefore, researchers have been extensively interested in solving the optimal placement problems of various electrical devices for a considerable period of time. Numerous solutions have been developed to address the optimal allocation of these devices in transmission and distribution networks, as well as in both islanded and grid-connected microgrids.

Since 1961, optimal allocation of various electric devices has been carried out in electric power systems. These devices and their objectives include:

1. Shunt capacitors for voltage control and loss reduction (66),
2. Flexible AC Transmission Systems (FACTS) for congestion management and system loadability improvement (67; 68),
3. Distributed generation (DG) and renewable distributed generation technologies for voltage stability improvement, loss and voltage deviation reduction (69; 70),
4. Transformers, feeders, and High Voltage/Medium Voltage (HV/MV) substations for cost reduction (71),
5. Meters for fault location observability improvement, (72)

6. Phasor Measurement Units (PMUs) for network observability and reliability improvement (73; 74),

7. Electric Spring (ES) devices for voltage profile improvement (75),

8. Switches, sectionalizers, circuit breakers, and reclosers for cost of energy losses, reliability improvement and total risk reduction (76; 77; 78),

9. Fault Current Limiters (FCLs) for elimination of the faulty section impact on the whole network, reliability improvement, loss reduction (79),

10. Battery Storage Device for short term interruptions reduction. (17) (80)

The primary aims of researchers concerning the optimal placement of electrical and electronic devices revolve around the minimization of power losses, various costs, fault current, peak power, and overall risk. Furthermore, their objectives encompass the maximization of power quality, voltage stability, network stability, network reliability, loadability of transmission and distribution networks, and environmental benefits.

1.4.1 Optimization Techniques for Optimal Location Problems in Power Systems

In the field of power systems, optimal location problems play a significant role in ensuring the efficient and reliable operation of the electrical grid. These problems involve determining the optimal placement of various devices within the network to achieve specific objectives, such as minimizing power losses, improving voltage stability, reducing system costs etc.

To address these optimization problems, a wide range of techniques have been developed and applied. These techniques can be broadly classified into different categories, including analytical methods, heuristic and meta-heuristic algorithms and artificial intelligence techniques. Figure 1.9 illustrates the different optimization categories and their methods for optimal location of electrical devices in the power

system. Following subsections will be presenting variety of algorithms for the optimal location problems.

1.4.1.1 Analytical Methods

Analytical methods typically rely on theoretical frameworks, mathematical analysis, and calculations to address various objectives. These methods commonly aim to achieve the following goals: minimizing power losses, determining the optimal size of components or devices, and improving the voltage profile within a system.

Through theoretical analysis, these methods strive to identify strategies and techniques that can effectively reduce power losses within a given system. This involves optimizing the configuration of components, adjusting operational parameters, and implementing control measures to minimize energy dissipation and increase overall system efficiency. Also, analytical methods seek to determine the optimal size of components or devices within a system. By considering factors such as load demands, generation capabilities, and system constraints, these methods aim to find the most suitable sizes or capacities for devices such as generators, transformers, and capacitors. This optimization process ensures that the system operates at an optimal point, balancing performance and resource utilization.

This paper introduces a strategy aimed at achieving the optimal integration of Battery Energy Storage Systems (BESSs) to enhance the load and Distributed Generation (DG) hosting capability of the utility grid. The proposed approach includes an efficient tool that determines the optimal capacity and day-ahead operation strategy for deploying BESSs under the control of the Distribution Network Operator (DNO). The strategy utilizes a cost-based multi-objective optimization framework that takes into account two key factors: 1) the cost associated with the distribution system, and 2) the battery cycling cost. Through quantitative analyses, the paper assesses the benefits and trade-offs of BESS installations, considering various service options (81).



Figure 1.9: Optimization Categories and Their Methods for the Optimal Location Problem

To achieve the optimal device placement, many analytical methods are employed in power system analysis and optimization (81; 82; 83). Some of these methods provide systematic approaches for evaluating different aspects of the power system and identifying the locations that yield the desired improvements. Several analytical approaches commonly employed to determine the optimal device placement comprise the following:

- Power Flow Analysis
- Mathematical Programming
- Sensitivity Analysis
- Graph Theory
- Voltage Stability Analysis
- Monte Carlo Simulation

1.4.1.1.1 Power Flow Analysis Power flow analysis is an essential tool for assessing the steady-state behavior of power systems and identifying areas that require optimization. It involves solving a set of nonlinear equations to determine the magnitude and phase angles of voltages and currents throughout the network. By analyzing the power flow, engineers can understand the system's loading conditions, identify bottlenecks, and evaluate the impact of device placement.

One commonly used method for power flow analysis is the Newton-Raphson method (84). It iteratively solves the power flow equations by linearizing the nonlinear equations and updating the state variables until convergence is achieved. The Fast Decoupled Power Flow (FDPF) algorithm is another widely employed technique that provides a faster and less computationally intensive solution by decoupling the real and reactive power equations (85). These power flow analysis techniques provide valuable insights into the system's operating conditions and help identify areas that

require optimization. The paper utilizes a conventional iterative search technique along with the Newton-Raphson method for load flow analysis for achieving optimal sizing and placement of generators in power systems. The objective is to efficiently reduce both cost and losses. Additionally, the paper emphasizes the optimization of a weighting factor, which plays a critical role in striking a balance between cost and loss considerations (83).

Different power flow methods (86; 87; 69) have been extensively investigated and assessed for their potential in identifying the optimal placement of Distributed Generation (DG). These methods typically aim to achieve multiple objectives, including reducing power losses, maximizing the size of DG units, and improving voltage levels. Two distinct Optimal Power Flow (OPF) formulations were employed to address two objectives: 1) determining the annual cost associated with spilled energy, and 2) optimizing the allocation of Energy Storage Systems (ESS) within the distribution system (88).

1.4.1.1.2 Mathematical Programming Mathematical optimization, also known as mathematical programming, involves the identification of the optimal element from a given set of alternatives, based on a specific criterion or objective. Mathematical programming techniques provide powerful tools for formulating and solving optimization problems related to the optimal location of electrical devices in power systems. These methods utilize objective functions and constraints to optimize device placement considering various factors such as system performance, costs, and operational constraints.

Linear programming (LP) (89), mixed-integer linear programming (MILP) (90), second-order cone programming (91), stochastic programming (92), robust optimization (93) and nonlinear programming (NLP) (94) are commonly used mathematical programming techniques in power system optimization.

LP formulates optimization problems with linear objective functions and constraints. It has been applied to various power system optimization problems, including

optimal generator placement (95), capacitor placement (96), and optimal power flow (88). LP techniques can efficiently find optimal device locations that minimize system losses, total cost, maximize power transfer capabilities, or achieve other specific objectives.

MILP extends LP by incorporating integer variables, allowing for discrete decisions in the optimization process. It is particularly useful for problems that involve the selection of discrete devices or discrete device operating states. MILP techniques have been applied to optimal placement of devices such as transformers (97), capacitors (98), DGs (99), renewable energy sources (100), and BSSs (101). By considering discrete device placement options, MILP models can provide more realistic and practical solutions for optimal device locations. Various algorithms, such as branch-and-bound and branch-and-cut, are employed to solve MILP problems efficiently (102).

NLP deals with optimization problems involving nonlinear objective functions or constraints. It is useful for complex power system optimization problems that require considering nonlinearity, such as optimal placement of FACTS devices (103) or distributed generation units (104; 105). NLP techniques, including gradient-based and evolutionary algorithms, have been used to determine optimal device locations that improve system performance and address specific objectives. These algorithms iteratively search for optimal solutions by considering the gradients or evolutionary operators to navigate the search space and converge to the global optimum (105).

The application of mathematical programming techniques in power system optimization has been well-documented in the literature. Mainly LP, MILP, and NLP were used to address various optimization problems and determine optimal device locations. By formulating the problem as a mathematical program and leveraging efficient solution algorithms, these techniques provide systematic approaches for identifying optimal locations that enhance power system performance, reduce costs, and satisfy operational requirements.

1.4.1.1.3 Sensitivity Analysis Sensitivity analysis is a powerful technique used to assess the impact of device locations on various system parameters and performance metrics in power systems. It plays a crucial role in identifying the optimal locations for electrical devices by quantifying the sensitivity of system variables to changes in device placement.

Sensitivity analysis evaluates how modifications in device locations influence important system characteristics such as power flows, voltage profiles, losses, or other performance indicators. By assessing the sensitivity of these variables in device placement, it can be seen where the installation of devices can yield substantial implications.

The sensitivity analysis process typically involves the following steps:

1. Variable Selection: Determining the system variables of interest based on the specific objectives and requirements. These variables can include power flows, voltage magnitudes, voltage angles, reactive power, or system losses.

2. Design of Experiments: Designing and investigating the effects of device placement variations on the selected variables. This can involve changing the locations of devices individually or in combinations, while keeping other system parameters constant. In the optimization or power flow software, loops will work to investigate the effects while placement variations are happening.

3. Simulation or Analysis: Power system simulations or analytical calculations are performed for each experiment in the designed set. This step involves running power flow studies, voltage stability analyses, or other relevant analyses to determine the values of the selected variables for each scenario.

4. Sensitivity Calculation: The sensitivity of each variable is calculated by comparing the changes in its value with corresponding changes in device locations. This quantifies the relationship between device placement and the selected system variables.

5. Sensitivity Interpretation: The sensitivity results can identify critical areas or locations that have a substantial influence on the system's performance. Locations with high sensitivity may indicate that device placement in those areas can significantly impact the desired objectives depending on the optimal location problem.

Overall, sensitivity analysis is a valuable analytical method in power system planning and operation. However, the omission of accounting for the nonlinearity inherent in the power flow model can detrimentally influence the precision of computational results in sensitivity-based methodologies. Thus, sensitivity analysis can be integrated with other optimization techniques to guide the determination of optimal device locations. By incorporating sensitivity data as constraints or objective functions in the optimization models, the selected locations can show a significant impact on improving the desired system performance.

For example, in the optimal placement of capacitors in radial distribution systems, sensitivity analysis helps determine the impact of capacitor locations on system losses and voltage profiles (106). By evaluating the sensitivity of these performance metrics to changes in capacitor locations, the optimal locations can be determined that yield the greatest reduction in losses and voltage improvement.

Sensitivity analysis has also been applied to the optimal placement of FACTS devices, such as Static Var Compensators (SVCs) and Thyristor Controlled Series Capacitor (TCSC) in transmission systems. In a study by Gautam et al., sensitivity analysis was utilized to evaluate the impact of SVC and TCSC locations for improving the capability of a transmission system to safely and reliably transmit electricity (107).

The real power flow sensitivity factor has been proposed as a method for determining the optimal position of FACTS devices in order to maximize the total transmission capacity of an interconnected system (108). In (109), a two-stage methodology was implemented to effectively minimize power losses within the system. The comprehensive approach was applied with incorporating sensitivity analysis to

identify the optimal placement of the STATCOM, while the Newton-Raphson method was utilized to ascertain the appropriate capacity for the STATCOM.

Furthermore, sensitivity analysis plays a crucial role in determining the optimal placement of renewable energy sources, such as wind turbines or solar panels, in power systems. The Incremental Transmission Losses (ITL) approach was employed in two different sensitivity analysis techniques: allocating wind generators in the network and analyzing the impact of intermittency in power injections on the electrical system (110).

1.4.1.1.4 Graph Theory Graph theory provides analytical methods for analyzing power system topology and identifying optimal locations for device placement. Power system networks can be represented as graphs, with nodes representing buses and edges representing transmission lines and adjacency matrix as shown in 1.10. Graph theory techniques, such as centrality analysis and shortest path analysis, are employed to assess the importance, influence, and connectivity of nodes within the network. These techniques aid in identifying optimal device locations.

One common graph theory technique is centrality analysis, including betweenness centrality and closeness centrality, measures the significance of nodes based on their positions and connectivity within the network. Some research papers (111; 112; 113) implement centrality analysis based graph theory method for optimal location of microgrids, reactive power compensators and capacitors. High-betweenness centrality nodes are those through which a large amount of power flow passes, making them potential optimal locations for device placement (106). High-closeness centrality nodes are those that have short distances to other nodes, indicating their potential as optimal locations for enhancing system connectivity and reducing power losses. By applying centrality analysis, critical nodes that have a significant impact on system behavior can be identified and optimal device locations can be determined accordingly.

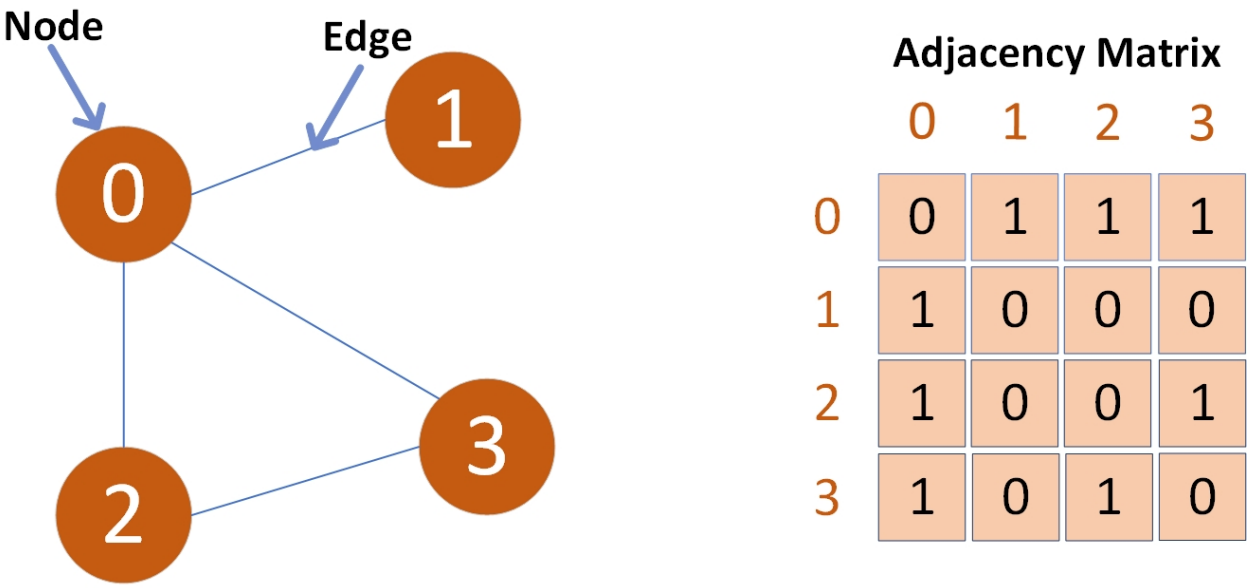


Figure 1.10: Simple Graph Theory and Its Adjacency Matrix

Another widely used graph theory method is the shortest path algorithm which is utilized to determine the most efficient routes between nodes in the network. In the context of power systems, shortest path analysis is employed to identify optimal paths for power transmission, reactive power compensation (114; 115). By considering the shortest path between nodes, optimal location of devices such as battery storages, FACTS devices, DGs and reactive power compensators can determined.

The shortest path analysis is conducted using various algorithms, such as Dijkstra's algorithm (116) or the Floyd-Warshall algorithm (117), to find the path with the minimum total cost or distance between two nodes. This analysis aids in determining optimal device placement along the shortest path, considering factors such as distance, losses, voltage drop, or other performance metrics.

Furthermore, graph partitioning techniques based on spectral analysis have been utilized in power systems. These methods partition the power system network into subgraphs based on the eigenvectors of the Laplacian matrix, helping to identify clusters or communities of nodes that can guide optimal device placement strategies [4]. By considering the interaction and interdependence of nodes within these clusters, engineers can determine the most effective locations for devices such as transformers or capacitors.

By employing graph theory techniques, including centrality analysis and shortest path analysis, power system topology, connectivity, and optimal routes can be analyzed effectively. These graph-based methods provide valuable insights into the importance of nodes, the connectivity of the network, and the optimal device placement considering factors such as power flow control and voltage stability.

1.4.1.1.5 Voltage Stability Analysis Voltage stability is a critical aspect of power system operation, and analyzing voltage stability helps in identifying weak areas that require device placement. Various techniques and indices are used for voltage stability analysis to assess the system's ability to maintain acceptable voltage levels under different operating conditions. Optimal device placement is one of the

feature of voltage stability analysis and can be determined by evaluating voltage stability indices and identifying locations where devices like capacitors or FACTS (Flexible AC Transmission Systems) devices can enhance system stability (118).

Continuation power flow analysis is a commonly used technique for voltage stability assessment (119). It involves solving a sequence of power flow equations while gradually varying a parameter (e.g., load level or reactive power support) to track the system's voltage stability limit. The results of continuation power flow analysis provide insights into critical points where voltage instability may occur, helping identify areas in need of device placement for voltage support.

Modal analysis is another approach for voltage stability analysis that considers the system's eigenvalues and eigenvectors (120). By evaluating the eigenvalues, which represent the system's stability margins, the proximity to voltage collapse can be assessed. Modal analysis can identify weak areas with low damping ratios and help determine the optimal locations for device placement to improve system stability.

Optimal device placement for voltage stability improvement can involve the installation of devices such as shunt capacitors, static VAR compensators (SVCs), or other FACTS devices. These devices can provide reactive power support, voltage control, and enhance system stability. Optimal allocation and sizing of these devices can be determined using various optimization techniques considering factors such as system constraints, costs, and voltage stability objectives (121; 122).

By applying voltage stability analysis techniques and considering voltage stability indices, weak areas or busses can determined. Thus, determining the optimal locations for installing the electrical devices. This helps in maintaining acceptable voltage levels, improving voltage stability margins, and mitigating the risk of voltage collapse.

1.4.1.1.6 Monte Carlo Simulation Monte Carlo simulation (MCS) is a probabilistic technique used to evaluate the performance of power systems under different operating conditions and uncertainties. By generating multiple scenarios through random sampling of system parameters, MCS provides insights into the robustness

and effectiveness of device placement strategies. The simulation results help in identifying the optimal locations that yield consistent improvements in system performance across a range of possible scenarios (123).

MCS has been applied in various aspects of power systems, including reliability assessment, risk analysis, and optimization. In the context of optimal location of electrical devices, MCS enables to evaluate the performance of different device placement strategies and identify optimal locations based on statistical analysis of the simulation results.

For instance, in a study by Marmidis et al. (124), MCS was employed to determine the optimal locations for wind turbines in a wind park power system. The optimization process is conducted by considering the criteria of maximizing potential wind power production and minimizing installation costs. Similarly, Donadel et al. proposed a novel methodology to determine the optimal placement of medium-sized DGs within a distribution system characterized by uncertain topologies. This approach takes into account the unique characteristics of small DGs and leverages Monte Carlo Simulation to assess and optimize their optimal locations (125).

Moreover, Monte Carlo simulation is utilized to identify the location where the deployment of FACTS devices yields the highest cost savings in conventional generation. A proposed methodology focuses on determining the optimal placement of FACTS devices, taking into account variations in demand and renewable generation output. The primary optimization technique employed in this study is a differential evolution algorithm, with the objective of minimizing generation costs (126).

These research illustrate the application of Monte Carlo simulation in determining the optimal location of electrical devices in power systems. By simulating various scenarios and analyzing the statistical distribution of system performance metrics, device placement that account for uncertainties and variations in operating conditions can be accomplished.

1.4.1.2 Heuristic and Meta-Heuristic Methods

Heuristic and meta-heuristic techniques have gained popularity in determining optimal device locations in power systems due to their ability to handle complex optimization problems with large solution spaces. Traditional optimization techniques may struggle with the computational challenges posed by power system planning, especially when considering numerous variables, constraints, and nonlinearity . Heuristic and meta-heuristic techniques offer effective approaches for finding near-optimal solutions in complex scenarios. These techniques are inspired by natural phenomena or problem-solving strategies and provide powerful tools for exploring the solution space and identifying optimal device locations (127; 128). By leveraging the principles of evolution, collective behavior, or problem-solving heuristics, these techniques can effectively navigate large solution spaces, consider multiple objectives, and handle system constraints, enabling the determination of optimal device locations in power systems.

However, it is worth noting that the performance of heuristic and meta-heuristic techniques heavily depends on the chosen parameters, problem formulation, and the quality of the solution space exploration. Proper tuning of algorithmic parameters and careful problem formulation are crucial to ensure reliable and high-quality results.

1.4.1.2.1 Heuristic Algorithms Heuristic techniques are problem-solving approaches that rely on practical rules or intuitive strategies. Unlike rigorous mathematical optimization methods, heuristics provide approximate solutions that are often quick to obtain. Heuristic techniques leverage domain knowledge and problem-specific insights to guide the search for optimal device locations. Heuristic techniques are particularly useful when the problem complexity is high and an exact optimal solution is challenging to obtain within a reasonable time frame. While heuristic techniques may not guarantee optimality, they provide practical and efficient approaches for determining near-optimal device locations in power systems. Examples

of heuristic techniques in power system optimization include Tabu Search, Simulated Annealing, and Harmony Search.

Tabu Search utilizes memory-based search procedures to explore the solution space efficiently, considering both local and global search movements. Nara et. al applies the tabu search algorithm to optimize the allocation and capacities of DGs in order to minimize distribution loss in power systems. The algorithm is used iteratively to find the best placement of DGs, taking into account their discrete capacities (129).

Simulated Annealing mimics the annealing process in metallurgy, gradually cooling a system to reduce defects and achieve an optimal solution. (130) applies a simulated annealing algorithm to determine the optimal placement of multiple DGs in the IEEE 33 bus radial distribution system. The study considers multiple objectives such as reducing power losses and improving voltage profiles. By estimating expenditure and savings, the algorithm identifies the optimal DG placements .

Harmony Search is inspired by the improvisation process of musicians, where each decision variable represents a musical note and the harmony refers to a feasible solution. Binary harmony search algorithm based optimal placement of phasor measurement units (PMUs) in power networks to achieve complete observability while considering different installation costs is proposed in (131). Objective of this paper is to minimize the number of PMUs and their associated installation costs.

1.4.1.2.2 Meta-Heuristic Algorithms In contrast, meta-heuristic techniques go beyond specific problem-solving strategies and instead focus on general frameworks for solving optimization problems. Meta-heuristic algorithms are designed to explore the solution space systematically, intelligently, and adaptively. These algorithms mimic natural phenomena, social behavior, or problem-solving processes to efficiently search for optimal solutions. Meta-heuristic techniques, such as genetic algorithms, particle swarm optimization, ant colony optimization operate based on iterative improvements to candidate solutions. They iteratively explore the solution space, gradually refining the solutions and dynamically adjusting search parameters. Unlike

heuristic techniques, metaheuristic techniques provide a more systematic approach to optimization, offering the potential for finding globally optimal or near-optimal device locations.

Genetic algorithms (GA) are widely employed in power system optimization. GA is inspired by the principles of natural selection and genetics. It involves the evolution of a population of potential solutions through genetic operators such as selection, crossover, and mutation. GA iteratively explores the solution space, allowing for the identification of optimal device locations (132). For example, genetic algorithms have been used for optimal placement and sizing of devices such as FACTS devices (133), capacitors (134), and distributed generation sources (135).

Particle Swarm Optimization (PSO) is another popular metaheuristic technique used for optimal device location in power systems. PSO is inspired by the collective behavior of bird flocking or fish schooling, where particles explore the search space by updating their positions based on their own best position and the best position found by the entire swarm (136). PSO has been successfully applied to determine optimal locations for devices such as FACTS devices (137), distributed generation sources (138), and phase shifting transformer (139).

Ant Colony Optimization (ACO) is a metaheuristic technique that emulates the behavior of ants searching for food. ACO algorithms utilize pheromone trails to guide the search process. Ants deposit pheromones to mark paths and other ants follow these trails to find better solutions (140). ACO has been employed for optimal device location in power systems, including capacitor placement (141) and optimal allocation of distributed generation sources (142).

1.4.1.3 Artificial Intelligence (AI) Techniques

Artificial intelligence techniques have gained prominence in power system optimization due to their ability to handle complex, nonlinear problems and learn patterns from historical data. AI techniques are also used for determining the optimal locations of devices in power systems. Within the realm of power system optimization, various

AI techniques have been applied for many purposes like optimal location, optimal sizing, cost reduction. There are many algorithm as AI techniques but artificial neural networks (ANNs), fuzzy logic, and machine learning algorithms are the most popular ones in the power system area.

1.4.1.3.1 Artificial Neural Networks (ANNs) ANNs have garnered significant attention in power system applications, including the determination of optimal device locations. ANNs consist of interconnected nodes that process information and learn patterns from input-output training data (143). The advantage of ANNs lies in their capacity to capture complex relationships between input parameters and the corresponding optimal device locations.

In the context of power system optimization, ANNs are trained using historical data where the input parameters represent key system characteristics, and the output corresponds to the optimal device locations. Once trained, ANNs can provide predictions for device locations based on new sets of input parameters. These predictions offer valuable insights to decision-makers in selecting the most suitable device placement strategies.

ANNS have been successfully employed in diverse power system optimization tasks mostly for fault location purposes (144), and some capacitor placement (145) and allocation of DGs (146). By harnessing the capabilities of ANNs, accurate and efficient solutions for optimal device location can be obtained.

1.4.1.3.2 Fuzzy Logic Fuzzy logic is another AI technique that is a prominent mathematical approach for addressing the challenges associated with decision-making in power system optimization problems. Fuzzy logic techniques are well-suited to handle uncertainties and imprecise inputs. This is achieved through the representation and manipulation of linguistic variables and subjective information (147).

Fuzzy logic-based approaches and fuzzy decision support systems have been utilized to determine optimal device locations in power systems. These approaches employ fuzzy rules and membership functions to model system parameters and constraints. By considering linguistic variables and uncertain information, fuzzy logic techniques enable the derivation of robust and flexible solutions for device placement problems.

The application of fuzzy logic has been observed in the power systems area where finding the optimal location of reactive power compensators (148), DGs (149), and other devices in power systems. By incorporating fuzzy logic techniques, the decision-making process is enhanced by accommodating subjective inputs and addressing uncertainties inherent in the system.

1.4.1.3.3 Machine Learning Algorithms Machine learning algorithms are pretty known approaches for wide variety of areas like chemical engineering, computer engineering, industrial applications, supply chain etc. They also have gained considerable traction in power system optimization due to their capacity to learn patterns from data and make accurate predictions. Various machine learning algorithms, such as support vector machines (SVM), decision trees, random forests, and deep learning approaches, have been deployed in the pursuit of optimal device location in power systems.

In the research, support vector machines have been applied to identify optimal locations for reactive power compensators (150), while decision trees and random forests have been utilized to determine the optimal placement of DGs (151; 152). Deep learning techniques, such as convolutional neural networks, have also been explored for fault location problem (153).

Machine learning algorithms offer the advantage of capturing intricate relationships and nonlinear dependencies between system parameters and optimal device locations. Consequently, they provide flexible and accurate solutions by leveraging the power of data-driven learning.

1.5 Network Distribution Systems

Electric utility companies use distribution systems to provide their customers with reliable, high-quality electricity. Most distribution systems use a simple radial circuit that is either above ground or underground. Radial system can be illustrated as in Figure 1.11. Radial networks are improved with reliability applying the switching schemes like primary auto loop, primary selective and secondary selective schemes. Secondary selective schemes are applied in industrial plants and other institutions, while primary selective schemes are applied in areas of concentrated load. However, utilities prefers spot and secondary grid network systems in congested areas like high-dense suburban or metropolitan areas to provide high reliability and operating flexibility (2). Spot and secondary networks are shown in Figure 1.12 and Figure 1.13, respectively.

Networks became more standardized by the 1970s.The establishment of grid networks in densely populated areas involved the implementation of 120/208V distribution systems and the construction of 277/280V spot networks to cater to significant load centers (154). Furthermore, utility companies like Consolidated Edison in New York developed evaluation techniques to determine the most appropriate design plan for new customers (155). Utilities explored the installation of modern advanced sensors in low voltage systems in the 1980s (156). In response to the emergence of new sensors, certain utility companies began integrating additional monitoring and control systems, such as Supervisory Control And Data Acquisition (SCADA), into their networks (157). The same technologies are now used by more advanced network systems. Network protectors do the same thing as their original counterparts, but they now use microprocessors instead of electromechanical relays. Usually, they are directly connected to the transformer to minimize the distance separating them from the transformer.

About 80 cities in North America currently have some form of low-voltage networks(LVNs). In some cases, they are only 120/208V grids, while in others they

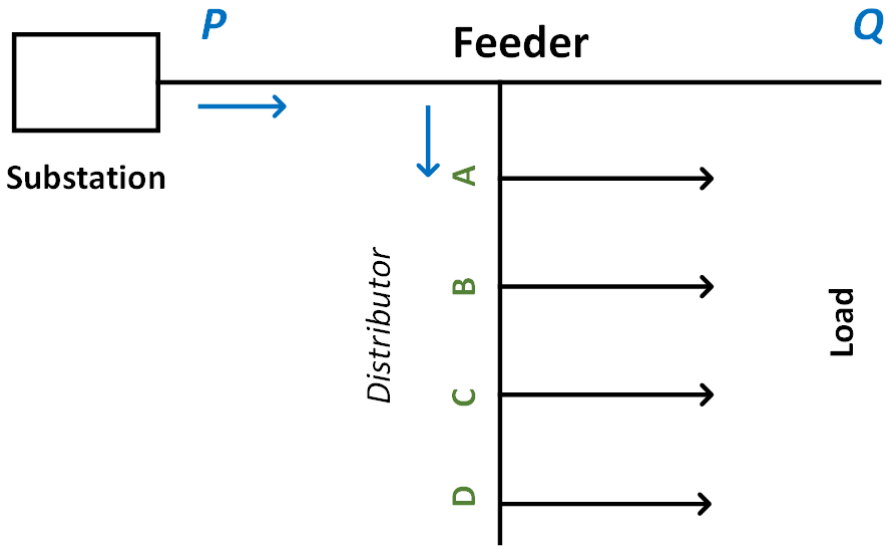


Figure 1.11: Radial Distribution System

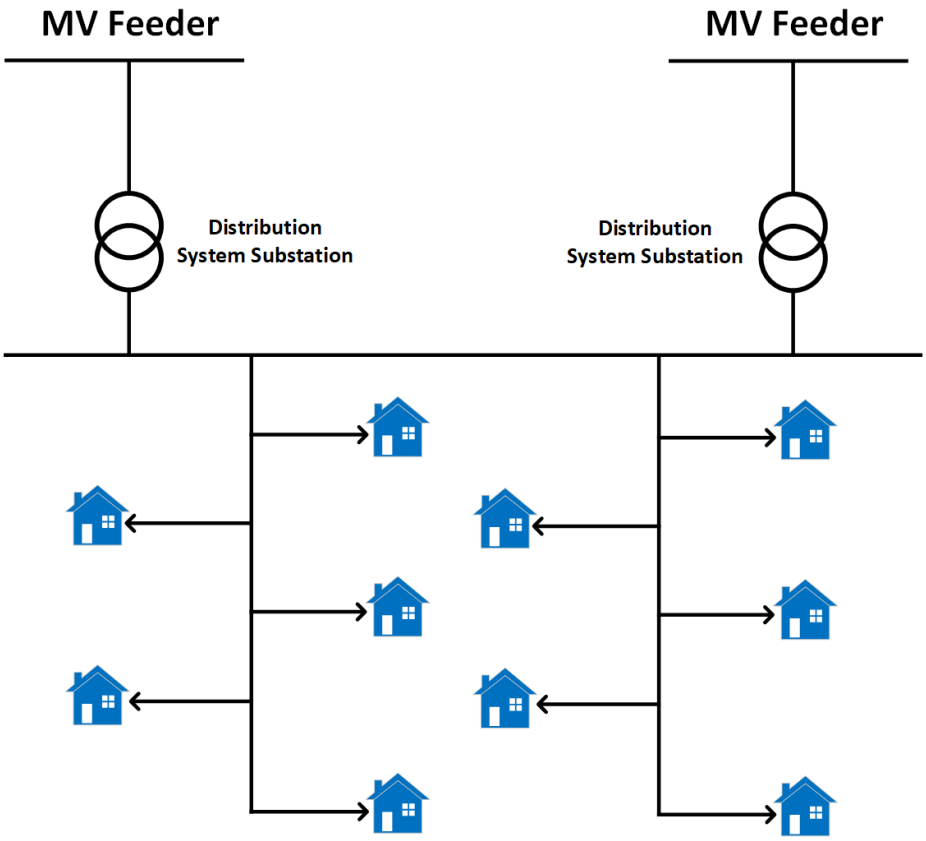


Figure 1.12: Spot Low-Voltage Network

are combination grids with both 120/208V and 277/480V spots. Despite their high costs, both of these distribution systems provide far greater reliability than that of radial feeders.

We will use three different network systems in this work. Two-parallel feeder system will be performed for verification of the some calculations of simulation software. Mostly, the IEEE 342-Node Low Voltage Networked Test System(LVTNS) will be used for simulation purposes since the system has secondary and spot networks where secondary network is 100% meshed grid. Finally, Consolidated Edison (ConEd) system, real distribution system data, will be used to simulate optimal power flows.

1.5.1 Two Parallel Transformers

A simple circuit with two parallel feeders is provided with two transformers between primary and secondary networks where secondary side of transformers are connected to common series and parallel loads. Secondary network transformers are rated at 1000 kVA each. Accordingly, the total loading aimed less or equal to be the total power supply by transformers. This distribution system is modeled and represented as in Figure 1.14.

1.5.2 IEEE 342-Node Low Voltage Networked Test System(LVNTS)

As part of the increasing network redesign of the grid network, the distributed distribution feeders have changed from the traditionally radial distribution feeders to an LVN that is supplied by a multitude of feeders. For the purpose of providing a benchmark of analysis for LVNs, the LVNTS was developed by the Testing Feed Group of the Distribution Analysis Subcommittee. LVNTS is a 342 node network that consists of 150 delta-connected primary nodes, as well as 192 grounded-wye secondary nodes. This test feeder, unlike existing test feeders, features a highly meshed system with unbalanced loads compared to other feeders. There are eight 13.2 kV primary

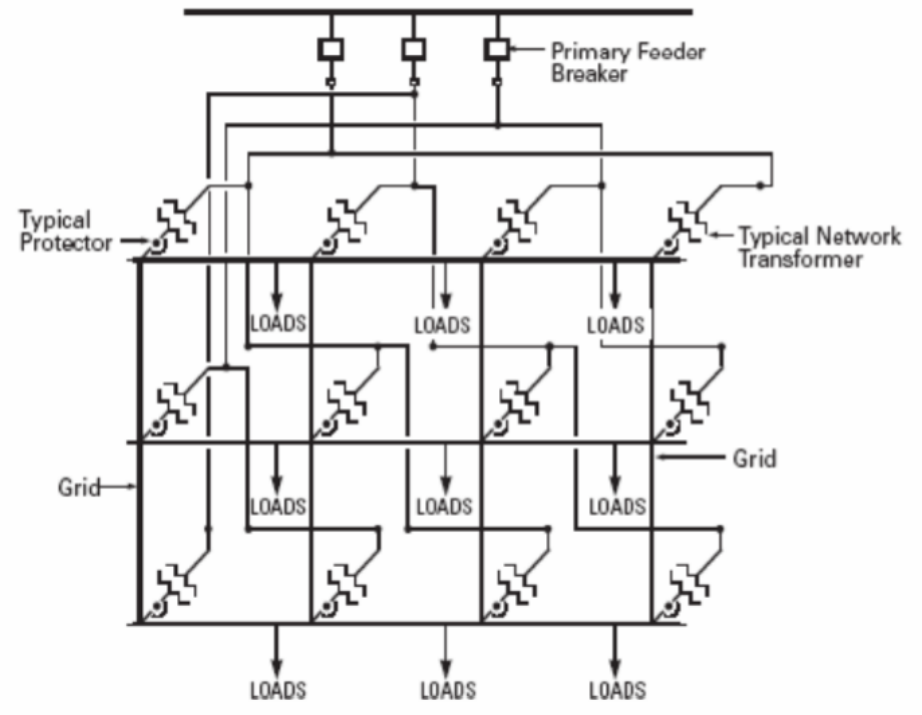


Figure 1.13: Secondary Grid Distribution System (2)

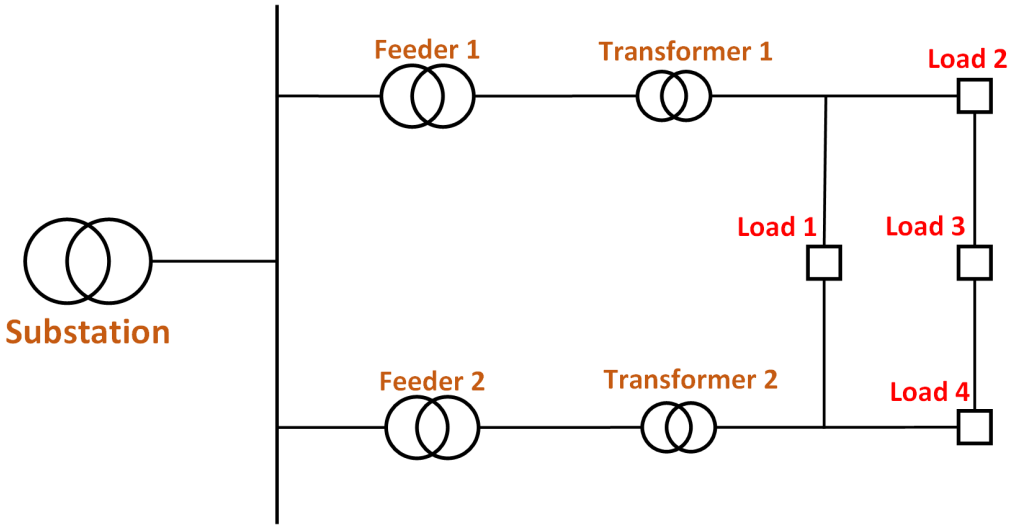


Figure 1.14: One-Line Diagram of Two-Feeder Distribution System

feeders feeding the LVNTS and they are supplied by a 230 kV substation with two 50 MVA 230/13.2 kV step-down transformers. The primary feeders provide power to a single grid system of 120/208V and eight spot networks of 277/480V via 68 delta/grounded-wye transformers. A grounded-wye system is used in both the grid and spot networks. Approximately 50 MVA of load is present on the system, which is represented as wye-connected constant power loads as well as Delta-connected constant power loads. In order to supply the Grid network, there are eight primary distribution feeders through 48 transformers of 1,000 kVA each. Figure 1.15 shows a one-line diagram of the LVNTS where blue lines stand for the spot network lines and red lines are the secondary network lines (3).

1.5.3 Consolidated Edison(ConEd) System

The Con-Ed system includes the small dense-loaded area. The distribution system has 292 secondary network transformers which are rated 500 kVA, 1000 kVA, 2000 kVA and 2500 kVA. Their voltage bases are 13.406 kV/0.216-0.48 kV. 7 feeders are supplying power to the different areas in the distribution system. In this project, 1000 kVA transformers are chosen for power flow studies because they are located in the small-meshed grids as illustrated in Figure 1.16. Out of the 292 secondary transformers, 83 of them are rated at 1000 kVA. Each small-meshed grid is interconnected with others through transformers, as shown in the Figure 1.16.

The remaining sections of the dissertation are organized as follows. In Chapter 2, the CVSR model is presented, including the steady-state model of the CVSR device. This chapter also provides a historical overview of CVSR devices, discusses their characteristics, and presents the reformulations of reactance and power flow equations considering the presence of the CVSR. Additionally, the formulation of transformer sensitivity with the CVSR is described.

Chapter 3 focuses on the application of CVSR devices to handle power congestions and control power flow in distribution systems. The chapter explores various scenarios and case studies, demonstrating the effectiveness of CVSR devices in managing power flow and mitigating overloading issues.

Chapter 4 introduces the optimization techniques employed in the dissertation for the optimal placement of CVSR devices. It provides detailed information about the optimization model used for the placement of CVSR devices to alleviate congestions. The chapter highlights the importance of accurate and efficient placement of CVSR devices in distribution systems.

The simulation results are presented in both Chapter 3 and Chapter 4, providing comprehensive insights into the optimal locations and effectiveness of CVSR devices in managing power flow and relieving overloading.

Finally, Chapter 5 concludes the dissertation by summarizing the main findings and contributions. It also discusses the limitations of the study and proposes future research directions to further enhance the optimization and application of CVSR devices in power systems.

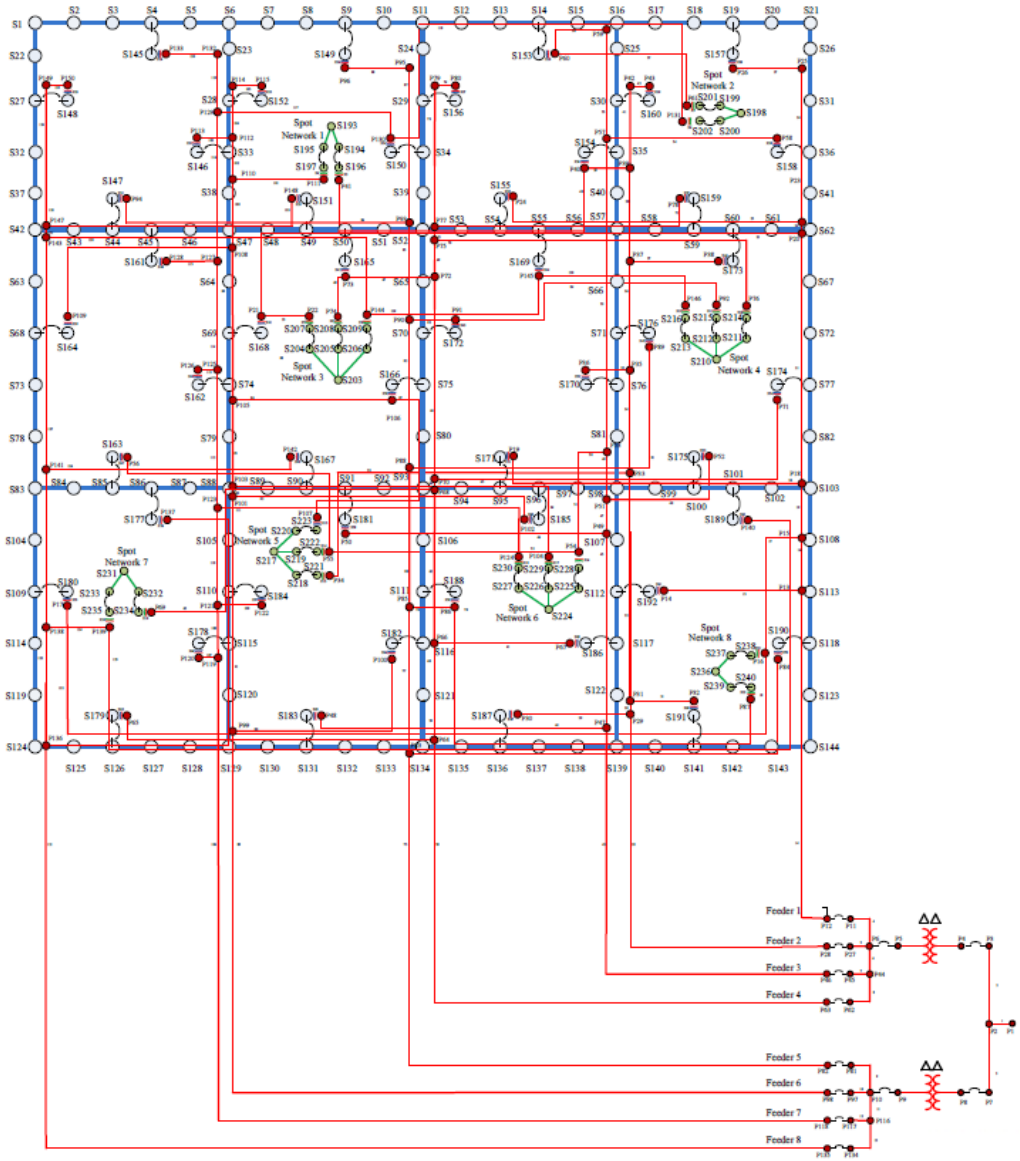


Figure 1.15: One-Line Diagram of the IEEE 342-Node LVNTS (3)

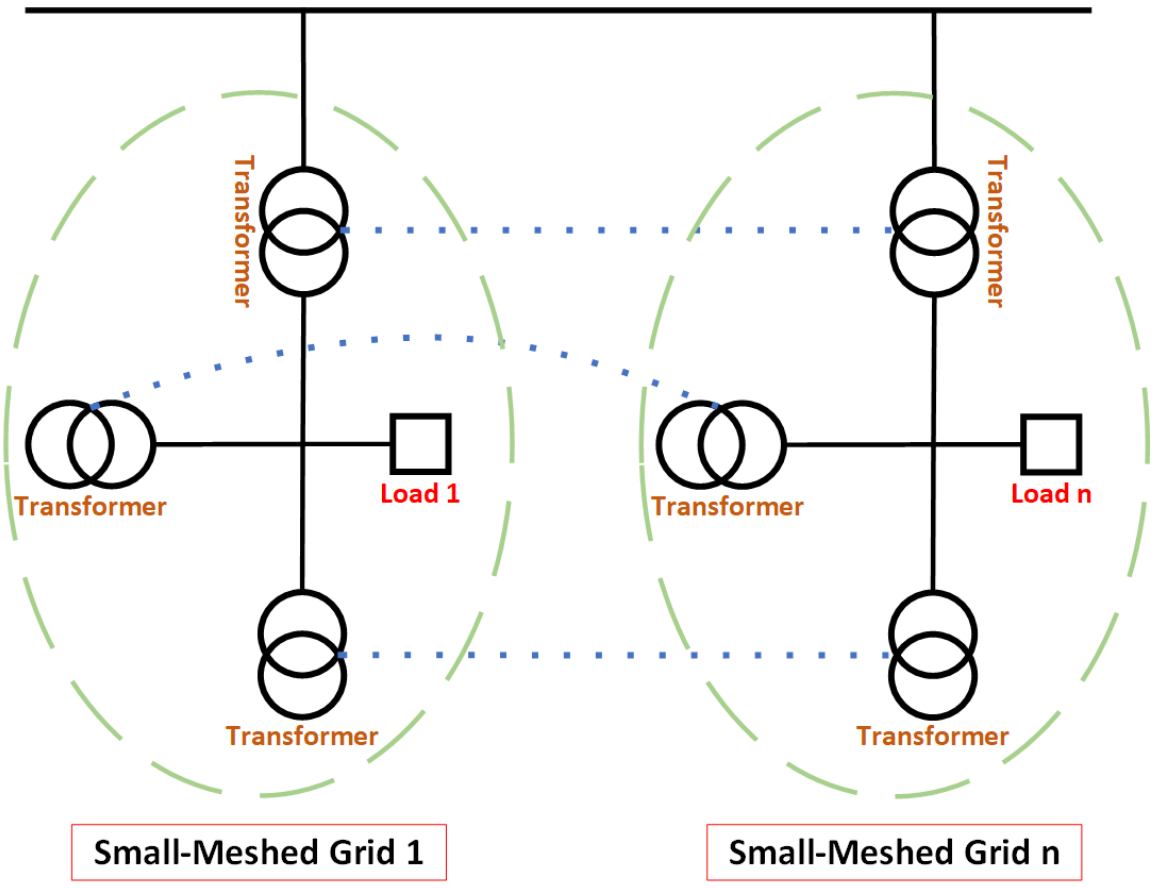


Figure 1.16: Small-Meshed Grids in Con-Ed System

Chapter 2

The Continuously Variable Series Reactor (CVSR) Model

In this chapter, details of the continuously variable series reactor(CVSR) device will be given such as characteristics of the CVSR, already applied CVSR devices in the literature,steady-state model of CVSR device. Moreover, sensitivity analysis section will be provided to show how power flow control is doable with CVSR devices while considering the effects of change of input variables.

2.1 Characteristics of CVSR Device

In this work, we use the CVSR device. Definition of the CVSR is a series reactor in its design limits that vary continuously. The concept provides adjustment of reactance by regulating the magnetization in a ferromagnetic core. The CVSR's operation in complete electric cycle is illustrated in Figure 2.1. The core of CVSR contains both AC and DC flux components, which determine the state of the CVSR along its nonlinear magnetic characteristic as AC line current is conducted along the center leg, and DC line current is conducted along the outer legs. A high reluctance airgap in the center leg provides a path for the DC flux component to pass through, directing the

flux to the outer loop of the core. Additionally, the airgaps determine the maximum reactance of the Airgaps in the center leg are a high reluctance path to the DC flux that directs the DC flux component to the outer loop of the core. The airgaps also establish the maximum reactance of the CVSR device. By adjusting the DC bias, one can move the operating point along the B-H curve, and thereby modulate the flow of power on the AC side within specified limits. These limits are determined by the saturation and linear regions of the B-H curve. In nominal conditions, ac current will change depending on the inductive reactance controlled by the dc bias.

2.2 History of CVSR Devices

Concept of the CVSR device is based on the saturable-core reactor (SCR) as the oldest. A SCR is essentially a reactor with a variable value. A saturable core is shared by the AC and DC windings, and therefore the DC current supplying the DC bias flux affects the inductance. This in turn changes the magnetization of the saturable core shared by the AC winding. The idea of a SCR was initially proposed by C. F. Burgess and B. Frankenfield in 1901 (158). Between 1920's and 1960's, SCR-based applications flourished (159; 160; 161) and steadily declined after the invention of solid-state devices. For several decades, SCR focused much of its R&D efforts on the development of low-power electronic-circuitry-based applications that were widely used in the fields of control, communications, and sensor technology. Between 1920 and 1960, SCR based applications exist in the literature. In the process of developing a regulator of the impedance type, the balanced amplifier using biased SCR was developed in 1947 (160). SCR is used in (162) to maintain oscillations like harmonics or sub-harmonics in 1946. High-frequency carrier in communication area is produced with SCR in 1955 (163).

There have been few reports of high-power SCR applications in electric power systems until the 1990s (164; 165). There are several technologies that have been well understood and utilized in the past but recently, the SCR technology has

been revisited and found to be promising for a number of applications in the power industry such as power flow control, fault current limiting, reactive power compensation, oscillation damping, etc. Several technological advances over the past several decades, including advances in power electronics and high-temperature superconductors, are enabling SCRs to be integrated into power-system applications that were inconceivable cost- and technology-wise several decades ago. In general, SCR devices are low-cost and long-lasting. As a result of utilizing the existing technologies of SCR in power system applications, there is a reduced risk of investment, making it possible to deploy these technologies on a wider scale and to achieve commercialization in a short period of time. Thus, basis of the CVSR device has been introduced in (7).

In 2015s, concept of the CVSR device has been established and its prototype was manufactured. The CVSR device has been studied in the literature starting 2015. The first usage of the CVSR device was in (1). The CVSR has been used to investigate effects of the CVSR on distance protection with coupling capacitor voltage transformers (CCVTs). According to the Table 2.1, maximum apparent reactance of CVSR device is 0.64 and 5.1 Ω for prototype and full-scale operations at 277V and 66.4 kV AC voltage, respectively. During the scaling of a three-phase system, a bank of three single-phase devices was used. Figure 2.1 is shown in the (1). An experimental field prototype, designed for 1000 A, 20 kW, has been constructed and tested with A 115 kV, 1500 A CVSR with DC controller (DCC) is offered to use in utility transmission grid applications (37). This CVSR device has capable with variable reactance changing between 2 and 5 Ω. Demonstration of the CVSR device can be seen in Figure 2.2. Using a modeling approach of a gyrator-capacitor in (23), it is possible to simulate the magnetic interaction within a prototype device along with the voltages and currents in a connecting electric circuit external to the device. Same CVSR device (37) in used to have simulation and experiments.

In 2016, a method to model CVSR operation is proposed for electromagnetic transient simulation purposes in the power system analysis (4). The CVSR device specifications are same as in the Table 2.1.

In (22), the proper allocation of CVSRs is described to assist in reducing the transmission expansion planning (TEP) problem's costs and provide flexibility. For the prototype system in this paper, the output reactance of the CVSR cannot exceed 20% of the line reactance:

$$0 \leq X_{CV,k} \leq 0.2X_k \tag{2.1}$$

Previously, three single-phase CVSR devices were used. However, single three-phase CVSR device is introduced in (5) in 2020. In a three-phase system, installing a bank of three single-phase units certainly offers some benefits, such as simpler unit design, decreased reserve requirements, lighter units and more. Although, other factors such as space constraints and the use of less ferromagnetic material can reduce the costs, and using a single three-phase CVSR may be the best choice. Concept of multi-magnetic materials is used in three-phase CVSR to improve the reaction characteristic. It consists of a symmetrical core made of a high permeability ferromagnetic material with five legs which are two outer gapless legs and three inner gapped legs. Schematic of three-phase CVSR is illustrated in Figure 2.3. The reactance changes can be between 3.15 to 0.06 Ω while DC bias current vary 0 to 200 A. However, no information is given about the rated AC voltage. Similar to (5), three-phase CVSR device is modelled analytically in (6). Different positioning of the five legs has been proposed in that paper. The first, third and fifth legs are with gaps yet the others are gapless legs with the DCC which configuration is shown in Figure 2.4. A control current ranging from 0 to 1000 amps can be used to control the device's reactance between 3.4 and 0.84 Ω.

Three-legged CVSR structure like previous ones is applied for power flow control in transmission network (166). Based on experimental results, the proposed CVSR can continuously modulate the reactance from 1.6 to 5 Ω when the AC current in the

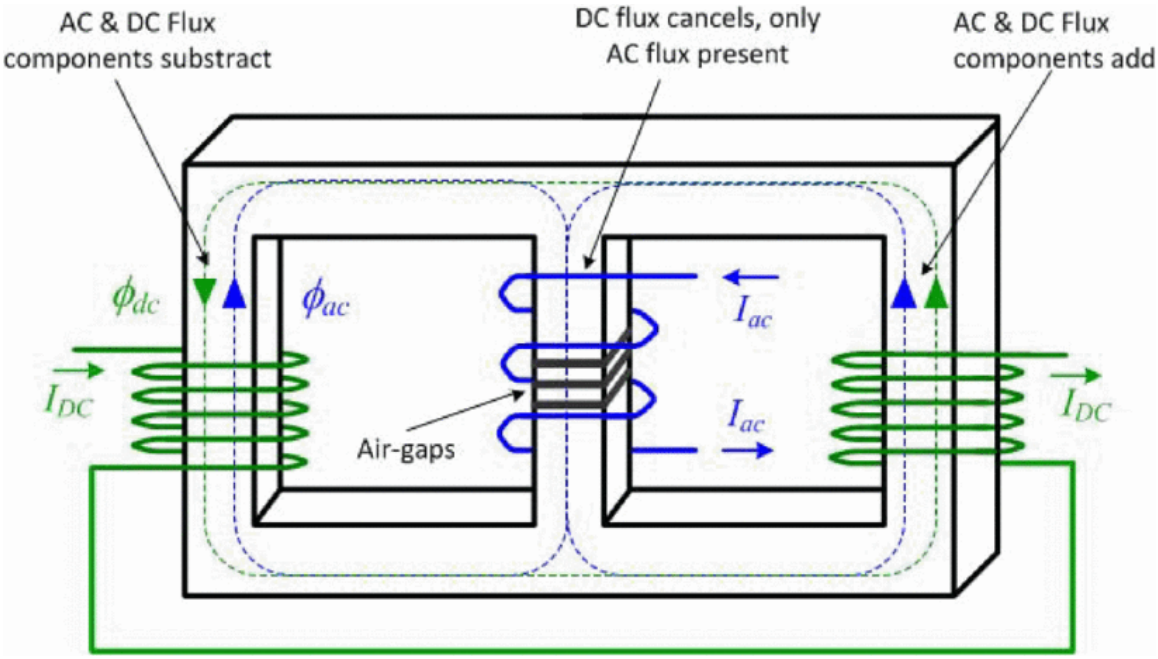


Figure 2.1: Schematic of CVSR Device. (4)



Figure 2.2: Demonstration of the CVSR Device.

Table 2.1: Parameters for Prototype and Full-Scale CVSR Device (1).

Parameter	**Description**	**Prototype**	**Full-Scale**
X_{max}	Maximum apparent reactance	0.64 Ω	5.1 Ω
X_{min}	Minimum apparent reactance	0.16 Ω	1.4 Ω
I_{rated}	Rated AC current	200 A	1.5 kA
V_{rated}	Rated AC voltage (line-to-neutral)	277 V	66.4 kV
$I_{dc(max)}$	DC bias current for minimum reactance	200 A	200 A
I_{fault}	Fault rating	4 kA	30 kA

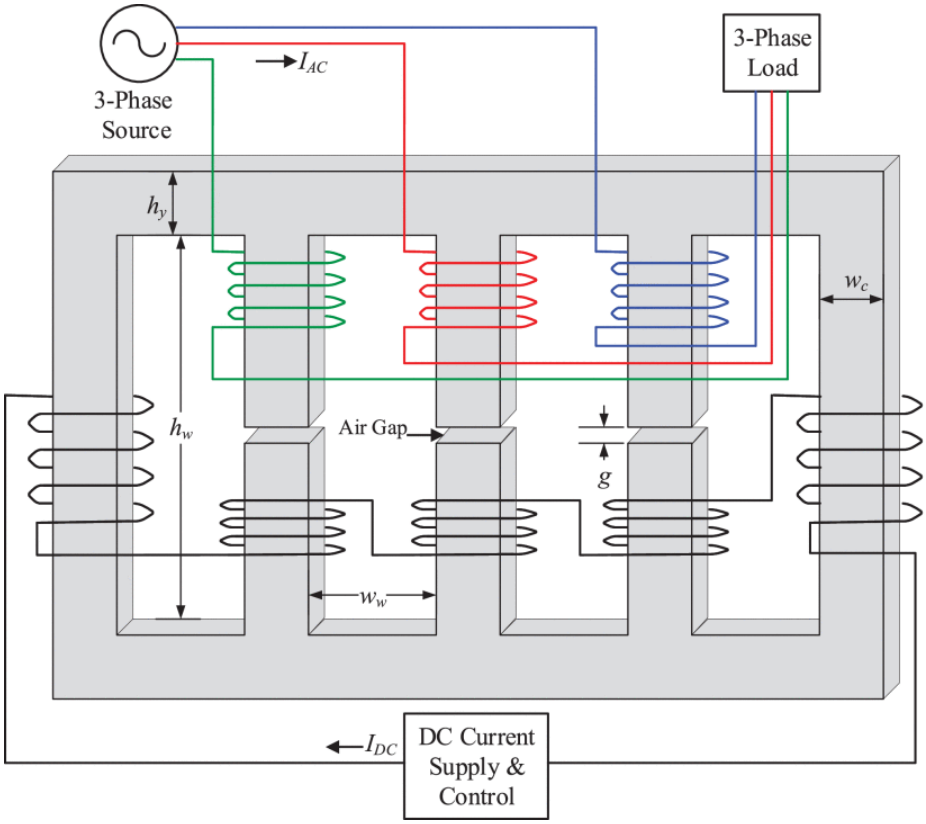


Figure 2.3: Three-Phase CVSR Prototype. (5)

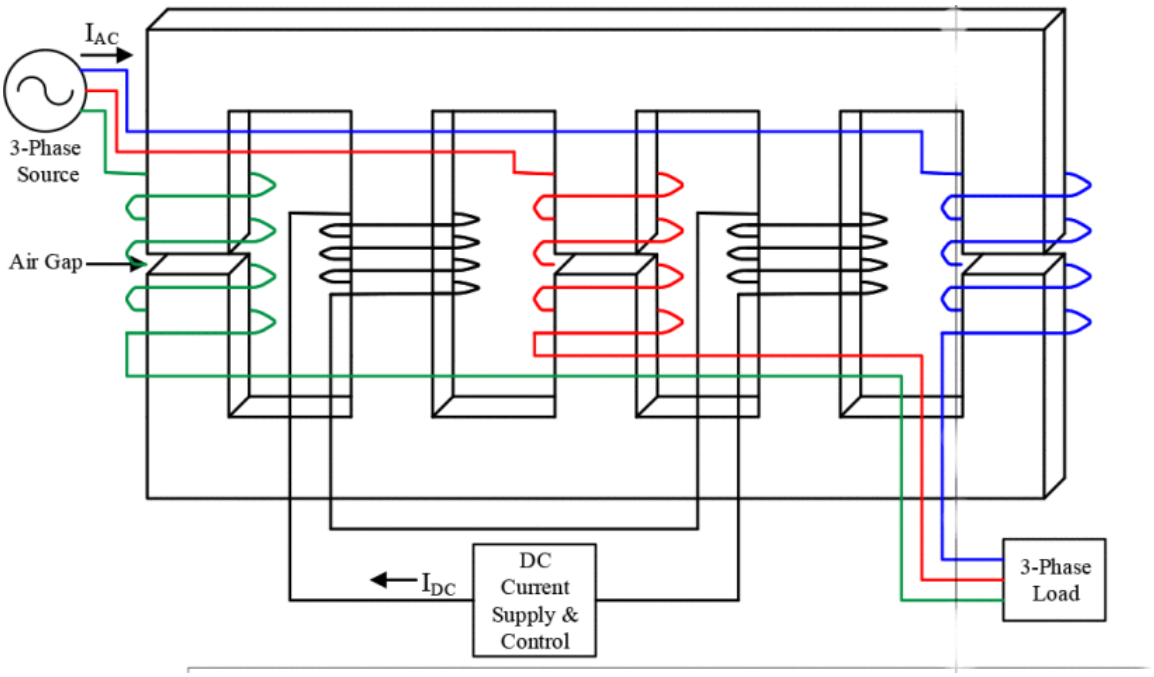


Figure 2.4: Second Version of Five-Legged Three-Phase CVSR Prototype.(6)

transmission system varies between zero and 1500 A, demonstrating the effectiveness of the design. By tuning the DC bias current flowing through the DC winding of the inductor, the apparent reactance of the AC winding of the inductor can be controlled. DC bias currents of zero magnitude will maximize the AC reactance. However, large DC bias currents will saturate the magnetic core, resulting in a significant decrease in AC reactance as shown in Figure 2.5.

2.3 Steady-State Model of CVSR Device

CVSRs are intended for use in normal operations of power systems, as well as for control of steady-state power flows. CVSR model has been presented in various systems. Transmission system is one of them. (22) ignored the resistance on the transmission lines. Therefore, the resistance is not included in the formulations. On the contrary, this work focuses on the CVSR application into the distribution system where the resistance of the lines and transformers are taken in to account. We assume no resistance at CVSR device. Moreover, any resistance loses are neglected and not affected to the line resistance. Figure 2.6 shows the procedure of a CVSR as a control device which is connected to the primary side of the transformer.

CVSRs cannot provide a negative reactance, unlike TCSCs. The CVSR can be installed on the transmission line where not overly compensated, i.e., $x_k \geq 0$.

2.3.1 Reformulations of Reactance and Power Flow Equations

Formulation of susceptance, B, and conductance, G, of the transformer will be updated with the variable reactance of the CVSR which is shown in following equations:

$$X'_{ij} = X_{ij} + X_{CV,k} \tag{2.2}$$

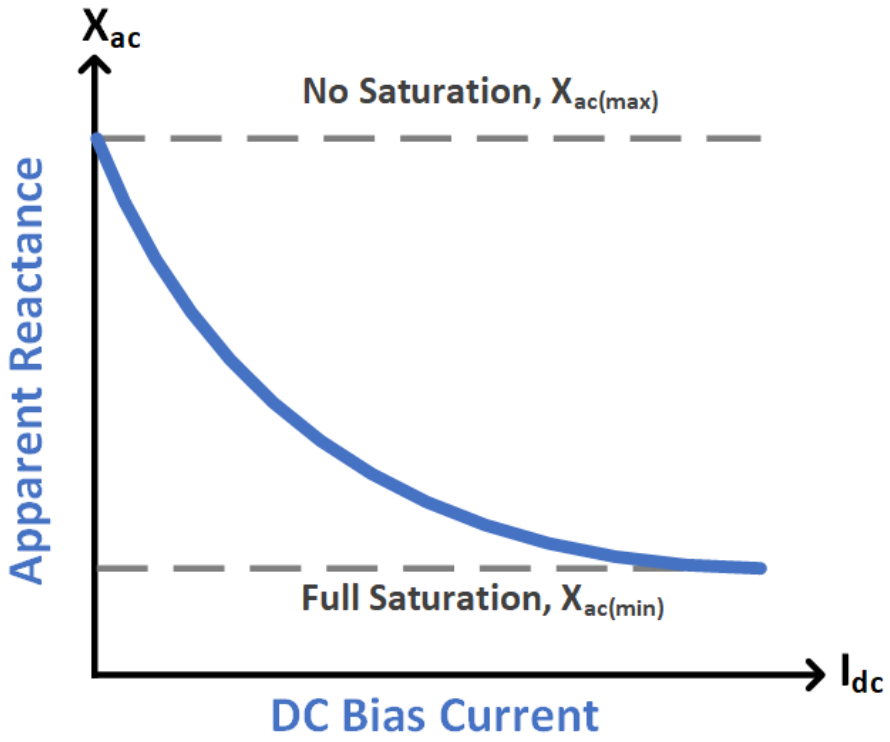


Figure 2.5: Relationship Between the Apparent Reactance and the DC Bias Current.

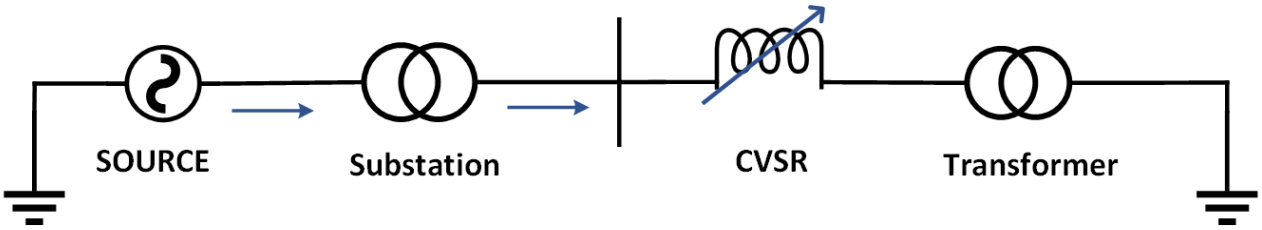


Figure 2.6: CVSR Device Connected to the Transformer.

$$B_{ij}^{'} = \frac{-X_{ij}^{'}}{X_{ij}^{2'} + R_{ij}^{2}} \tag{2.3}$$

$$G_{ij}^{'} = \frac{R_{ij}}{X_{ij}^{2'} + R_{ij}^{2}} \tag{2.4}$$

$$Y_{ij}^{'} = G_{ij}^{'} + B_{ij}^{'} \tag{2.5}$$

Thus, $X_{CV,k}$ will be added in the admittance,$Y^{'}$, matrix easily.

$$Y^{'} = \begin{bmatrix} Y_{ii}^{'} & -Y_{ij}^{'} \\ -Y_{ij}^{'} & Y_{jj}^{'} \end{bmatrix} \tag{2.6}$$

where

$$Y_{ij}^{'} = \begin{cases} Y_i + \sum Y_{ij}^{'}, & if \qquad i = j \\ -Y_{ij}^{'}, & if \qquad i \neq j \end{cases} \tag{2.7}$$

In normal situation, active and reactive power flow can be written as (84) :

$$P_{ij} = V_i V_j \left(\frac{R_{ij}}{R_{ij}^2 + X_{ij}^2} cos(\delta_{ij}) + \frac{X_{ij}}{R_{ij}^2 + X_{ij}^2} sin(\delta_{ij}) \right) \tag{2.8}$$

$$Q_{ij} = -V_i V_j \left(\frac{R_{ij}}{R_{ij}^2 + X_{ij}^2} sin(\delta_{ij}) - \frac{X_{ij}}{R_{ij}^2 + X_{ij}^2} cos(\delta_{ij}) \right) \tag{2.9}$$

With the CVSR device, (2.8) and (2.9) are converted to (2.10) and (2.11), respectively, by using the equation (2.2). CVSR is ready to control active and reactive power flow with this simple implementation of the CVSR reactance.

$$P_{ij}^{'} = V_i V_j \left(\frac{R_{ij}}{R_{ij}^2 + X_{ij}^{2'}} cos(\delta_{ij}) + \frac{X_{ij}^{'}}{R_{ij}^2 + X_{ij}^{2'}} sin(\delta_{ij}) \right) \tag{2.10}$$

$$Q_{ij}^{'} = -V_i V_j \left(\frac{R_{ij}}{R_{ij}^2 + X_{ij}^{2'}} sin(\delta_{ij}) - \frac{X_{ij}^{'}}{R_{ij}^2 + X_{ij}^{2'}} cos(\delta_{ij}) \right) \tag{2.11}$$

2.4 Sensitivity Analysis with the CVSR Device

Transformer sensitivity analysis is a model that determines how the power flow of the transformers are affected based on the changes with input variables. Reactance value of the CVSR device in ohms will be the input for the sensitivity analysis. Then, optimisation problem is involved and optimal reactance value can be determined. Thus, the analysis gives some outcomes in a way that can neglect the overloading on the transformers.

Transformer sensitivity analysis should be done for each transformer to create transformer sensitivity matrix. There are multiple steps to do. The first, initial power flow results must be obtained with the base system (overloaded system). Transformer sensitivity matrix is divided into combination of three sensitivity groups. These groups are the effect of active CVSR device on transformer A to transformer B, vice versa and transformers' itself. The first and the second groups of sensitivities build the off-diagonal values of transformer sensitivity matrix, and diagonal elements are built by the third sensitivity group. Figure 2.7 shows how the transformer sensitivity matrix looks like the sensitivity groups.

Finally, transformer sensitivity matrix must be obtained with the base system in a given range of reactance of the CVSR device. Meaning, transformer sensitivity matrix is calculated offline and used in the power flow optimization simulations as a constant matrix. For each network and load changes, transformer sensitivity matrix should be recalculated.

$$\frac{\partial P'_{ij}}{\partial X_{CV,k}} = V_i V_j \left(\frac{sin(\delta_{ij})}{(X_{ij} + X_{CV,k})^2 + R_{ij}^2} - \left(\frac{2sin(\delta_{ij})(X_{ij} + X_{CV,k})^2 - 2R_{ij}cos(\delta_{ij})(X_{ij} + X_{CV,k})}{((X_{ij} + X_{CV,k})^2 + R_{ij}^2)^2} \right) \right) \tag{2.12}$$

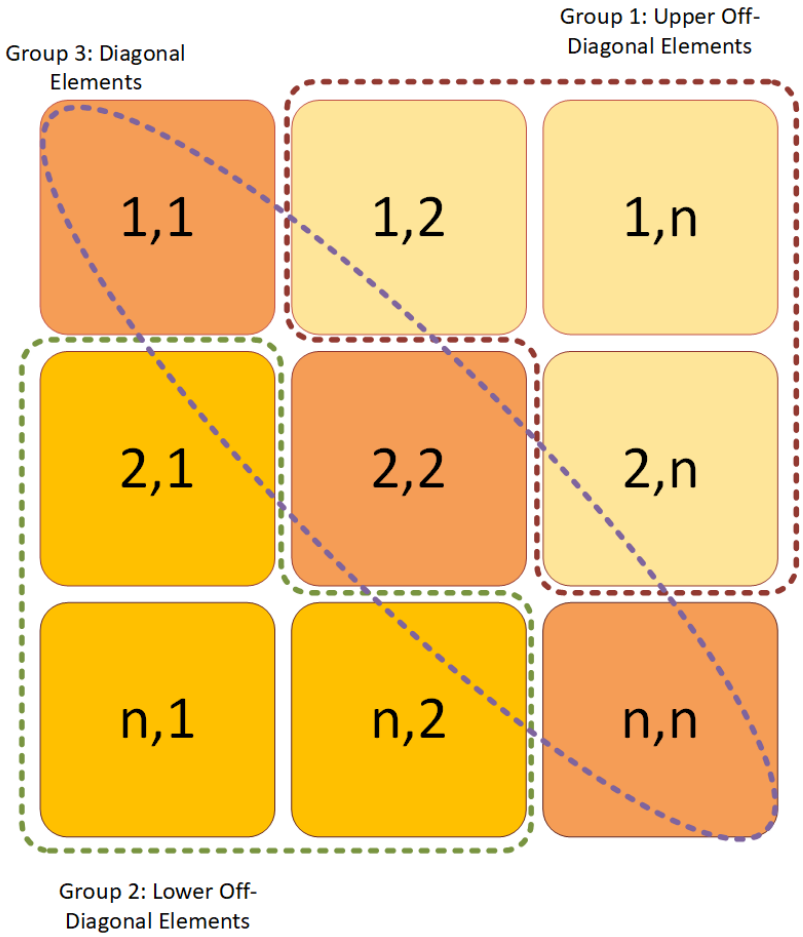


Figure 2.7: Transformer Sensitivity Matrix.

$$\frac{\partial Q'_{ij}}{\partial X_{CV,k}} = V_i V_j \left(\frac{cos(\delta_{ij})}{(X_{ij} + X_{CV,k})^2 + R_{ij}^2} - \right.$$

$$\left. \left(\frac{2cos(\delta_{ij})(X_{ij} + X_{CV,k})^2 - 2R_{ij}sin(\delta_{ij})(X_{ij} + X_{CV,k})}{((X_{ij} + X_{CV,k})^2 + R_{ij}^2)^2} \right) \right) \tag{2.13}$$

where $X_{CV,k} = 0 : 1 : X_{CV}^{max}$. X_{CV}^{max} is the maximum value of the reactance increment for each CVSR device which value should be determined before going through the sensitivity analysis.

Equation (2.12) and (2.13) represents the partial derivative of (2.10) and (2.11) with respect to reactance of the CVSR device, respectively. Thus, these equations will give the transformer sensitivity matrix, $T_{sm,k}$. Figure 2.8 shows the example of transformer sensitivities when the reactance is increasing in a certain limit of reactance increment. In the next chapter, transformer sensitivity matrix will be calculated as an offline calculation and used in the optimization modelling.

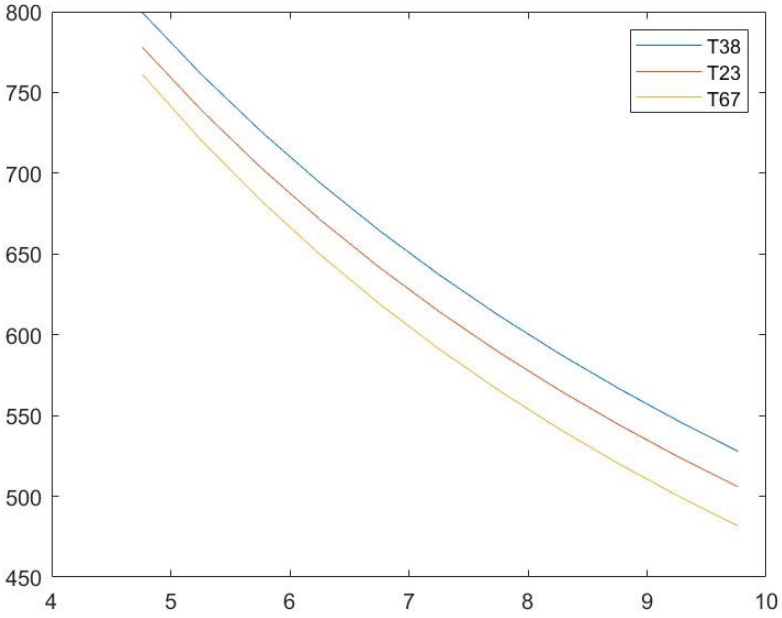


Figure 2.8: Sensitivity Analysis in Plots.

Chapter 3

Application of the CVSR Device for Power Flow Control

3.1 Introduction

The main application of the CVSR in this work is to use it for controlling power flow in distribution power systems that have a meshing connection and where the CVSR regulates the reactance of the transformer. In order to prevent overloading of transformers or relieving congestions in the distribution network, the CVSR device can be used to control the primary side of the transformer's reactance and, consequently, control the flow of electrical power through the transformer. As a result, the system can maintain normal operation without requiring any equipment upgrades. Generally, a variation of a few ohms is sufficient to relieve overloading. The CVSR can be used to control the device's reactance up to 3.4 Ω according to (6). However, we will assume that the CVSR can increase the reactance 3 Ω at maximum. The CVSR size and requirements can be determined based on transformer capacity and loading conditions. In comparison to similar devices from FACTS, the CVSR is significantly more economical. Due to the lower cost of CVSRs compared to equivalent FACTS devices (such as TCSCs and UPFCs), multiple CVSRs may be incorporated into a

power transmission or distribution system to enhance its flexibility in terms of its capacity. Thus, the CVSR will be implemented to control power flow in the variety of distribution systems in chapter 3. In this part of the work, small distribution system with two-parallel transformer with CVSR devices will be introduced.

3.1.1 Two-Parallel Transformers

With two parallel feeders and two transformers, a simple distribution circuit is established. The secondary side of the transformers is connected to parallel and series loads respectively. These secondary transformers each have a rating of **1000 kVA** where the total loading is 1540 kVA. Thus, the total load aimed to be less than or equal to the amount of total power supplied by transformers. Figure 3.1 depicts a model and representation of this distribution system with CVSR devices connected to the primary side of the transformers.

For this system, Y-primitive and Y matrices are validated by hand comparing to OpenDSS results. For the Y-primitive matrix of transformer can calculated as follows:

$$Z_{sc} = \frac{r + jx}{100} \tag{3.1}$$

where Z_{sc} is short circuit impedance, r is load-loss or resistance in percentage, x is leakage reactance in percentage.

$$Z_{sc}(1V) = \frac{r + jx}{100} \frac{1}{S_T} \tag{3.2}$$

where S_T is kVA base.

$$\overline{Y_1}(1V) = B\overline{Y_{sc}}B^T \tag{3.3}$$

where $\overline{Y_1}(1V))$ is nodal admittance matrix on one turn which is commonly used in positive sequence models. B is incidence matrix.

$$\overline{Y_W} = N\overline{Y_1}N^T = NB\overline{Y_{sc}}B^T N^T \tag{3.4}$$

where $\overline{Y_W}$ is winding admittance matrix. N is a turn ratio matrix.

$$\overline{Y_{Prim}} = A\overline{Y_W}A^T = ANB\overline{Y_{sc}}B^T N^T A^T \tag{3.5}$$

where $\overline{Y_{Prim}}$ is primitive matrix of that transformer. A is incidence matrix.

We used a CVSR device that is connected to the primary side of Transformer-1 in this small distribution system which is illustrated in Figure 3.1. Artificial overloading is made by doubling the Load 2 where its nominal was 400 kVA. Power flow on the Transformer-1 and Transformer-2 are simulated in Figure 3.2. As we can see Transformer-1 is overloaded about 30 kVA when the base Ohm value is 4.76 Ω in Figure 3.2a. Then, the benefit of the CVSR device is used to increase reactance for relieving extra loading at the Transformer-1. 1 Ω increment is enough for Transformer-1 back to below its maximum limit. However, this extra loading is shifted to the Transformer-2 which can be seen in Figure 3.2b. Transformer-2 remains in the limits with the value of 975.5 kVA when 1 Ω increment on the Transformer-1 by a CVSR device exists. As a result, Figure 3.2 shows the effectiveness of the CVSR on relieving the overloading in this small distribution system.

3.2 Optimization Model

Optimization model consists the online and offline calculations. Online calculations are made through the MATLAB (167). On the other hand, the OpenDSS (168) software is used for the offline calculations in the optimization. Specifically, bus voltages, bus angles, active and reactive power flows at all buses are imported from the OpenDSS.

The optimization model works with given parameters and outputs from the OpenDSS. With given distribution parameters, the first, the base system is run through the OpenDSS with obtaining the outputs as active and reactive power flows. Then, transformer sensitivity matrix will be built with power flow results from the

OpenDSS. Finally, optimization can be run. Thus, simulation results will be obtained by using objective function and constraints. Figure 3.3 illustrates data flow of offline calculations from the OpenDSS to the MATLAB to simulate optimization.

Main purpose of this research is to maintain the power flows on the transformers in some range while minimizing the reactance increment (in ohms) of the CVSR devices. Thus, the objective function is to minimize the summation of reactance increments on the CVSR devices.

$$\min_{\mathbf{A}} \sum_{k=1}^{\mathrm{K}} X_{CV,k}$$

$$\mathbf{A} \in \{X_{CV,k}, P_k, Q_k, S_k\} \tag{3.6}$$

where $\mathbf{A}$ is the set of continuous variables,

System constraints ensure that the loading on the transformers are in control and not exceeding the limits.

$$S_k = T_{sm,k} \times X_{CV,k} + S_{in,k} \tag{3.7}$$

$$S^{min} \leq S^k \leq S^{max} \tag{3.8}$$

$$X_{CV}^{min} \leq X_{CV,k} \leq X_{CV}^{max} \tag{3.9}$$

In the constraint 3.7, apparent power flow is recalculated by using the transformer sensitivity matrix, $T_{sm,k}$, and initial apparent power flow of each transformer, $S_{in,k}$ at operating point. At the initial point, reactance supplement was zero by the CVSR devices. Constraint 3.8 and 3.9 represent the minimum and maximum power flow limits at each transformer, and minimum and maximum limits of reactance increment supplied by each CVSR device, respectively.

3.2.1 Linear Formulation

Nonlinear relationship is fairly complicated in the power flow formulation. However, it is relatively linear in practice. It can be clarified with the simple inequality:

$$X_{ij} < X_{CV} \tag{3.10}$$

This inequality does not change. Thus, sensitivities does not alter relatively and it gives the linear results after adding the X_{CV} in to the problem formulation. Consequently, if the transformer sensitivity slopes are close to the linear behavior, linearized formulation can be applied in this situation to neglect nonlinearity in the optimization problem. Thus, the optimization problem can be modeled as linear and solved with linear solvers. Figure 3.4 illustrates the approach that nonlinearity simply converted to the linearity for the transformer sensitivity. Average value of base and end points of the transformers' power flow is considered for the every transformer sensitivity calculations. Accordingly, transformer sensitivity matrix will be recalculated in a linear form as:

$$T_{sm,k}^{lin} = \frac{S_{f,k} - S_{in,k}}{X_{CV}^{max} - X_{CV}^{min}} \tag{3.11}$$

Consequently, equation 3.7 will be updated to equation 3.11 with new linearized sensitivity matrix, $T_{sm,k}^{lin}$, in equation 3.10 when the linearized approach is used. Thus, equation 3.11 shows the new calculation of linearized transformer sensitivity matrix. Usually $T_{sens,k}^{lin}$ is negative value since the power flow decreases while increasing the reactance on the CVSR devices.

3.2.2 Piecewise Linear Formulation

A piecewise approximation can be very important for some data. The piecewise approximation is one method of creating a function by adding binary variables and reformulating the constraints that allows the nonlinear problem to be solved by linear

solvers (169). In this paper, we use piecewise approximation to divide nonlinear function into the linear segments, which is illustrated in Figure 3.5. Since the nonlinear function is converted to the piecewise linear segments, objective function and constraints will be update as follows:

$$\min_{\mathbf{A}} \sum_{k=1}^{\mathrm{K}} \sum_{s=1}^{S_n} X_{CV,k,s}$$

$$\mathbf{A} \in \{X_{CV,k,s}, P_{k,s}, Q_{k,s}, S_{k,s}, I_{k,s}\} \tag{3.12}$$

subject to:

$$T^{pw}_{sm,k,s} = \frac{S_{k,s+1} - S_{k,s}}{X^{max}_{CV} - X^{min}_{CV}}; \qquad s = 1, ..., \mathrm{S_n} \tag{3.13}$$

$$\sum_{s=1}^{\mathrm{S_n}} I_{k,s} = 1 \tag{3.14}$$

$$S_{k,s} = \begin{cases} S_{k,1} = S^{max}_{k,0} + T^{pw}_{sm,k,1} \times X_{CV,k,1} + S_{in,k} \\ if I_{k,1} = 1 \quad \therefore \forall I_{k,s} = 0 \\ S_{k,2} = S^{max}_{k,1} + T^{pw}_{sm,k,2} \times X_{CV,k,2} \\ if I_{k,2} = 1 \quad \therefore \forall I_{k,s} = 0 \\ \vdots \\ S_{k,s} = S^{max}_{k,s-1} + T^{pw}_{sm,k,s} \times X_{CV,k,s} \\ if I_{k,s} = 1 \quad \therefore \forall I_{k,s} = 0 \end{cases} \tag{3.15}$$

$$S^{min} \leq \sum_{s=1}^{\mathrm{S_n}} S_{k,s} \leq S^{max} \tag{3.16}$$

$$X^{min}_{CV} \leq \sum_{s=1}^{\mathrm{S_n}} X_{CV,k,s} \leq X^{max}_{CV} \tag{3.17}$$

where each segment is denoted by s. Constraint 3.13 is formulated to create transformer sensitivity matrix for each segment where the value of $T^{pw}_{sm,k,s}$ is usually

negative. Binary variables of the constraint 3.15 are equal to the one in constraint 3.14. Meaning, only one condition can be active constraint in 3.15 for the optimization problem. Constraint 3.15 is more complex comparing to the constraint 3.7 since 3.15 is reformulated using piecewise approximation. $S_{k,0}^{max}$ is assumed as zero. Constraints 3.15-3.17 are updated version of 3.7-3.9, respectively.

3.3 Case Studies

3.3.1 System Description and Simulation Setup

The proposed model is applied to two different systems: the IEEE 342-LVTNS (3) and ConEd system. They have different numbers and sizes of transformers and loads. Therefore, the CVSR device concept is applied to these two systems with different aspects.

For the simulation purposes, OpenDSS is generally used for offline calculations. The first, initial power flow value, $S_{in,k}$, is calculated by OpenDSS where $X_{CV,k} = 0$. If $S_{initial,k}$ is higher than S^{max}, optimal reactance increment must be calculated in MATLAB. Following that, MATLAB's YALMIP toolbox (170) is employed to create a mathematical model, and CPLEX (171) is used to solve the optimization problem. In the subsequent two subsections, the simulation results for the respective distribution systems are presented, showcasing the outcomes obtained from the optimization process.

3.3.2 IEEE 342-LVTNS

Since we desire to test the capability of the CVSR devices to control power flow on transformers in heavily meshed and networked distribution system with numerous parallel transformers, we picked the IEEE 342-Node Low Voltage Networked Test System (LVNTS).

The IEEE 342-Node LVNTS has two delta-delta step down transformers, 47 grid network transformers rating at 1 MVA and 20 spot network transformers rating at 1.5-2.5 MVA. We focus on the grid network where the base voltage is 13.8 kV/208 V (primary/secondary side of grid network transformers). Thus, initial reactance is calculated as 9.52 Ω with given 0.05 pu value in the OpenDSS system data. On the other hand, minimum and maximum reactance increment of the CVSR devices, $X_{CV,k}$, are calculated for 0.06 and 3.15 Ω, respectively (6). Although, in this work, they are assumed to be exact numbers of 0 and 3 Ω for minimum and maximum limits, respectively.

3.3.2.1 Linear Optimization

The first, overloading scenario with one CVSR device is applied to the IEEE system. Loading at Bus S22 is multiplied by 8 and becomes 1160 kVA, normally was 145 kVA. After running the simulation with increased loading, the loading at the Transformer-23 (T-23) is increased to 1132 kVA while other nearby transformers are not overloaded, over 1 MVA in this case. At least 132 kVA loading must be relieved from the T-23. Therefore, a CVSR device is placed at the T-23 to relieve congestion. According to the OpenDSS results, 1.5 Ω increment is good enough relieving some loadings at T-23 to become 977.4 kVA while other close transformers' power flow are increased but still in the limits. Table 3.1 shows that one CVSR device can handle the overloading in this case. Then, simple linear optimization is applied to this problem for more accuracy using the transformer sensitivity matrix since 1.5 Ω increment decreases the T-23 power flow to 977.4 kVA. There might be an optimal ohm increment which can decrease the power flow just below or equal to the maximum limit. Thus, the linear optimization improved the results comparing to the non-optimization one. Table 3.2 indicates that 1.33 Ω increment is enough to relieve overloads at T-23 to become 1 MVA in optimization result from the MATLAB. Meanwhile, 1.33 Ω makes the power flow at T-23 is 992.31 kVA. Accordingly, relative error in percent is calculated and it

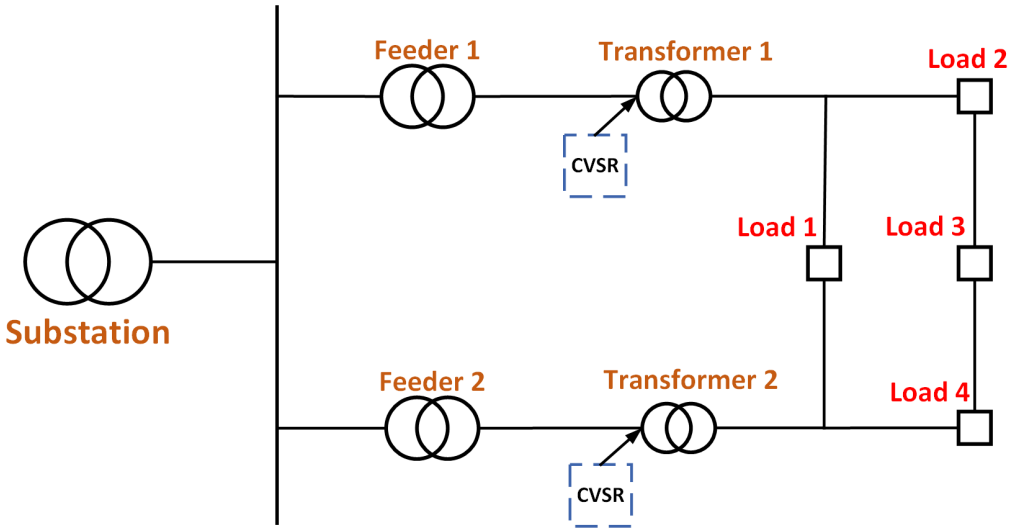
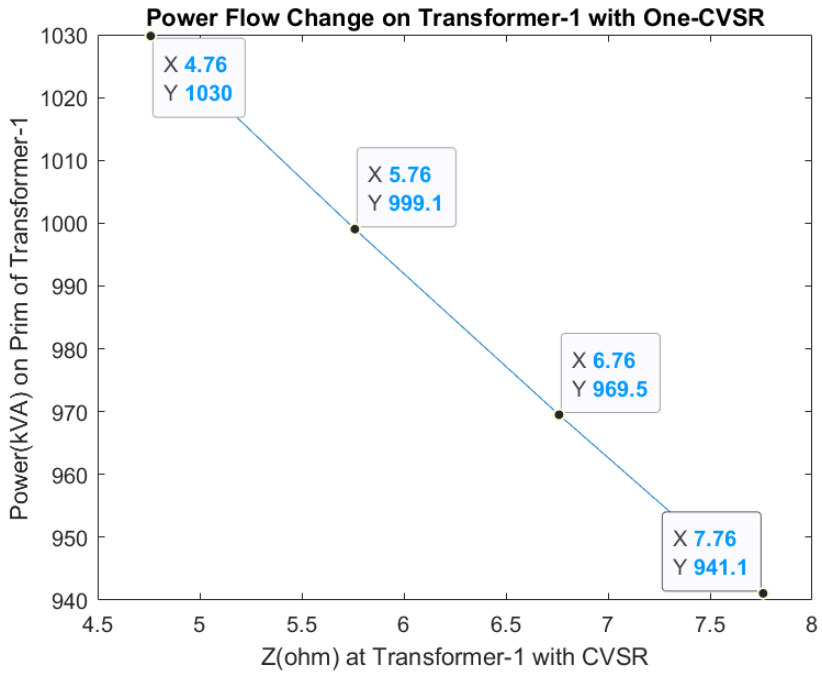


Figure 3.1: Simple Diagram of Two Feeders Distribution System with CVSR devices

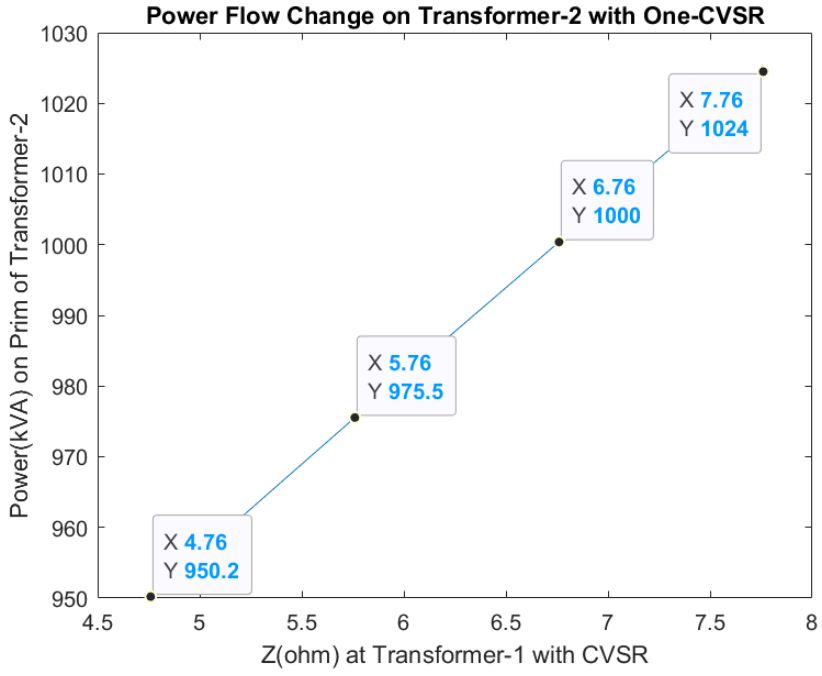
Table 3.1: Power Flow Results of T-23 T-24 and T-32 with only One CVSR device

Loads	Transformers					
S22	T-23		T-24		T-31	
Coefficient=8	*kVA*	*ohm*	*kVA*	*ohm*	*kVA*	*ohm*
	1132	4.76	945.3	4.76	728.3	4.76
	1076	5.26	960.6	4.76	740.2	4.76
	1024	5.76	974.3	4.76	750.9	4.76
	977.4	6.26	986.9	4.76	760.7	4.76
	934.2	6.76	998	4.76	769.5	4.76

[a] Only T-23 has CVSR device.



(a) Transformer-1



(b) Transformer-2

Figure 3.2: Power Flow of Transformers when the CVSR is Only Implemented to the Transformer-1

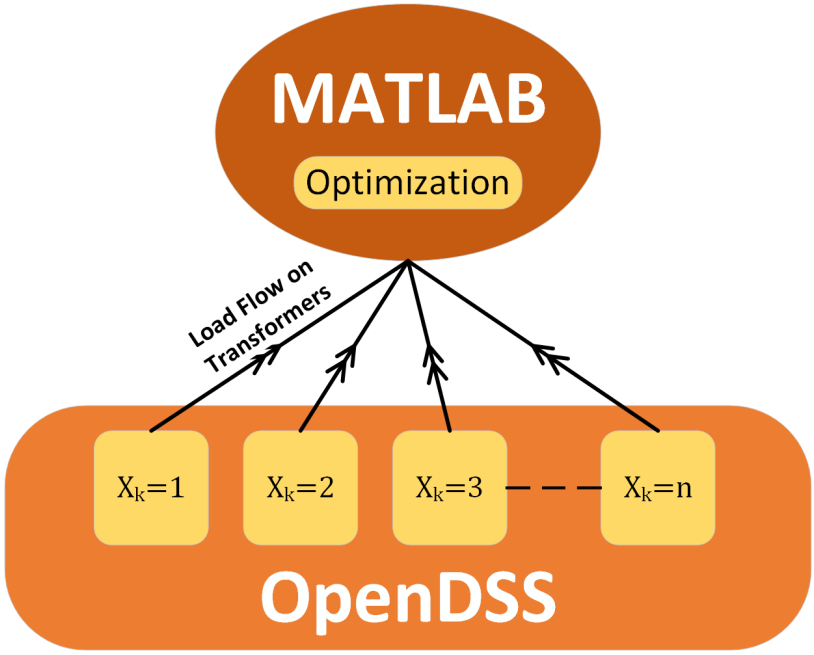


Figure 3.3: Interaction Between MATLAB and OpenDSS.

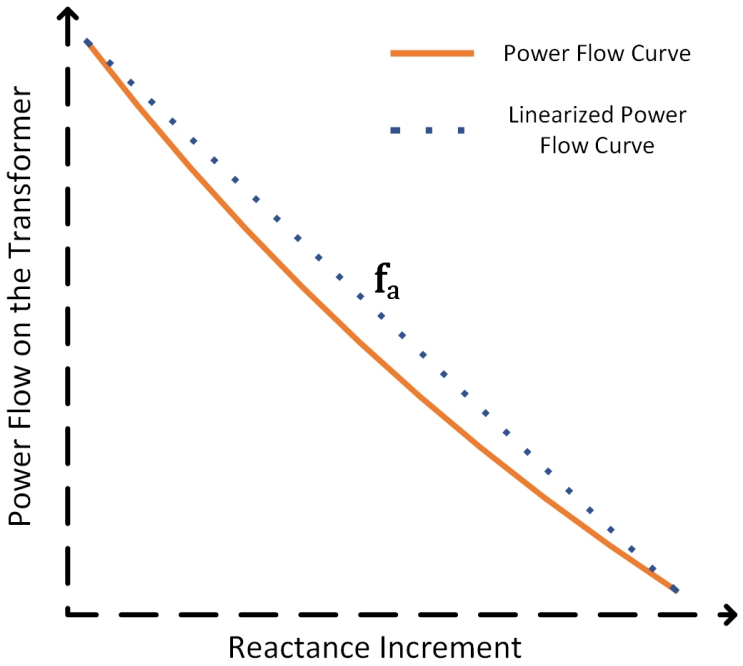


Figure 3.4: Linear Illustration of Power Flow on a Transformer with Reactance Increments.

shows us the accuracy of the optimization is close to the benchmark results by the OpenDSS.

3.3.2.2 Piecewise Linear Optimization

Even the simple linear formulation improves the results, more improvements can be done using the piecewise formulation. Thus, piecewise optimization is implemented in the IEEE 342-LVTNS by usig the Eqs. 3.12 - 3.17. Like in the Figure 3.5, power flow curves of transformers are divided into 2, 4 and 5 equal segments. Meaning, 1.5 Ω range for 2-Segment, 0.75 Ω range for 4-Segment, and 0.6 Ω range for 5-Segment are used in the simulations. Differently from linear optimization, two CVSR devices are practiced at T-23 and T-24 transformers. Additionally, we evaluate three different upper-limit of power flows of transformers with or without the CVSR devices. They are 1000 kVA, 950 kVA and 900 kVA. Normally, 1000 kVA is the rating of secondary network transformers in the IEEE 342-LVTNS but we include the two more limits to observe if the 3 Ω can be enough to reduce power flow below that limits.

Results of piecewise optimization show the improvement of optimality of reactance increment in Table 3.3 and Table 3.4. For limiting the power flow on 1000 kVA, only 1.297 Ω increment is enough for 2-Segment piecewise optimization. 4-Segment and 5-Segment numbers improved the results more with 1.283 Ω and 1.275 Ω increment, respectively. Overall, all cases give encouraging results which are close to the benchmark (OpenDSS) results. Since 4-Segment or 5-Segment optimization results are promising, they can be used for simulation purposes for the project. However, 5-Segment optimization suffers from computational burden since the transformer sensitivity matrix data increases exponentially. For example, 2-Segment with 3 transformers in the system has $2^2 * 3^2 = 36$ matrix data, while 5-Segment with 3 transformers in the system has $5^2 * 3^2 = 225$.

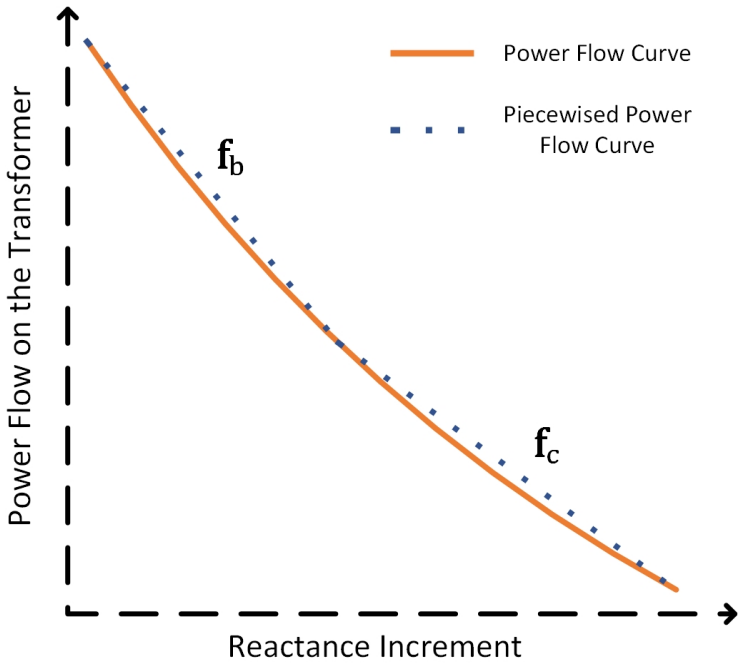


Figure 3.5: Piecewise Linear Illustration of Power Flow on a Transformer with Reactance Increments.

Table 3.2: Linear Optimization Result Comparison with the Benchmark Results

Loads	**Transformers**					
S22	**T-23**		**T-24**		**T-31**	
Coefficient=8	***kVA***	***ohm***	***kVA***	***ohm***	***kVA***	***ohm***
Optimization Result from Matlab(Linprog)	**1000**	**6.09**	**980.5**	**4.76**	**755.8**	**4.76**
OpenDSS (Benchmark)	**992.3**	**6.09**	**982.8**	**4.76**	**757.55**	**4.76**
Relative Error in Percentage	**0.774%**	–	**0.238%**	–	**0.236%**	–

[a] Only T-23 has CVSR device.

Table 3.3: Piecewise Optimization: 2,4 and 5-Segment Comparison when Transformers are limited to 1000 kVA

Base Reactance and Active Powers Before Optimization					
X_{hl} − 23 **(Ohm)**	X_{hl} − 24 **(Ohm)**	P_{23} **by OpenDSS**	P_{23} **by Optimization**	P_{24} **by OpenDSS**	P_{24} **by Optimization**
4.76	4.76	1133.96 kVA	1133.96 kVA	944.72 kVA	944.72 kVA
2-Segment Piecewise Optimization Results					
4.76 + 1.3	4.76 + 0	997.80 kVA	1000 kVA	981.44 kVA	980.70 kVA
4-Segment Piecewise Optimization Results					
4.76 + 1.28	4.76 + 0	999.11 kVA	1000 kVA	981.11 kVA	980.70 kVA
5-Segment Piecewise Optimization Results					
4.76 + 1.27	4.76 + 0	999.85 kVA	1000 kVA	980.91 kVA	980.74 kVA

[a] Only T-23 has CVSR device.

Table 3.4: Piecewise Optimization: 2,4 and 5-Segment Comparison when Transformers are limited to 950 kVA

Base Reactance and Active Powers Before Optimization					
$X_{hl} - 23$ **(Ohm)**	$X_{hl} - 24$ **(Ohm)**	P_{23} **by OpenDSS**	P_{23} **by Optimization**	P_{24} **by OpenDSS**	P_{24} **by Optimization**
4.76	4.76	1133.96 kVA	1133.96 kVA	944.72 kVA	944.72 kVA
2-Segment Piecewise Optimization Results					
4.76 + 2.03	4.76 + 0.56	945.66 kVA	950 kVA	944.59 kVA	950 kVA
4-Segment Piecewise Optimization Results					
4.76 + 1.99	4.76 + 0.53	947.48 kVA	950 kVA	947.07 kVA	950 kVA
5-Segment Piecewise Optimization Results					
4.76 + 1.99	4.76 + 0.52	947.59 kVA	950 kVA	947.65 kVA	950 kVA

[a] Only T-23 has CVSR device.

3.3.3 ConEd System

Similar to the IEEE 342-Node LVTNS, overloading simulations are conducted for mini-meshed grids in the Con-Ed system. 6 transformers and 1 loading are focused for overloading purposes as can be seen in Figure 1.16. Three transformers (T-191, T-238 and T-74) are much closer comparing to the others (T-189, T-240 and T-79). Similar to the IEEE 342-Node LVTNS, minimum and maximum limits of the CVSR reactance increment are assumed to be exact numbers of 0 and 3 Ω, respectively.

3.3.3.1 Linear Optimization

At the first, Load.90 is multiplied by 1.80, just randomly. The results are observed through the 6 graphs in the Figure 3.6. Farther transformers are not affected much comparing to the closest transformers. Since all three closest transformers are overloaded after the load increment. There is not a small amount of range to increase reactance on these transformers. We can see power flows if T-191 has CVSR device and total 3 Ω reactance increment. At some point, overloading on T-191 is relieved but T-74 and T-238 are more overloaded. Eventually, the error is observed with the 1.80 multiplication because new loading at Load.90 (3317 kVA) is too much and higher than the capacity of closest three transformers (3000 kVA). Thus, 1.80 multiplication showed us there are no other transformers taking the remaining loading of 317 kVA.

After 1.8x loading, 1.62x loading is applied to the Load.90 where the total loading becomes 2986 kVA. Comparing to the 1.8x loading, 1.62x loading is enough for three closest transformers to handle the overloading with one CVSR device. So, it is sufficient to have CVSR device only on T-191 with reactance increment of 0.2 to 1.0 Ω which is shown in Figure 3.7.

Simple linear optimization is studied for the result validation with OpenDSS power flow results in Table 3.5. We aim to balance the closest three transformers in the mini-meshed grid. 960 kVA is the amount we set for all transformer to be while other close

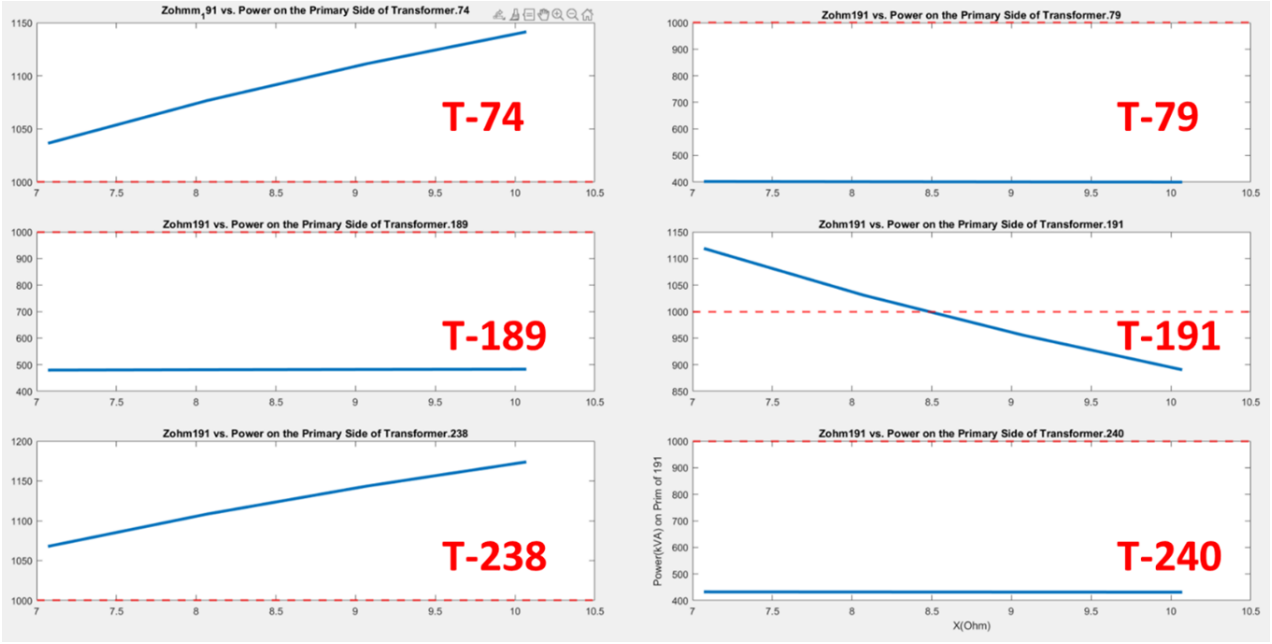


Figure 3.6: Power Flow of Transformers at Load.90 Multiplied by 1.80.

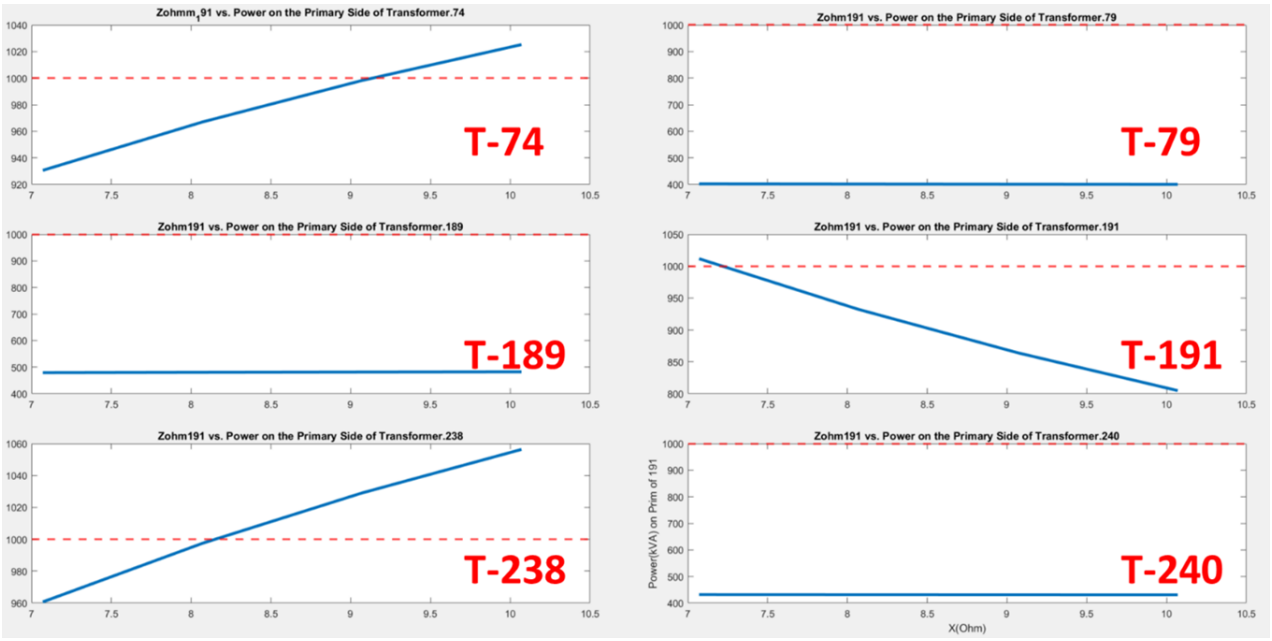


Figure 3.7: Power Flow of Transformers at Load.90 Multiplied by 1.62.

transformers below the 1 MVA while the load coefficient is 1.62 in this simulation result. Optimization results are very close to the benchmark result.

3.3.3.2 Piecewise Linear Optimization

Next, we want to see if we can balance the total loading of overloaded three transformers with 2-segment piecewise optimization. Table 3.6 shows the results of 2-segment ann 4-segment piecewise optimization by MATLAB and OpenDSS. Comparison between 2-Segment and 4-Segment piecewise optimization is performed. Total load on the three transformers after overloading is 2903 kVA while the MATLAB-Optimization is 2894 kVA and OpenDSS results 2896 kVA.

Table 3.6 shows that 4-Segment piecewise optimization improved the accuracy with less reactance increments. MATLAB findings are very close to the OpenDSS calculations.

Table 3.5: Simple Linear Optimization Result Validation when Transformers are limited to 960 kVA.

Transformer	Initial Loading (kVA)	1.62x Load Increment (kVA)	CVSR Reactance (Ohm)	OpenDSS (Benchmark) (kVA)
T.191	648.3	1011.7	1.73	950.9
T.174	572	930.58	0.89	967.1
T.238	597.9	950.7	1.22	959.7
T.79	404.4	402.1	-	401.3
T.189	478.5	479.4	-	480.3
T.240	430.5	431.9	-	431.9

Table 3.6: Piecewise Optimization Result Validation.

2-Segment Piecewise Optimization Results					
Transformer	**Initial Loading (kVA)**	**1.62x Load (kVA)**	**CVSR Reactance (Ohm)**	**MATLAB (kVA)**	**OpenDSS (Benchmark) (kVA)**
T.191	648.3	1011.7	0.73 Ohm	966	962.7
T.74	572	930.58	0 Ohm	964	969.3
T.238	597.9	960.7	0.29 Ohm	964	964.4
4-Segment Piecewise Optimization Results					
Transformer	**Initial Loading (kVA)**	**1.62x Load (kVA)**	**CVSR Reactance (Ohm)**	**MATLAB (kVA)**	**OpenDSS (Benchmark) (kVA)**
T.191	648.3	1011.7	0.69 Ohm	966	964.6
T.74	572	930.58	0 Ohm	964	966.9
T.238	597.9	960.7	0.27 Ohm	965	965.2

Chapter 4

Optimal Location of CVSR devices

4.1 Introduction

Previously in Chapter 3, CVSR proved its capability for controlling power flow in various distribution systems including radial and meshed grids. To avoid transformer overloading and alleviate congestion within the distribution network, the implementation of the CVSR device offers a viable solution. By exerting control over the reactance of the transformer's primary side, the CVSR device effectively regulates the flow of electrical power through the transformer. This mechanism enables the system to sustain normal operation without necessitating any equipment upgrades. Typically, a slight variation of a few ohms proves adequate in mitigating overloading situations. As in the Chapter 3, we will again assume that a CVSR device only increase the reactance by 3 Ω at its peak capacity.

In this chapter, we will focus on the optimal location of CVSR devices while keeping the power flow on the transformers are below their maximum limits. While the cost of CVSRs is considerably lower than that of comparable alternatives, it is crucial to minimize the overall expenditure associated with CVSR devices in large distribution systems. This is particularly important, considering the load levels and risk factors inherent in such systems.

This section of the study involves employing the IEEE 342-Node Low Voltage Networked Test System (LVTNS), integrated with CVSR devices, to address the optimal device placement problems under different scenarios. In the next sections, the optimal location of CVSR devices in a distribution system will be determined through various approaches.

4.2 Optimization Model

Same as the chapter titled "Application of the CVSR Device for Power Flow Control", the optimization model involves both real-time and pre-computed computations in this chapter too. Real-time or online calculations are done in the MATLAB, while the OpenDSS software handles the pre-computed or offline calculations for the optimization. The OpenDSS is utilized to import bus voltages, bus angles, as well as active and reactive power flows at all buses for each loop while we change the reactance value of primary side of secondary network transformers in the distribution system.

The optimization model operates based on provided parameters and inputs derived from the OpenDSS. Given the distribution parameters, the initial step involves running the base system through the OpenDSS to acquire outputs in the form of active and reactive power flows. For the online calculations or main optimization problem, there area some approaches like analytical, heuristic and meta-heuristic, and artificial intelligence (AI) methods. Since the IEEE 342-LVTNS is not that large system for heuristic, meta-heuristic and AI methods to involve, we will focus on the analytical approaches with more consistent and precise solutions. However, heuristic and AI techniques can be used for faster results while these techniques do not guarantee the optimal solution.

Depending on the approaches for optimal location of CVSR devices, the sensitivity matrix of the transformers will be constructed using the power flow outcomes obtained from the OpenDSS. Subsequently, main optimization problem can be executed, and

the simulation outcomes will be attained by applying the objective function and constraints. While many papers focus on to minimize real or reactive power loss, minimizing the reactance while keeping number of CVSR devices minimum is the main objective in this dissertation.

In the subsequent subsections, we will introduce four different algorithms to tackle the optimal placement problem of CVSR devices in the power system. These algorithms include the shortest path algorithm, loading-based algorithm, transformer sensitivity-based algorithm, and piecewise optimization-based algorithm. Figure 4.1 provides a visual representation of the flow chart for these optimization methods, illustrating the sequential steps involved in each algorithm. By employing these different approaches, we can explore various strategies and find the most effective and efficient solutions for the optimal placement of CVSR devices in the power system.

4.2.1 Shortest Path Algorithm

One of the common shortest path algorithm is Dijkstra's algorithm which is a graph-based algorithm that efficiently finds the shortest path between one node and another node and vice versa in a weighted graph. By utilizing the shortest path algorithm, we can identify the CVSR locations that are in closest proximity to all loads within a graph. The flowchart in Figure 4.2 illustrates how Dijkstra's shortest path algorithm works step by step. This algorithm will be adapted to solve the optimal placement problem of CVSR devices in the power system. This approach enables us to determine optimal CVSR positions without requiring specific information about the loading levels. Hence, the optimal location results obtained through the shortest path algorithm remain unaffected by any load increments. As a result, the shortest path algorithm will only exist in 4.3.2 Case 1: Base Load in the following sections.

However, this method is lack of any information from loading levels. Only the location and line distances of transformers and loading busses will be used in this approach. When compared to other techniques employed in this study, the shortest

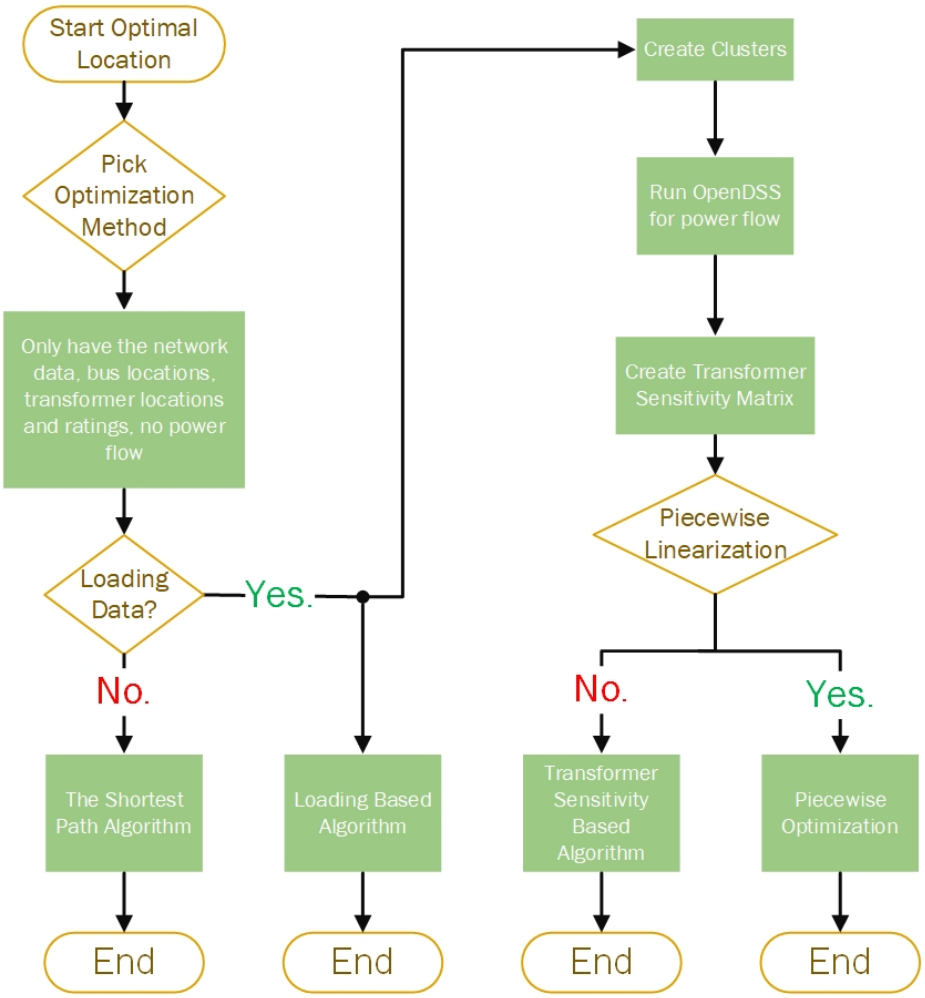


Figure 4.1: Flowchart of Optimization Methods for CVSR Optimal Location Problem

path algorithm yields faster results, although it may exhibit comparatively lower accuracy.

4.2.2 Loading Based Algorithm

Another algorithm that we will use for the optimal location problem is the loading based technique. We propose the loading based method which is a simple technique for determining the optimal location of CVSR devices in power systems. On the contrary of shortest path algorithm, this method focuses on assessing the loading conditions of the system components, namely, loadings and transformers, to identify areas that require device placement for system stability and relieve possible congestions.

A key aspect of the loading-based method is the determination of loading indices that quantify the stress levels on different components of the power system. Therefore, we use graph theory to determine the loading penetration levels on the transformers. Load penetration refers to the extent to which electrical loads are distributed or dispersed among transformers in a power distribution system. It is influenced by two factors: load distances to transformers and load amounts in kVA. The load distance to transformers refers to the proximity of electrical loads to the available transformers in the distribution system. Loads that are located closer to a specific transformer are more likely to be connected to that transformer. Conversely, loads that are located farther away from a transformer may be connected to different transformers in the system. Load amounts in kVA also impact load penetration. The total load connected to a transformer is determined by the cumulative kVA rating of the loads connected to it. These indices provide a measure of the loading conditions and can be used as indicators to identify areas where the system is operating close to its limits or experiencing significant congestion. Flowchart of loading based algorithm provides steps to achieve optimal location of CVSR devices in figure 4.3.

The loading based method aims the optimal locations of CVSR devices where the most transformers were affected by the loadings. Meaning, if there are more

```
1: for each vertex v in Graph                          ▷ Initialization
2:    dist[v] := infinity                              ▷ Initial source to v is infinite
3:    previous[v] := undefined                         ▷ Previous Bus in optimal path from source
4: dist[source] := 0                                   ▷ Distance from source to source
5: Q := All Buses in Graph                             ▷ All Buses in the graph are unoptimized
6: while Q is not empty                                ▷ Main Loop
7:    u := bus in Q with smallest dist[]
8:    remove u from Q
9:    for each neighbor v of u                         ▷ where v has not yet been removed from Q.
10:      alt := dist[u] + dist_between(u,v)
11:      if alt ¡ dist[v]                              ▷ Relax (u,v)
12:         dist[v] := alt
13:         previous[v] := u
14: previous[]
```

Figure 4.2: Djkstra's Shortest Path Algorithm for Optimal Location of CVSR Devices

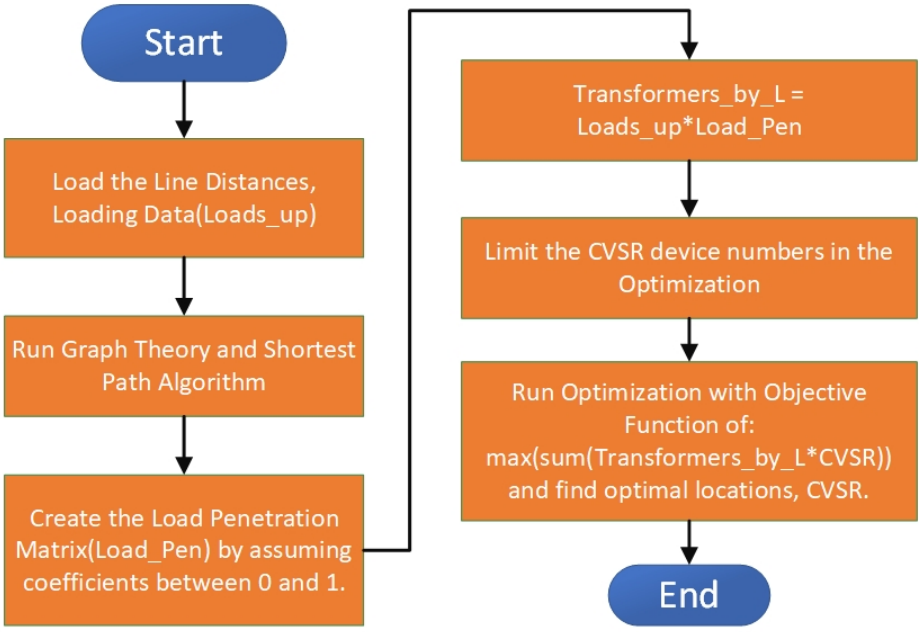


Figure 4.3: Flowchart of Loading Based Algorithm

loading in kVA-wise around a transformer, it will be a candidate to become one of the CVSR locations to be chosen. In Figure 4.4, the loading based algorithm is visually depicted using small and large circles to represent small and large loads in load penetration wise, respectively, around a single transformer. This illustration provides an understanding of how the algorithm works.

4.2.3 Transformer Sensitivity Based Algorithm

Transformer sensitivity based method is used to determine the possible locations of CVSR devices with help of transformer sensitivity matrix (TSM). TSM consists the sensitivities of target transformers that are affected based on changes in reactance values of CVSR devices. Comparing to the loading based method, transformer sensitivity based algorithm has more info like offline power flow outputs, sensitivity matrix to run in the main optimization problem.

The reactance value, measured in ohms, of the CVSR device serves as the input for the sensitivity analysis. A transformer sensitivity analysis is conducted for each transformer to construct the TSM. The process consists of several steps. Firstly, initial power flow results are obtained for the base system. The TSM is then divided into three sensitivity groups. These groups account for the impact of an active CVSR device on transformer A to transformer B, vice versa, and the transformers themselves. The off-diagonal elements of the TSM are formed by the first and second sensitivity groups, while the diagonal elements are formed by the third sensitivity group. Figure 2.7 depicts the structure of the TSM, illustrating the arrangement of sensitivity groups. As the number of transformers in the system increases, the number of elements in the TSM also increases as shown in Figure 4.5. For instance, if the distribution network consists of only 2 transformers, TSM would be a 2x2 matrix with two segments for piecewise optimization. In the case of the IEEE 342-LVTNS, which has a total of 48 secondary network transformers, generating the TSM would involve creating a matrix of size 48 x 48 x 2 (4608 elements) with two segments of piecewise

linearized TSM. The time required to compute the TSM for the entire network of transformers increases exponentially with the number of transformers, as shown in Figure 4.6. Even generating the sensitivity matrix for just 14 transformers would take more than 3 days to complete. After conducting further research, a clustering method was employed to reduce the computation time to approximately 10-15 minutes by using clusters with only two transformers in each.

After creating the sensitivity matrix, main optimal location optimization involves with constraints and objective function to minimize both the number of CVSR devices and the reactance values associated with these devices.

4.2.4 Piecewise Optimization Based Algorithm

Piecewise optimization based method is a mathematical optimization technique that we will apply to address the optimal location problem of CVSR devices in IEEE 342-LVTNS. This technique enables the modeling of non-linear relationships and discrete decision variables commonly encountered in power system optimization. Piecewise linear optimization allows the representation of discrete decisions, such as the selection of CVSR device locations from a finite set of options. The basic idea behind piecewise optimization is to approximate non-linear relationships with linear segments within predefined intervals or regions. This approximation allows us for the formulation of the optimization problem as a mixed-integer linear program (MILP), which can be efficiently solved using various optimization algorithms like CPLEX, Gurobi etc.

The optimal location problem is formulated as an optimization model where decision variables represent the binary selection of CVSR device locations. Constraints capture the system requirements, such as power flow limits of transformers, CVSR reactance limits, maximum number of CVSR devices to be used, and operational constraints. Objective function quantifies minimizing the number of CVSR devices and minimizing their reactance values.

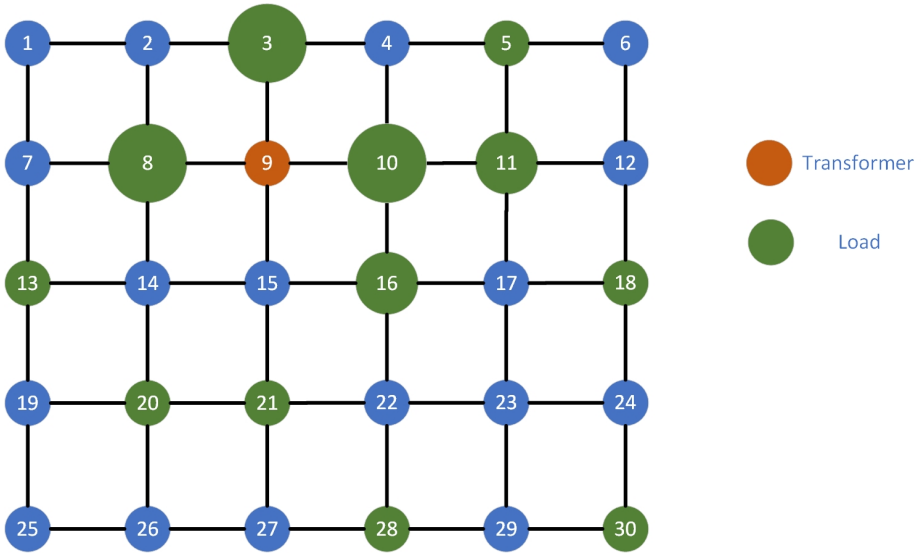


Figure 4.4: Loading Based Method Illustration with Small and Large Loads around a Transformer

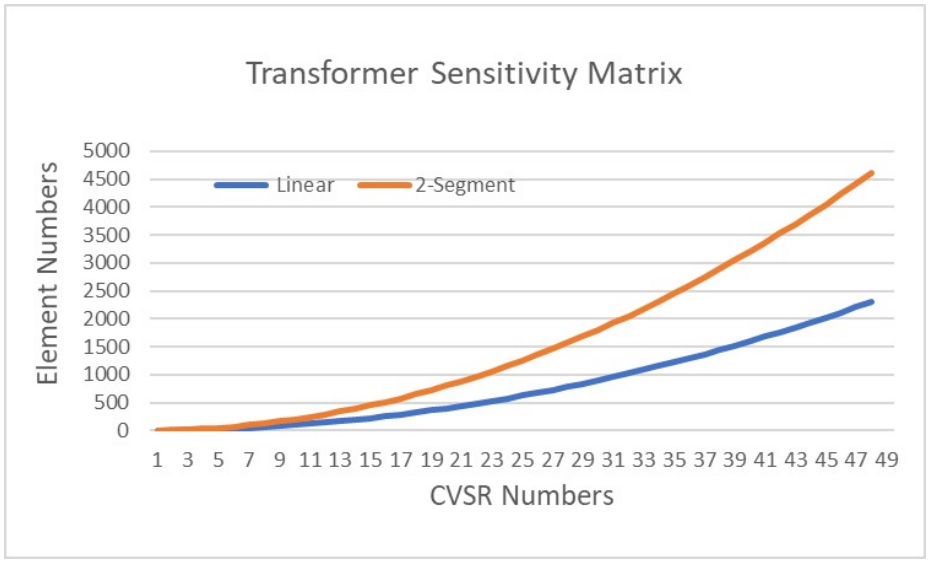


Figure 4.5: Impact of Increasing CVSR Devices on Transformer Sensitivity Matrix Elements

The advantages of using piecewise linear optimization for the optimal location problem in power systems include its ability to handle discrete decisions, capture non-linearities, and provide efficient and effective solutions. However, it is important to note that the accuracy of the approximation depends on the chosen number of intervals and the quality of the linear approximations within each interval.

Further numerical details will be provided within the case study sections, offering a comprehensive understanding of the specific numerical aspects involved.

4.3 Case Studies

4.3.1 System Description and Simulation Setup

The IEEE 342-Node LVNTS comprises two delta-delta step-down transformers, 47 grid network transformers rated at 1 MVA, and 20 spot network transformers rated between 1.5-2.5 MVA. Our focus is primarily on the grid network, where the base voltage is 13.8 kV/208 V on the primary and secondary sides of the grid network transformers, respectively. Accordingly, the initial reactance is calculated as 9.52 Ω based on the provided data in the OpenDSS system, with a given value of 0.05 pu. Additionally, the minimum and maximum reactance increments of the CVSR devices, denoted as $X_{CV,k}$,, are determined as 0.06 Ω and 3.15 Ω, respectively, as stated in (6). For the purpose of this study, we approximate values of 0 and 3 Ω as the minimum and maximum limits, respectively, for the reactance increments while (6) stated the minimum and maximum values as 0.06 Ω and 3.15 Ω.

The various optimal location models will be implemented and evaluated on the IEEE 342-LVTNS in the following sections. Consequently, the application of the CVSR device concept is tailored to suit the specific characteristics and requirements of the IEEE system. Moreover, number of CVSR devices are determined depending on the case studies.

In the field of electrical engineering, the concept of electrical length refers to a dimensionless parameter that is determined by dividing the physical length of an electrical conductor (such as a cable or wire) by the wavelength of the alternating current at a specific frequency propagating through the conductor. Since the line geometry, also referred to as wire, of all secondary network lines is same in the IEEE 342-LVTNS, we can say electrical length is directly proportional to physical length. Therefore, physical length of lines will be taken into account for optimization purposes.

Three cases will be evaluated in this chapter. Some details are given below for each cases:

- **Case 1: Base Load**
- **Case 2: x1.39 Base Load for All Loadings**
- **Case 3: Area-Based Load Increment**

For simulation purposes, OpenDSS is employed for offline calculations. Initially, the power flow value, denoted as $S_{in,k}$, is computed using OpenDSS, considering that the reactance increment value, $X_{CV,k}$, is set to 0. If the obtained initial power flow value, $S_{initial,k}$, exceeds the maximum allowable value, denoted as S^{max}, the MATLAB software is utilized to calculate the optimal reactance increment and determine the optimal location. Subsequently, the YALMIP toolbox is utilized in MATLAB to model and CPLEX to solve the optimization problem. The following subsections present the simulation results for the respective distribution system.

4.3.2 Case 1: Base Load

Firstly, we will examine the base load scenario, where the loadings in the network will remain unchanged without any increase or decrease. In this case, the transformers in the system operate below their maximum limits, and there are no overloaded secondary transformers. This particular scenario holds significance for power

distribution system planning purposes, as it provides valuable insights into the system's performance under normal operating conditions without any load-related issues.

The transformers in the system have loading levels ranging from 525 kVA to 741 kVA. None of the transformers are overloaded or approaching 90 percent of their maximum rating.

4.3.2.1 Shortest Path Algorithm

For the shortest path algorithm, we use graph theory and Dijkstra's shortest path algorithm built in MATLAB. Since none of the transformers are overloaded, this case study will give us opinion where we can place the CVSR devices as a power system planning problem. We aim to find the best five locations for the CVSR devices to be placed. For each transformer and loading locations, Dijkstra's algorithm gives us a distance value. The distance matrix illustration, with row vectors representing the loading buses and column vectors representing the transformer buses, can be found in Figure 4.7. Only Bus 19 has both load and transformer on it. Thus, distance between load at Bus 19 to transformer at Bus 19 will be zero.

After finding all distances between loads and transformers, ***mink*** is used to find five transformers that are close to the all loads in total distances. Figure 4.8 shows the optimal location of CVSR devices that can be placed. The CVSR device locations are denoted by red circles, while the green squares represent all transformer locations, including those with and without CVSR devices. The magenta dots indicate the five points in the network with the highest loading. Logically, optimal locations of CVSR devices are assigned in the center of the network.

4.3.2.2 Loading Based Algorithm

Once again, none of the transformers in this case study are overloaded, which makes it relevant for planning purposes. Initially, we employed Dijkstra's algorithm to

determine the distances between loads and transformers. These distances were then transformed into a load penetration matrix, taking certain assumptions into account. Additionally, load data for all buses was utilized to generate the load effect matrix.

By executing the main MATLAB file for optimization, we obtained the desired outcomes. Figure 4.9 illustrates the optimal placements of CVSR devices based on the results. Similarly to the figure 4.8 in the shortest path algorithm, the red circles in the figure indicate the locations of the CVSR devices, while the green squares represent the locations of all transformers. The magenta dots highlight the five points in the network with the highest loading. Comparing to the shortest path algorithm, loading based algorithm improved the optimal locations of CVSR devices. While the most of the locations remain same, one location changed from Bus-95 to Bus-49.

4.3.2.3 Transformer Sensitivity Based Algorithm

Comparing to two previous algorithms, transformer sensitivity based algorithm simply uses more data. Transformer sensitivity matrix is obtained by using the power flow data from OpenDSS. Following the creation of the sensitivity matrix, the main optimization process for determining the optimal CVSR device locations entails incorporating constraints and an objective function. The objective is to minimize the number of CVSR devices required and the reactance values associated with these devices. Like in Chapter 3, we use the linearized version of nonlinear power flow data Thus, the optimization results improved the optimal locations of CVSR devices.

The optimal locations of CVSR devices in the IEEE 342-LVTNS are depicted in Figure 4.10. The figure showcases the optimal locations of CVSR devices indicated by the red circles. The green squares represent the locations of all transformers in the network. Additionally, the magenta dots highlight the five points in the network with the highest loading, providing insights into areas of potential congestion. It is observed that the transformer sensitivity-based algorithm has resulted in changes to three CVSR locations compared to the loading-based method. Notably, the CVSRs at Bus-50 and Bus-70 remain unchanged, while the locations of the other CVSR devices

have been updated. These changes highlight the importance of having more data for achieving higher accuracy in the optimization process. With additional data, such as transformer sensitivity analysis, more precise and informed decisions can be made regarding the optimal locations of CVSR devices. This demonstrates the value of incorporating comprehensive data sets to improve the accuracy and effectiveness of the optimization results.

4.3.2.4 Piecewise Optimization Based Algorithm

Given the similarities between the transformer sensitivity based algorithm and the piecewise optimization based algorithm in terms of their performance in overloaded scenarios, as well as their equivalence in the Case 1: Base Load case, we will now proceed to Case 2: x1.39 Base Load. The same figure, Figure 4.10, depicting the optimal locations of CVSR devices using the transformer sensitivity-based method, is applicable in this method as well.

4.3.3 Case 2: x1.39 Base Load for All Loading Busses

As a secondary case study, we will uniformly increase the loadings in the entire network of the IEEE 342-LVTNS system by a factor of x1.39. Previously, all loads are multiplied by 1.5 but optimization problem was not solved since the transformer capacities were not enough to shift the load each other. In other words, the demand was surpassing the supply. Therefore, we used factor of x1.39 for loadings. This intentional increase in loadings aims to create a scenario where some transformers within the network become overloaded. Since there are 9 transformers are overloaded, namely, T-33,T-35,T-36,T-41, T-42, T-43, T-44, T-45, T-52 at Bus-49, Bus-54, Bus-35, Bus-45, Bus-69, Bus-50, Bus-70, Bus-55, Bus-71 and Bus-76, respectively. This case provides valuable insights for both operational and planning purposes. It allows us to assess the system's performance under specific conditions and determine the optimal locations for CVSR devices with their corresponding reactance values. This

evaluation helps identify areas within the distribution system where the installation of CVSR devices is necessary to enhance system performance and ensure efficient operation. Furthermore, it enables proactive planning to address potential challenges and optimize the distribution system's overall performance. Differently from Case 1, the optimization is utilized to find 10 optimal locations in Case 2.

Please note that the shortest path algorithm is not included in this case study as it would yield the same results and plots regardless of the load increment.

4.3.3.1 Loading Based Algorithm

In this approach, the optimization problem is designed to select the optimal locations for 10 CVSR devices where 9 transformers are overloaded. Similar to the method used in 4.3.2.2 Case 1: Loading Based Algorithm , we utilized Dijkstra's algorithm to calculate the distances between the loads and transformers. These distances were subsequently transformed into a load penetration matrix, considering specific assumptions. Moreover, the load data for all buses in the system was incorporated to construct the load effect matrix.

The optimal locations for 10 CVSR devices were determined, and they are depicted in Figure 4.11. It is evident that the optimal locations remain the same as those shown in Figure 4.9, with the addition of CVSR devices at Bus-49, Bus-55, Bus-76, Bus-90, and Bus-91. Five of the optimal locations remain the same because the load increment was uniformly applied to each load.

4.3.3.2 Transformer Sensitivity Based Algorithm

The optimal locations of CVSR devices in the IEEE 342-LVTNS are illustrated in Figure 4.12. The figure displays the 10 optimal locations of CVSR devices, represented by the red circles. The green squares depict the locations of all transformers within the network while the magenta dots indicate the 15 points in the network with the highest loading. The transformer sensitivity-based algorithm has resulted in modifications to

four of the CVSR device locations when compared to the loading-based method. Specifically, the CVSRs at Bus-49, Bus-50, Bus-55, Bus-70, Bus-76, and Bus-91 remain unchanged, while the remaining CVSR device locations have been altered. These adjustments highlight the significance of having an additional data, such as transformer sensitivity matrix, for achieving greater accuracy and informed decisions regarding the optimal placement of CVSR devices in the optimization process. This emphasizes the importance of incorporating comprehensive data-sets to enhance the accuracy and efficiency of optimization outcomes.

4.3.3.3 Piecewise Optimization Based Algorithm

Piecewise optimization based algorithm is more developed model among other techniques in this case study. Additional to the transformer sensitivity based method, this model has power flow limits of transformers and piecewise TSM (PTSM). This optimization model is solved with mixed integer linear programming (MILP) solver, i.e. CPLEX. Since we use more data, the optimal location results are improved. Figure 4.13 shows the optimal locations of CVSR devices in the meshed distribution system. The figure displays the 10 optimal locations of CVSR devices, indicated by the red circles. The green squares represent the locations of all transformers in the network, while the magenta dots highlight the 15 points in the network with the highest loading. By visualizing the distribution of CVSR device locations, transformer locations, and areas of high loading, we can gain insights into the effectiveness and impact of the optimization process. Comparing to the transformer sensitivity based algorithm, eight of the CVSR locations are same. Differently, piecewise optimization based approach selected the CVSR locations at Bus-75 and Bus-54.

The effectiveness of the optimization results is evident as we observe the optimal reactance values and locations of CVSR devices in Figure 4.14. The figure demonstrates how the allocation of CVSR devices in optimal locations, with appropriate reactance values, contributes to relieving the overloaded transformers in the network. As a result, the transformers are constrained to operate below their

maximum rated capacity of 1 MVA. This showcases the successful mitigation of overloading issues and ensures the reliable and efficient operation of the distribution system.

Moreover, we can observe the comparison of initial power flow, optimal power flow, and OpenDSS(Benchmark) power flow in Figure 4.15. The initial power flow analysis reveals the presence of overloaded transformers in the system. To address this issue, the optimal power flow analysis is conducted, taking into account the optimal reactance values obtained from the optimal locations of CVSR devices. By incorporating these optimal values into the power flow calculations, the proposed piecewise optimization-based method demonstrates its effectiveness in alleviating overloading problems. The results of the optimization closely match the benchmark results obtained from the OpenDSS power flow analysis. This close agreement between the optimization results and the benchmark results validates the accuracy and reliability of the proposed method.

4.3.4 Case 3: Area-Based Load Increment

In the final phase of our case studies, we introduce load increment in a specific area of the IEEE 342-LVTNS system which is depicted in Figure 4.16. This selective load increment allows us to assess the system's performance and examine the impact of higher loadings in that particular area. To facilitate the analysis, the IEEE 342-LVTNS system is divided into 12 distinct areas, enabling us to evaluate the behavior of the system under varying load conditions.

On the other hand, the loading levels vary significantly, making it impractical to apply the same load increment coefficient uniformly across all transformers. To address this issue, we divide the loads into two categories: small loads and large loads. The large loads are approximately twice the size of the small loads. This differentiation allows for a more precise and tailored approach to load increment. By incorporating this load distribution strategy into the optimization process, we

can effectively manage the overloading conditions and ensure a balanced allocation of CVSR devices. In this case study, we explore the impact of load increments on the specific area of the IEEE 342-LVTNS system. We consider three different load increment scenarios for small and large loads: (x1.8, x1.5), (x1.9, x1.6), and (x1.8, x1.8), respectively. For the (x1.8, x1.5) load increment scenario, we use same three algorithms to determine the optimal locations for two CVSR devices. The same applies to the (x1.9, x1.6) load increment scenario, but with a constraint that limits the number of CVSR devices to four locations for all algorithms. Lastly, for the (x1.8, x1.8) load increment scenario, the number of CVSR devices is limited to six locations. The goal is to identify the most effective positions to install CVSR devices in order to mitigate the overloading of transformers in the network. By limiting the different number of CVSR devices regarding the different load increments, the optimization process aims to achieve a balance between performance and cost-effectiveness. We aim to investigate the ability of CVSR devices with a reactance value of 3 Ω to handle the increased loadings when placed in the optimal locations.

4.3.4.1 Loading Based Algorithm

In the area-based loading increment case of Case 3, we apply the loading-based algorithm using the same approach as in Case 1 and 2. The Dijkstra's algorithm is employed to calculate the distances between the loads and transformers in the specific area.

In the first scenario, the small loads in the specific area are increased by a factor of x1.8, while the larger loads are multiplied by 1.5. The optimal two CVSR locations in the specific area are illustrated in Figure 4.17. OpenDSS power flow results indicate that transformers T-23 and T-24 at Bus-24 and Bus-4, respectively, are slightly overloaded in the specific area. However, it is interesting to note that the CVSR devices are located at Bus-49 and Bus-50, which are not directly within the loaded area. This observation suggests that the loading-based algorithm may not be effectively capturing the localized overloading conditions in the specific area.

The algorithm's focus on the overall load increment in the distinct area might lead to suboptimal placement of CVSR devices, resulting in CVSRs being placed in locations that do not directly address the overloaded transformers. This highlights the limitations of the loading-based algorithm in handling localized load increments and emphasizes the need for more data and advanced optimization techniques to accurately identify and address overloading conditions in specific areas.

In the second scenario, where the small loads are increased by a factor of x1.9 and the large loads are increased by a factor of x1.6, the total load in the specific area is further increased compared to the previous scenario. The results from OpenDSS with the given loading conditions indicate that transformers T-23, T-24, and T-32, located at Bus-27, Bus-4 and Bus-33 are overloaded. Using the loading-based algorithm, four optimal locations for CVSR devices are determined at transformers T-32, T-41, T-33, and T-42, located at Bus-33, Bus-69, Bus-49, and Bus-50, respectively. These locations are illustrated in Figure 4.18. Although there is an improvement compared to the first scenario, it is clear that the loading-based algorithm still falls short in accurately identifying the overloaded transformers within the specific area.

In the final scenario, both small and large loads are increased by x1.8 comparing to the base loading. According to that load changes, transformers of T-23, T-24, T-25, T-32, and T-40 at Bus-27, Bus-4, Bus-28, Bus-33, and Bus-45, respectively, are overloaded. The loading based algorithm finds six optimal location of CVSR devices in this overloaded area which is illustrated in Figure 4.19. The optimal locations of CVSR devices are attached to the T-32, T-41, T-33, T-42, T-40, and T-43 located at Bus-33, Bus-69, Bus-49, Bus-50, Bus-45, and Bus-70 respectively. Similar to the second scenario, the optimal location results are not improved much since only two of the CVSR locations are matching with the overloaded transformers.

4.3.4.2 Transformer Sensitivity Based Algorithm

Transformer sensitivity based algorithm is applied to the three scenarios same as loading based algorithm. Initially, small loads and large loads are multiplied by 1.8

and 1.5 of base loadings, respectively. The transformers T-23 and T-24 at Bus-24 and Bus-4 are overloaded according to the results we obtained from OpenDSS. Figure 4.20 presents the two optimal locations of CVSR devices in one of 12 distinct areas. It is noteworthy that the algorithm successfully matches the optimal locations of CVSR devices with the overloaded transformers in the system, achieving 100% accuracy in terms of location-based optimization.

Another scenario involves with increasing the small loads and large loads by x1.9 and x1.6 factors, respectively. Before giving the results of transformer sensitivity based optimization, OpenDSS is run and we know that transformers T-23, T-24, and T-32 at Bus-27, Bus-4, and Bus-33, respectively, are overloaded. We obtained the four optimal locations for CVSR devices in the specific area by modelling and solving the optimal location problem with transformer sensitivity based algorithm. Figure 4.21 shows these optimal locations. It is evident that all the overloaded transformers, namely T-23, T-24, and T-32, have received CVSR devices. Additionally, an additional CVSR device is placed on transformer T-40at Bus-45. This selection of T-40 suggests that it could be close to reaching its overloading level, warranting the installation of a CVSR device for preventive measures.

In the final scenario, same coefficient of x1.8 is applied to the small and large loads. Accordingly, OpenDSS power flow results give the five overloaded transformers of T-23, T-24, T-25, T-32, and T-40 at Bus-27, Bus-4, Bus-28, Bus-33, and Bus-45, respectively. Utilizing the transformer sensitivity-based algorithm once again, we were able to determine the optimal locations for six CVSR devices in the specific area. Figure 4.22 showcases these optimal locations. It is worth noting that the algorithm effectively identifies and addresses the overloading issues by placing CVSR devices on the transformers that are experiencing overloading. Specifically, the overloaded transformers T-23, T-24, T-25, T-32, and T-40 have all received CVSR devices to alleviate the overloading conditions. Additionally, a CVSR device is installed on transformer T-31 at Bus-44 for preventive measures, as this transformer may be approaching its overloading level.

The results of three scenarios demonstrate the effectiveness of the transformer sensitivity-based algorithm in accurately identifying the specific transformers that require CVSR devices to mitigate overloading. By considering the sensitivities of transformers to load variations, the algorithm can optimize the placement of CVSR devices and effectively alleviate overloading issues in the system.

4.3.4.3 Piecewise Optimization Based Algorithm

The utilization of more data has led to improved results in determining the optimal locations for CVSR devices in the meshed distribution system. Similar to the previous algorithm sections, we will investigate same three scenarios in this algorithm too. At the first, we will increase the small and large loadings by a factor of x1.8 and x1.5, respectively. The accompanying Figure 4.23 provides a visual representation of two optimal locations for the CVSR devices. The optimal locations match with the overloaded transformers. Meaning that the optimization method works very well. Moreover, initial (overloaded) and optimal (relieved) power flows on the transformers can be seen in Figure 4.24.

Transformers T-23, T-24, and T-32 are overloaded in the second scenario with x1.9 and x1.6 factors of increment on small and large loads, respectively.The optimization process aims to identify the optimal locations for four CVSR devices in this scenario. Figure 4.25 illustrates the optimal locations in the upper-left corner of the IEEE 342-LVTNS. Comparing these results to those obtained from the transformer sensitivity-based method, one different optimal location is observed. Although both approaches effectively address the overloaded transformers, it can be observed from Figure 4.26 that placing the CVSR devices at T-23 and T-24 may lead to an overload condition at T-25 due to the additional loads being shifted to the nearest transformer. Thus, the piecewise optimization based algorithm provides a more accurate result with optimal locations.

Lastly, all loads are multiplied by 1.8 in that area in the IEEE 342-LVTNS. Therefore, transformers T-23, T-24, T-25, T-32, and T-40 are overloaded according

to the OpenDSS power flow simulation. Piecewise optimization based algorithm applied into this scenario while finding the six optimal locations of CVSR devices. Figure 4.27 shows the optimal CVSR devices' locations where they are placed at transformers of T-23, T-24, T-25, T-32, T-40, and T-31 at Bus-27, Bus-4, Bus-28, Bus-33, Bus-45, and Bus-44. The results are same as transformer sensitivity based method's results. Additionally, shifting loadings from overloaded transformers to other nearby transformers can be seen in Figure 4.28. Piecewise optimization has enough data for relieving overloaded transformers and preventive actions to overload new transformers. Both algorithms proved their capabilities in regards of optimal location problem of CVSR devices.

The results obtained from the three scenarios demonstrate the effectiveness of the piecewise optimization-based algorithm in accurately identifying the transformers that require CVSR devices to mitigate overloading. By considering the load variations and dividing the system into smaller areas, the algorithm optimizes the placement of CVSR devices and effectively addresses overloading issues. The algorithm takes into account the specific characteristics of the transformers and their responses to varying loads, ensuring that the CVSR devices are strategically placed where they are most needed. This approach allows for a targeted and precise solution, resulting in accurate and efficient alleviation of overloading problems in the system.

Overall, the piecewise optimization-based approach outperforms other algorithms in every scenario. The algorithm consistently identifies the transformers that require intervention to alleviate overloading, resulting in efficient and accurate outcomes. By leveraging the advantages of piecewise optimization, this approach proves to be a highly effective solution for addressing overloading issues in the distribution system.

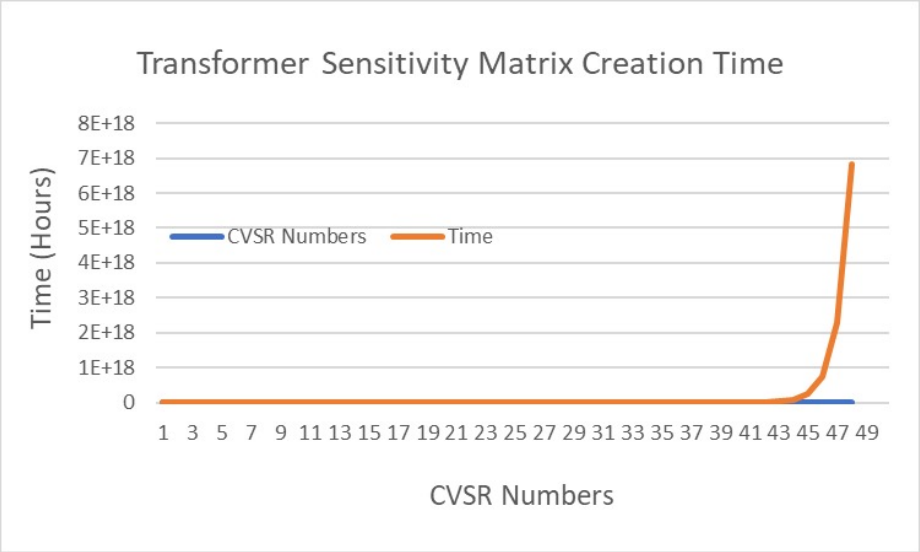


Figure 4.6: Effect of Increasing CVSR Devices on Transformer Sensitivity Matrix Creation Time

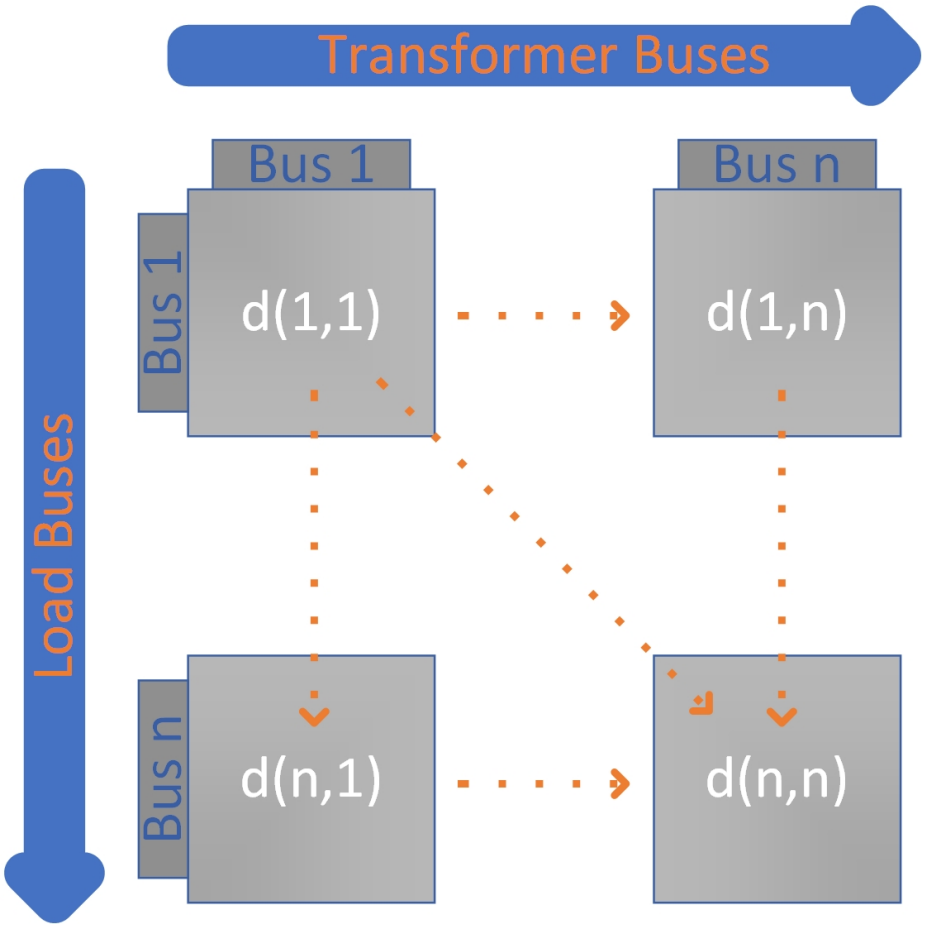


Figure 4.7: Distance Matrix of Transformer and Load Buses

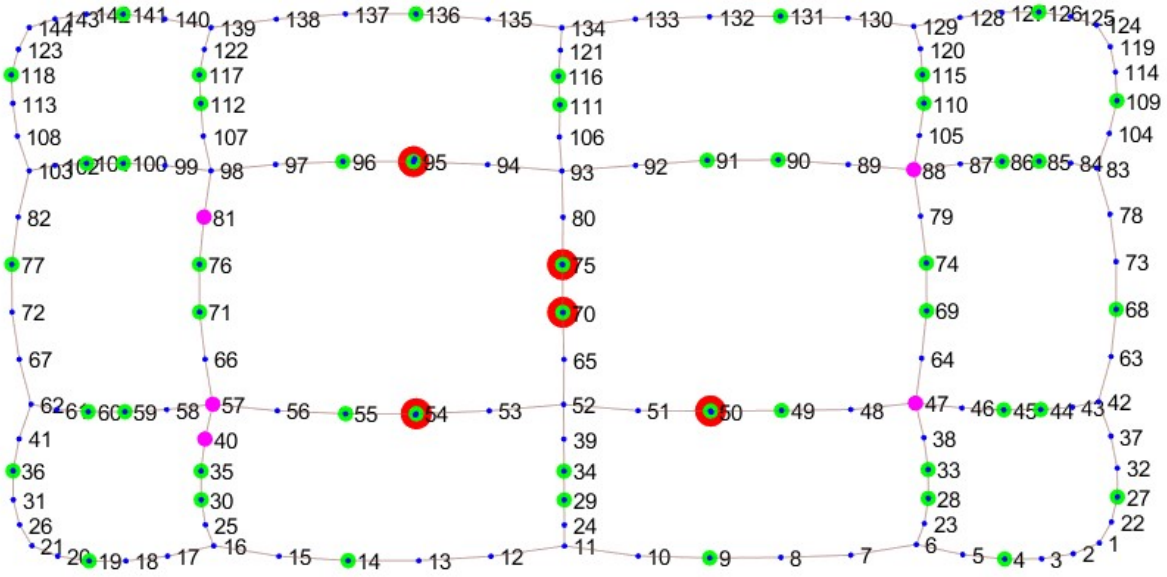


Figure 4.8: Optimal Location of CVSR devices using by Dijkstra's Shortest Path Algorithm

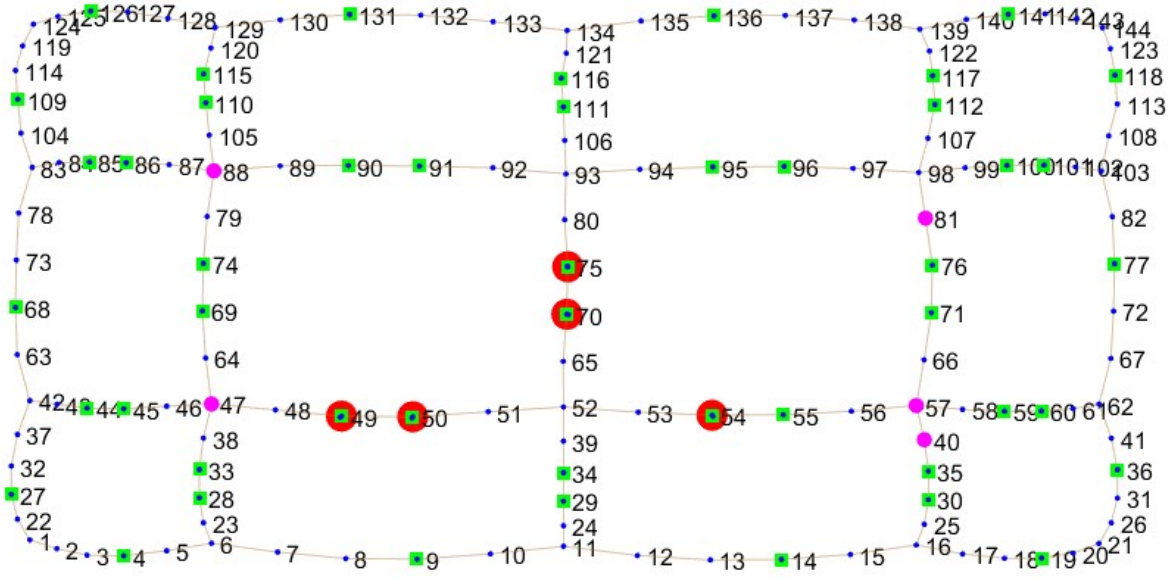


Figure 4.9: Optimal Location of CVSR devices using by Loading Based Algorithm

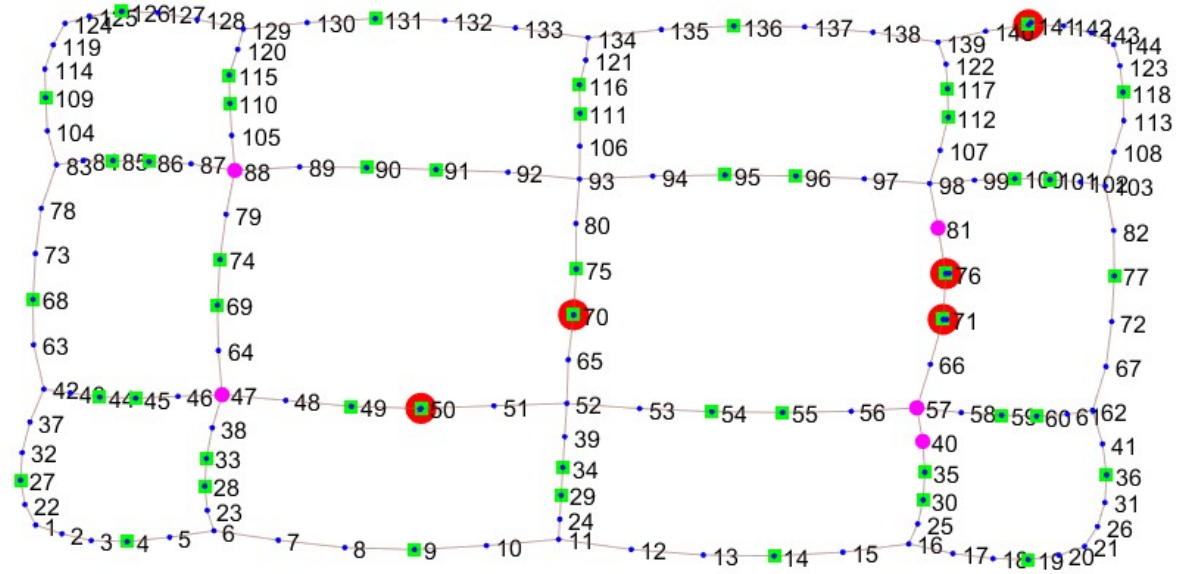


Figure 4.10: Optimal Location of CVSR devices using by Transformer Sensitivity Based Algorithm

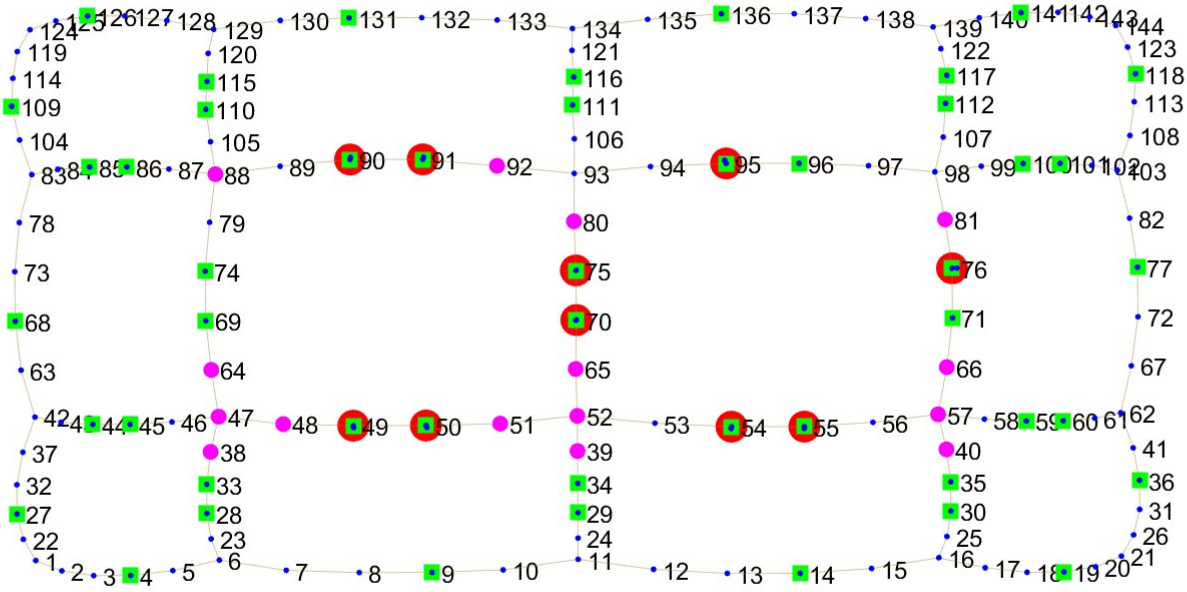


Figure 4.11: Optimal Location of CVSR devices using by Loading Based Algorithm

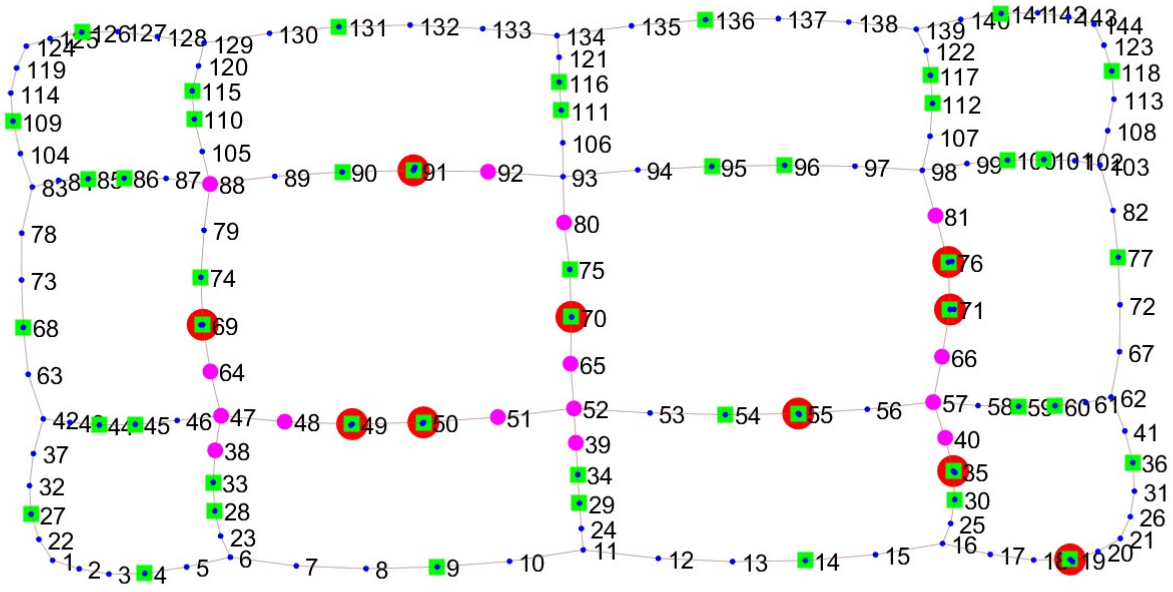


Figure 4.12: Optimal Location of CVSR devices using by Transformer Sensitivity Based Algorithm

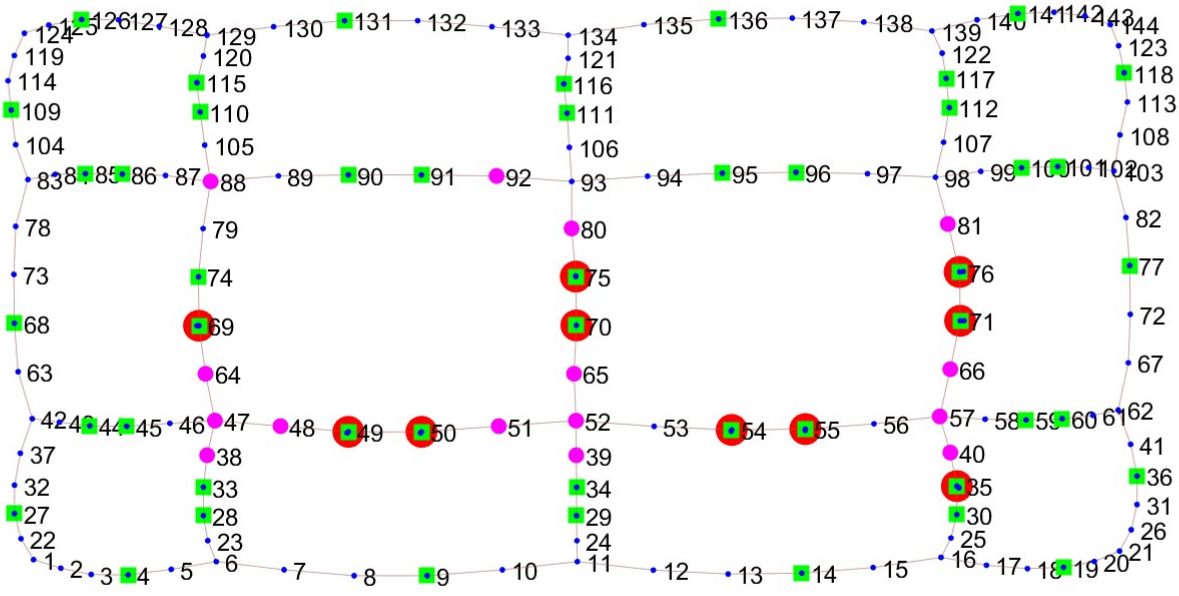


Figure 4.13: Optimal Location of CVSR devices using by Piecewise Optimization Based Algorithm

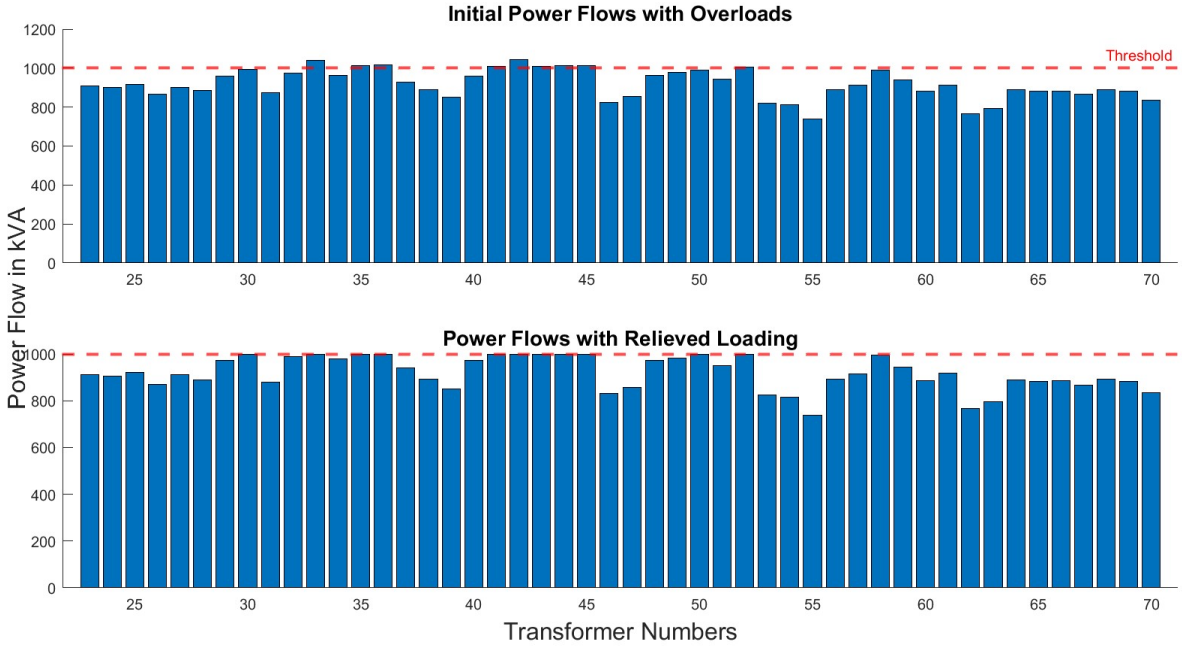


Figure 4.14: Initial Power Flow with Overloaded Transformers and Relieved Transformers after the Optimization

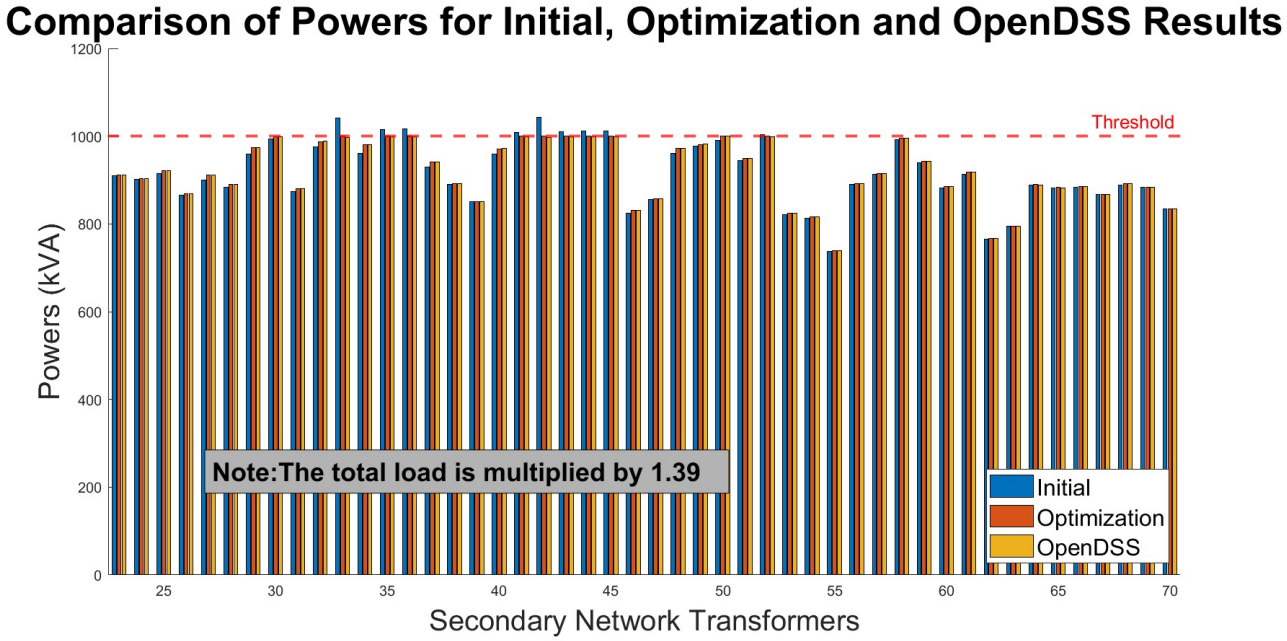


Figure 4.15: Power Flow Comparisons of Initial, Optimization and Benchmark(OpenDSS) Results

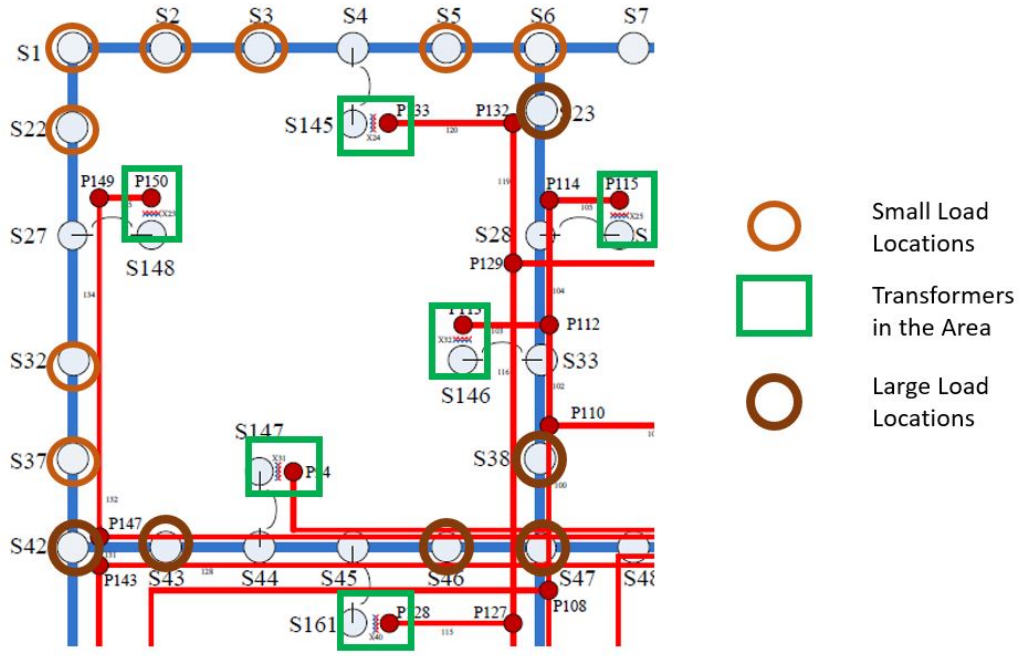


Figure 4.16: Particular Area of Load Increment in the IEEE-342 LVTNS

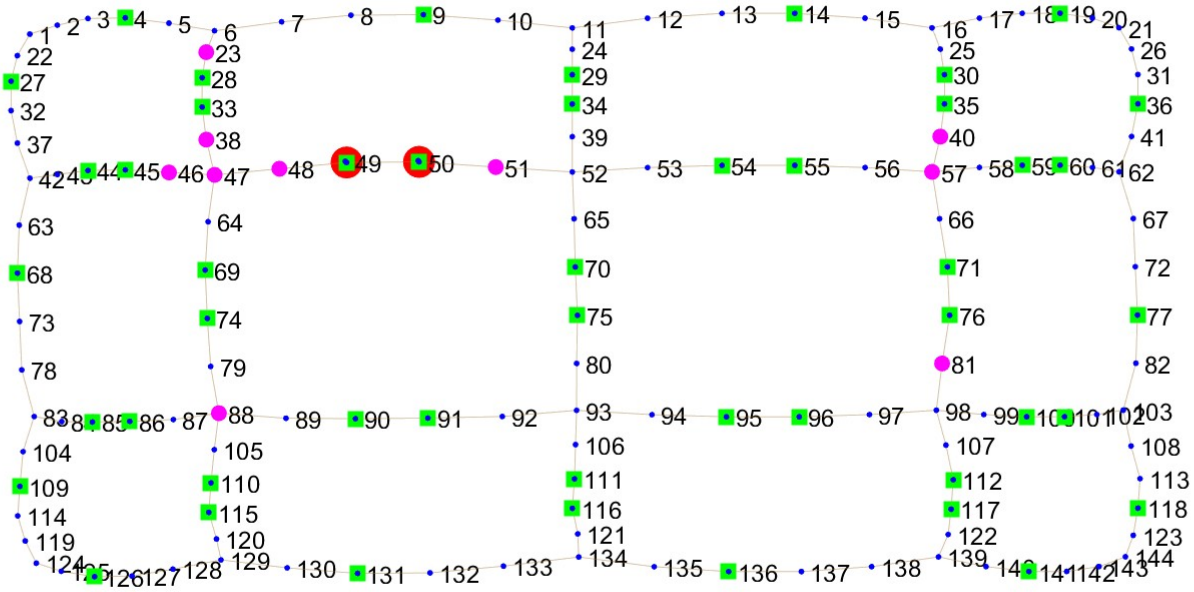


Figure 4.17: Optimal Location of Two CVSR Devices Using Loading Based Algorithm

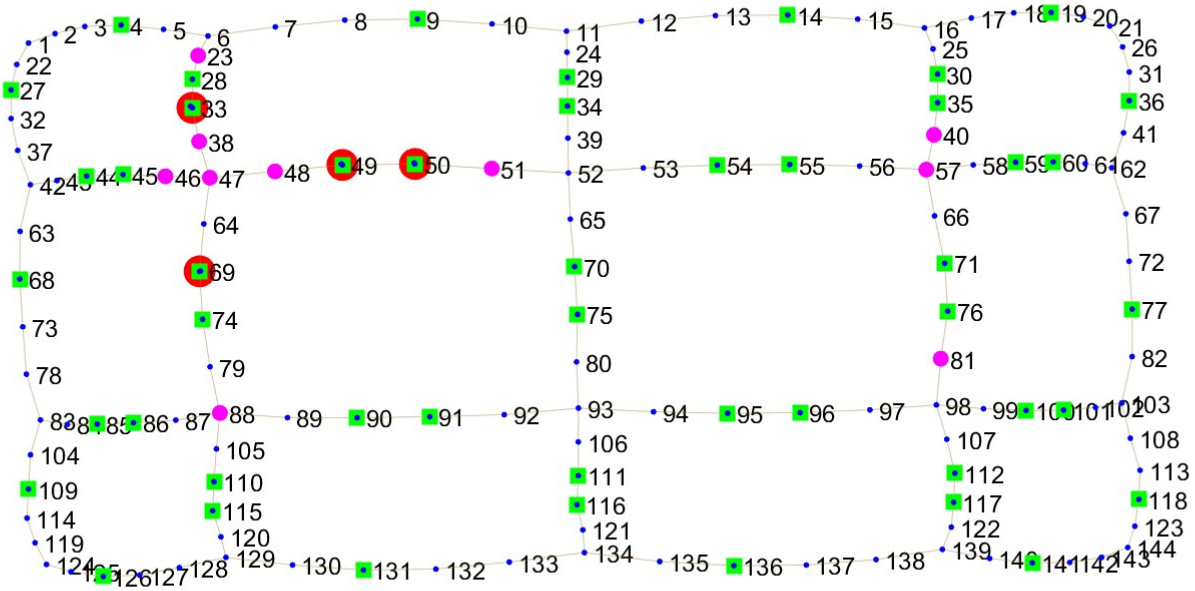


Figure 4.18: Optimal Location of Four CVSR Devices Using Loading Based Algorithm

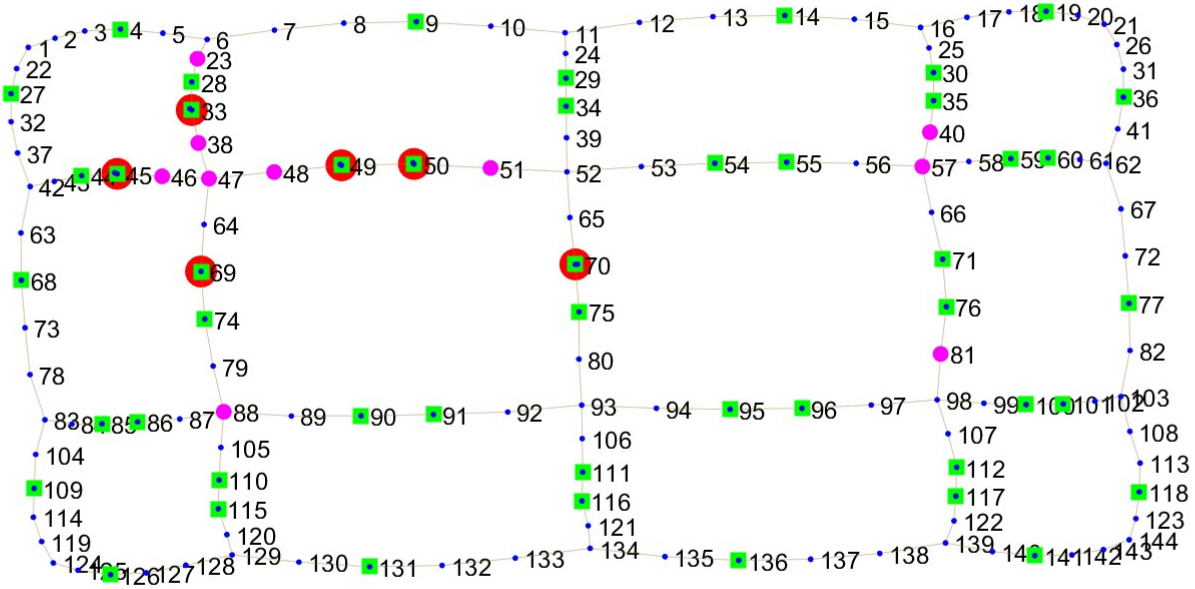


Figure 4.19: Optimal Location of Six CVSR Devices Using Loading Based Algorithm

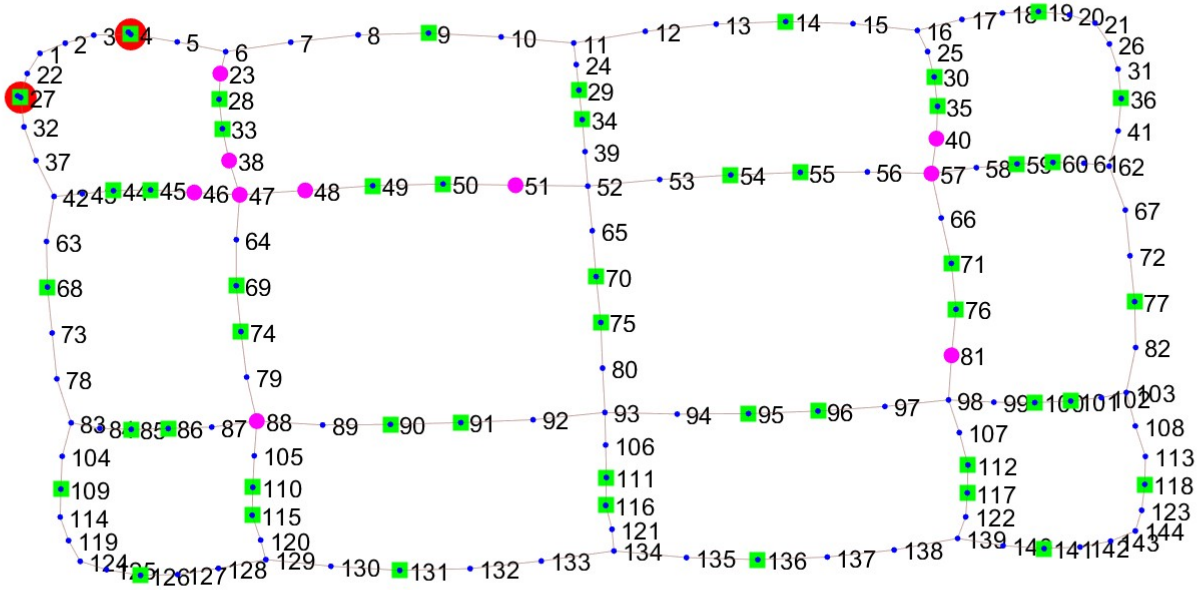


Figure 4.20: Optimal Location of Two CVSR Devices Using Transformer Sensitivity Based Algorithm

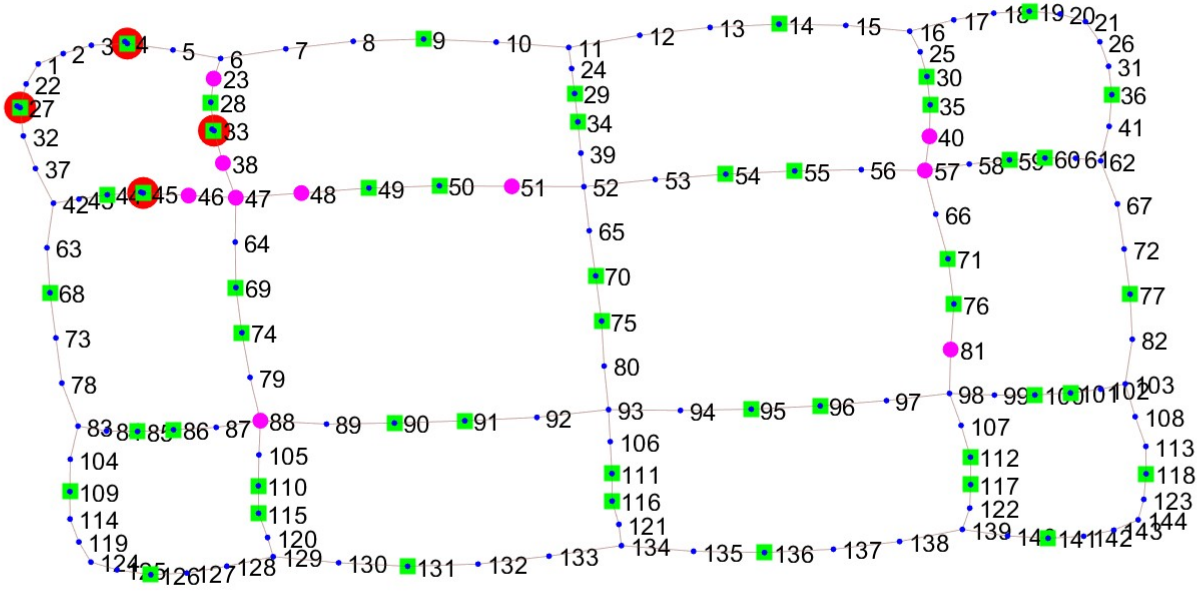


Figure 4.21: Optimal Location of Four CVSR Devices Using Transformer Sensitivity Based Algorithm

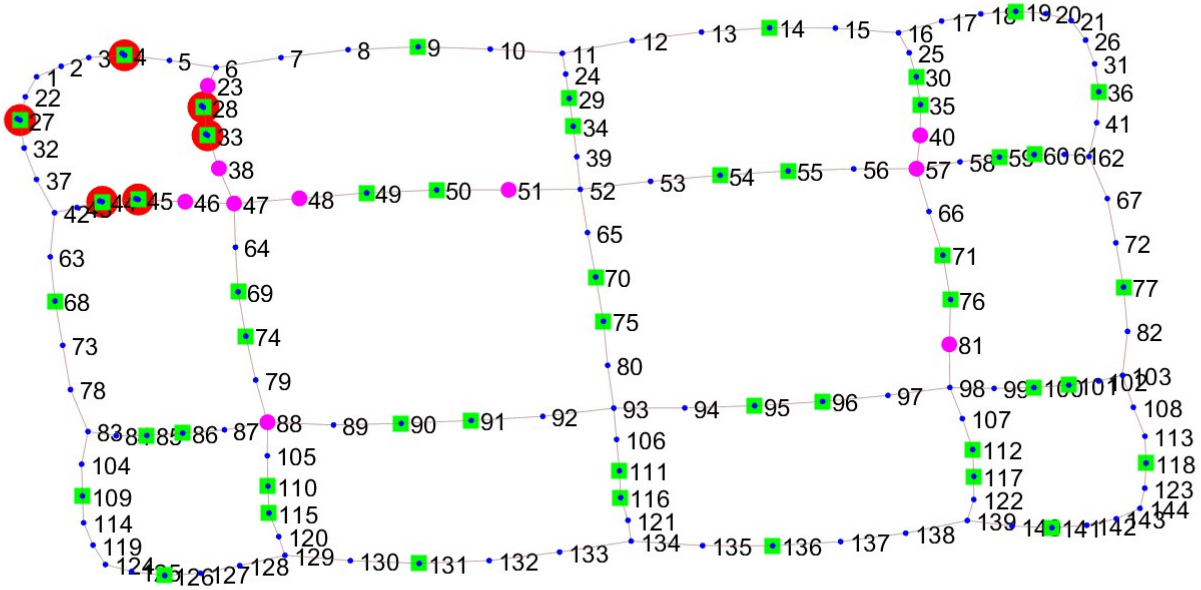


Figure 4.22: Optimal Location of Six CVSR Devices Using Transformer Sensitivity Based Algorithm

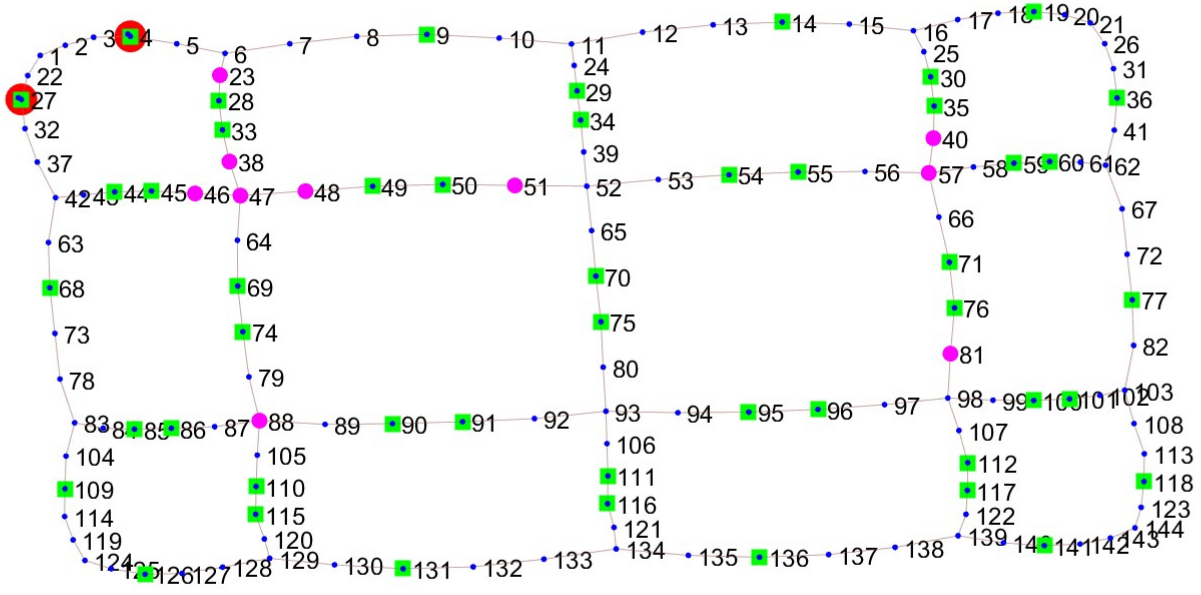


Figure 4.23: Optimal Location of Two CVSR Devices Using Piecewise Optimization Based Algorithm

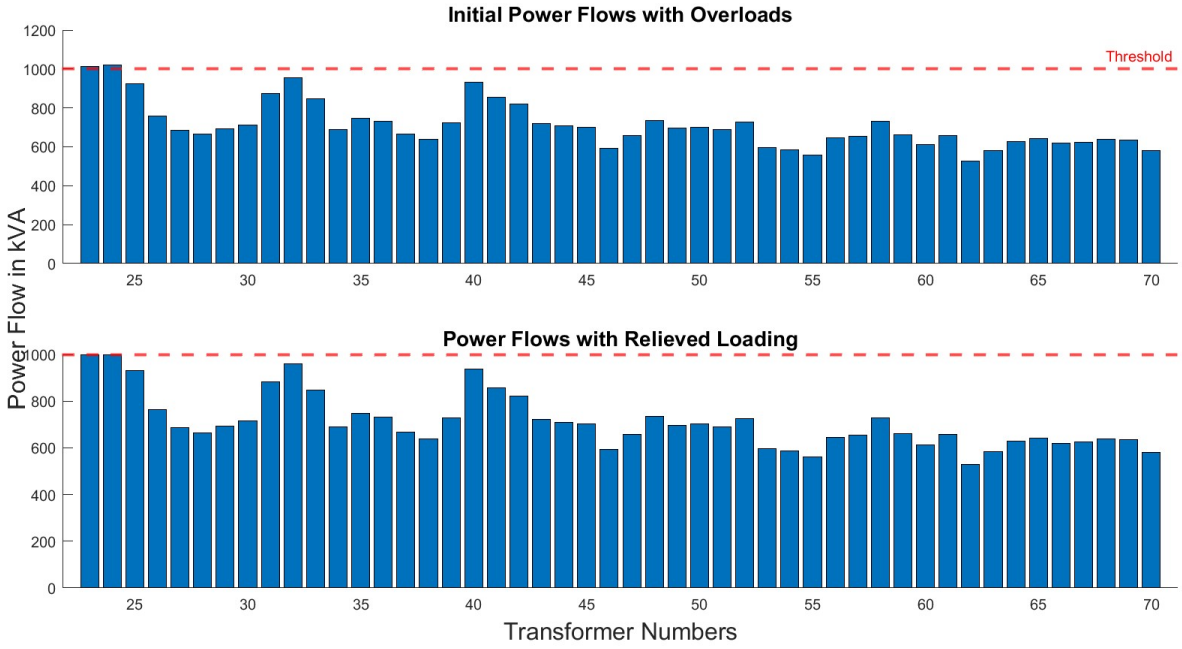


Figure 4.24: Scenario 1: Initial Power Flow with Overloaded Transformers and Relieved Transformers after the Piecewise Optimization

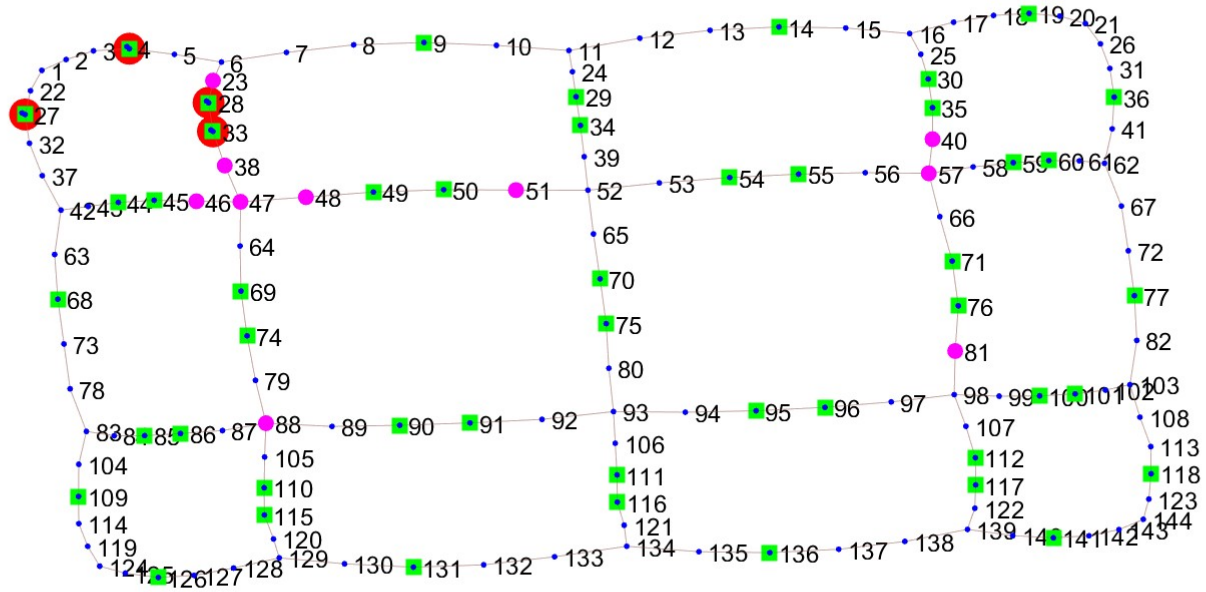


Figure 4.25: Optimal Location of Four CVSR Devices Using Piecewise Optimization Based Algorithm

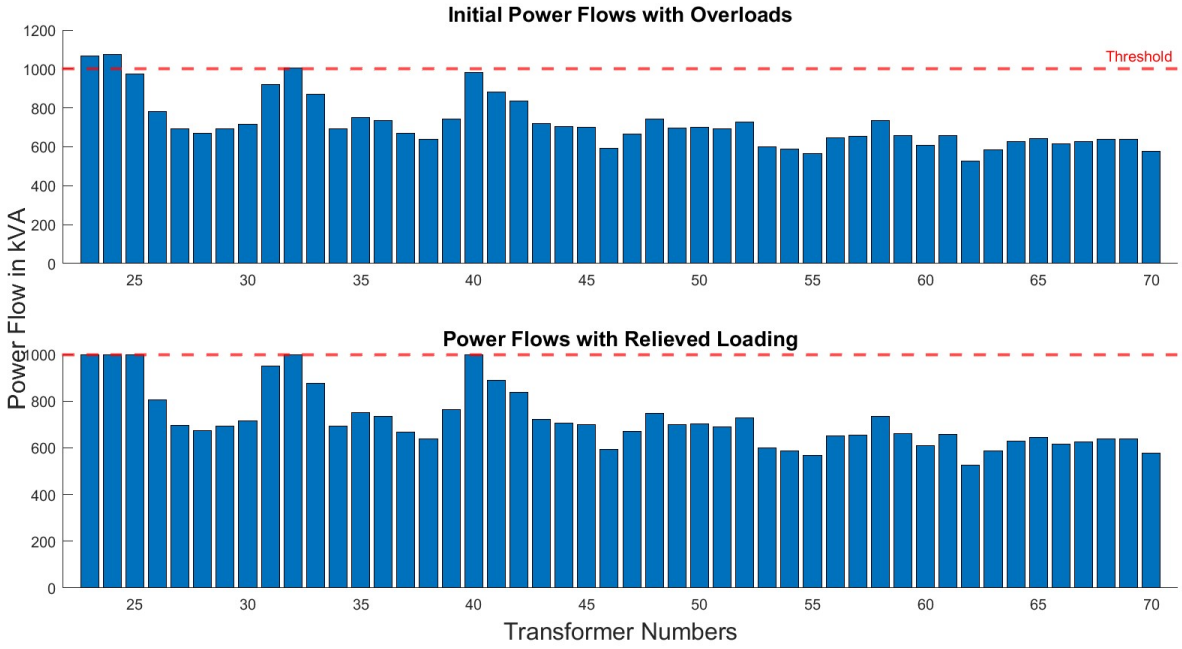


Figure 4.26: Scenario 2: Initial Power Flow with Overloaded Transformers and Relieved Transformers after the Piecewise Optimization

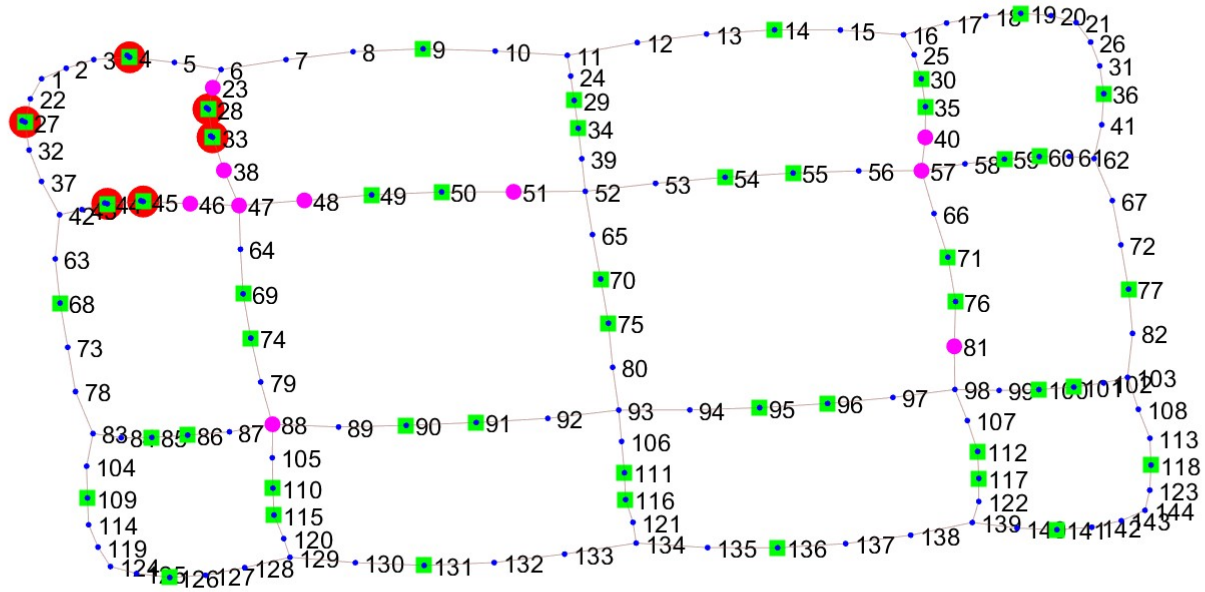


Figure 4.27: Optimal Location of Six CVSR Devices Using Piecewise Optimization Based Algorithm

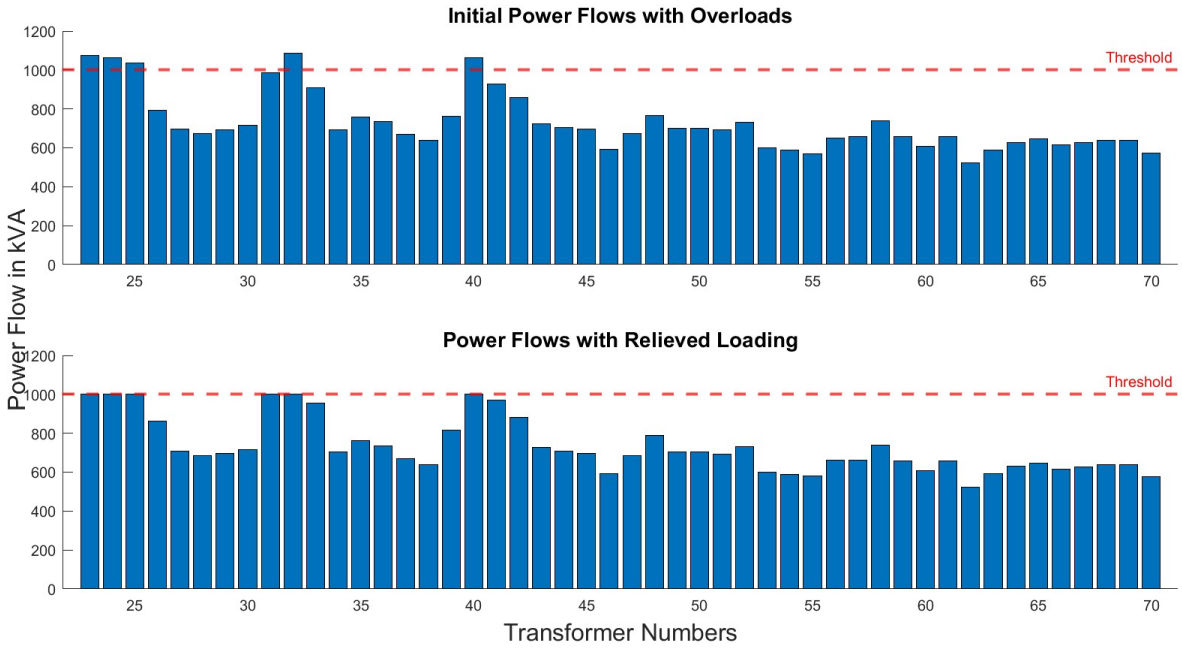


Figure 4.28: Scenario 3: Initial Power Flow with Overloaded Transformers and Relieved Transformers after the Piecewise Optimization

Chapter 5

Conclusion and Future Work

5.1 Conclusion

Overloading of the transformers, especially, in dense urban areas, may be occurred with many uncertain events. To address this issue, this paper proposes the model of the CVSR devices to control power flow on the grid network transformers. Reactance increment of the continuously variable series reactor (CVSR) devices regulates the total reactance on the primary side of the transformers to control power flow among transformers to relieve overloading. It is proven in the literature that using CVSR devices will significantly decrease the cost of transformer upgrades or purchases. The IEEE 342 node low voltage networked test system (LVNTS) is used to perform simulations. Results show that small amount of reactance increments relieve the enough loading on the transformers. We also observed that piecewise approximation to convert from nonlinear to linear functions works properly where the results are close to the benchmark results that obtained on the OpenDSS software. Examining more closely, 4-Segment piecewise optimization fits the best for this project for better accuracy with no computational burden for the Chapter 3.

Chapter 4 examines a range of algorithms, such as the shortest path algorithm, sensitivity-based methods, graph theory techniques, and piecewise optimization

approaches. The main objective of this chapter is to optimize the positioning of power flow control devices, specifically CVSR devices, in order to mitigate transformer overloading within the distribution system. These algorithms are applied to determine the most suitable locations for installing CVSR devices, taking into account factors such as transformer sensitivities, graph theory analysis, and piecewise optimization techniques. Each algorithm brings a distinct perspective and methodology, enabling a thorough analysis and comparison of their effectiveness in addressing transformer overloading challenges. Simulations are conducted using the IEEE 342-LVNTS, a fully meshed test system that offers a realistic and representative platform. Since the IEEE 342-LVTNS is not that large system for heuristic, meta-heuristic and AI methods to involve, we will focus on the analytical approaches with more consistent and precise solutions. However, heuristic and AI techniques can be used for faster results while these techniques do not guarantee the optimal solution. The results obtained from the simulations provide evidence of the effectiveness and precision of the piecewise optimization method in alleviating transformer overloading. This approach not only identifies optimal locations for CVSR devices but also minimizes the number of devices needed. This reduction in device count brings advantages by reducing the overall costs and complexities associated with implementing power flow control solutions in the distribution system. By employing these algorithms and evaluating their performance on the IEEE 342-LVNTS, this chapter delivers valuable insights into the optimal placement of power flow control devices, specifically CVSR devices, to tackle transformer overloading in the distribution system. By achieving the dual objective of relieving overloading and minimizing the number of CVSR devices, the piecewise optimization method proves to be a practical and efficient approach for power system operators and planners. These results highlight the potential of the piecewise optimization technique to enhance the performance and reliability of distribution systems while optimizing resource utilization.

5.2 Future Work

While this study has made significant progress in optimizing the placement of power flow control devices, specifically CVSR devices, for mitigating transformer overloading in the distribution system, there are several avenues for further research and development. The following areas can be explored as part of future work:

1. **Expansion to other test systems:** The current research has primarily focused on the IEEE 342-LVNTS and the ConEd small meshed grids. To enhance the applicability and generalizability of the proposed algorithms and methodologies, future work could involve testing and evaluating them on other test systems of varying scales and complexities. This would provide a more comprehensive understanding of the algorithms' performance under different network configurations and characteristics.

2. **Consideration of dynamic conditions:** The optimization of power flow control devices typically assumes steady-state operating conditions. However, in practical scenarios, the distribution system is subject to dynamic variations such as uncontrollable loads, intermittent renewable energy sources, environmental effects, and changes in system topology. Future work could incorporate dynamic models and algorithms that account for these variations to optimize the placement of power flow control devices under transient and dynamic conditions.

3. **Integration of advanced optimization techniques:** While the algorithms employed in this study have demonstrated promising results, future work could explore the integration of advanced optimization techniques, such as evolutionary algorithms, swarm intelligence, or machine learning algorithms, to further enhance the efficiency and effectiveness of the optimization process. These advanced techniques could enable more robust and efficient solutions, especially for large-scale distribution systems.

4. **Identification of open mains:** Open mains refer to the loss of lines or power devices that cause an open circuit in the distribution system. CVSR devices can mitigate overloading, and future studies can be conducted to identify hidden open mains in heavily meshed distribution systems. As a future work, research can focus on the detection and analysis of open mains using CVSR devices, developing algorithms or techniques to locate and address these issues effectively.

In conclusion, the future work on optimizing the placement of power flow control devices for mitigating transformer overloading in the distribution system involves expanding the research to other test systems, considering dynamic conditions, exploring advanced optimization techniques, and studying the identification of open mains. These future directions would contribute to the ongoing development and improvement of strategies for enhancing the performance and reliability of power systems.

Bibliography

[1] M. Young, A. Dimitrovski, Z. Li, Y. Liu, and R. Patterson, "Continously variable series reactor: Impacts on distance protection using ccvts," in *2015 IEEE Power & Energy Society General Meeting*. IEEE, 2015, pp. 1–5. xii, 3, 47, 50

[2] M. Behnke, W. Erdman, S. Horgan, D. Dawson, W. Feero, F. Soudi, D. Smith, C. Whitaker, and B. Kroposki, "Secondary network distribution systems background and issues related to the interconnection of distributed resources," National Renewable Energy Lab., Golden, CO (US), Tech. Rep., 2005. xiii, 37, 40

[3] K. Schneider, P. Phanivong, and J.-S. Lacroix, "Ieee 342-node low voltage networked test system," in *2014 IEEE PES general meeting— conference & exposition*. IEEE, 2014, pp. 1–5. xiii, 41, 43, 65

[4] M. Young, Z. Li, and A. Dimitrovski, "Modeling and simulation of continuously variable series reactor for power system transient analysis," in *2016 IEEE Power and Energy Society General Meeting (PESGM)*. IEEE, 2016, pp. 1–5. xiii, 3, 48, 49

[5] S. Pokharel and A. Dimitrovski, "Modeling of an enhanced three-phase continuously variable reactor," in *2020 IEEE Power & Energy Society General Meeting (PESGM)*. IEEE, 2020, pp. 1–5. xiii, 48, 51

[6] ——, "Analytical modeling of a three-phase magnetic amplifier-based continuously variable reactor," in *2020 IEEE/PES Transmission and Distribution Conference and Exposition (T D)*, 2020, pp. 1–5. xiv, 48, 51, 59, 66, 87

[7] A. Dimitrovski, Z. Li, and B. Ozpineci, "Applications of saturable-core reactors (scr) in power systems," in *2014 IEEE PES T D Conference and Exposition*, 2014, pp. 1–5. 1, 8, 47

[8] T. Wass, S. Hornfeldt, and S. Valdemarsson, "Magnetic circuit for a controllable reactor," *IEEE transactions on magnetics*, vol. 42, no. 9, pp. 2196–2200, 2006. 1

[9] D. Divan and H. Johal, "Distributed facts-a new concept for realizing grid power flow control," in *2005 IEEE 36th Power Electronics Specialists Conference*. IEEE, 2005, pp. 8–14. 2

[10] B. Singh, P. Tiwari, and S. Singh, "Enhancement of power system performances by optimally placed facts controllers by using different optimization techniques in distribution systems: A taxonomical review," in *2018 5th IEEE Uttar Pradesh Section International Conference on Electrical, Electronics and Computer Engineering (UPCON)*. IEEE, 2018, pp. 1–7. 2

[11] B. Tamimi and C. A. Cañizares, "Modeling and application of hybrid power flow controller in distribution systems," *IEEE Transactions on Power Delivery*, vol. 33, no. 6, pp. 2673–2682, 2018. 2

[12] Y. Kucherov and S. Utts, "The facts and hvdc equipment application for reliability, flexibility and controllability increase in the metropolitan area power system," in *11th IET International Conference on AC and DC Power Transmission*. IET, 2015, pp. 1–6. 2

[13] P. M. Saradva, K. T. Kadivar, M. H. Pandya, and A. J. Rana, "Application of d-statcom to control power flow in distribution line," in *2016 International*

Conference on Energy Efficient Technologies for Sustainability (ICEETS), 2016, pp. 479–484. 2, 7

[14] V. Khadkikar and J. L. Kirtley, "Interline photovoltaic (i-pv) power system—a novel concept of power flow control and management," in *2011 IEEE Power and Energy Society General Meeting*. IEEE, 2011, pp. 1–6. 2

[15] N. Wade, P. Taylor, P. Lang, and J. Svensson, "Energy storage for power flow management and voltage control on an 11kv uk distribution network," in *CIRED 2009-20th International Conference and Exhibition on Electricity Distribution-Part 1*. IET, 2009, pp. 1–4. 2, 12

[16] S.-S. Chen, L. Wang, W.-J. Lee, and Z. Chen, "Power flow control and damping enhancement of a large wind farm using a superconducting magnetic energy storage unit," *IET Renewable Power Generation*, vol. 3, no. 1, pp. 23–38, 2008. 2, 12

[17] O. Ciftci, M. Mehrtash, and A. Kargarian, "Data-driven nonparametric chance-constrained optimization for microgrid energy management," *IEEE Transactions on Industrial Informatics*, vol. 16, no. 4, pp. 2447–2457, 2019. 2, 12, 19

[18] S. Iyer, A. Ghosh, and A. Joshi, "Power flow control in a distribution system through an inverter interfaced distributed generator," in *2006 IEEE Power Engineering Society General Meeting*, 2006, pp. 7 pp.–. 2

[19] J. Zhu, H. Leng, H. Tang, R. Zhang, H. Gong, and L. Li, "Summary on the network reconfiguration algorithms for smart distribution grids," *Hunan Electric Power*, vol. 35, no. 6, pp. 1–5, 2015. 2

[20] X. Wang, X. Liu, S. Jian, X. Peng, and H. Yuan, "A distribution network reconfiguration method based on comprehensive analysis of operation scenarios in the long-term time period," *Energy Reports*, vol. 7, pp. 369–379, 2021. 2, 13

[21] A. Dimitrovski, Z. Li, and B. Ozpineci, "Magnetic amplifier-based power-flow controller," *IEEE Transactions on Power Delivery*, vol. 30, no. 4, pp. 1708–1714, 2015. 3, 8

[22] X. Zhang, K. Tomsovic, and A. Dimitrovski, "Security constrained multi-stage transmission expansion planning considering a continuously variable series reactor," *IEEE Transactions on Power Systems*, vol. 32, no. 6, pp. 4442–4450, 2017. 3, 8, 48, 52

[23] M. Young, A. Dimitrovski, Z. Li, and Y. Liu, "Gyrator-capacitor approach to modeling a continuously variable series reactor," *IEEE Transactions on Power Delivery*, vol. 31, no. 3, pp. 1223–1232, 2015. 3, 47

[24] A. D. Del Rosso and S. W. Eckroad, "Energy storage for relief of transmission congestion," *IEEE Transactions on Smart Grid*, vol. 5, no. 2, pp. 1138–1146, 2014. 4, 12

[25] L. Ni, F. Wen, W. Liu, J. Meng, G. Lin, and S. Dang, "Congestion management with demand response considering uncertainties of distributed generation outputs and market prices," *Journal of Modern Power Systems and Clean Energy*, vol. 5, no. 1, pp. 66–78, 2017. 4

[26] N. G. Hingorani and L. Gyugyi, *FACTS Concept and General System Considerations*, 2000, pp. 1–35. 5

[27] A. Siddique, Y. Xu, W. Aslam, and M. Rasheed, "A comprehensive study on facts devices to improve the stability and power flow capability in power system," in *2019 IEEE Asia Power and Energy Engineering Conference (APEEC)*, 2019, pp. 199–205. 5

[28] L. Gyugyi, C. Schauder, S. Williams, T. Rietman, D. Torgerson, and A. Edris, "The unified power flow controller: a new approach to power transmission

control," *IEEE Transactions on power delivery*, vol. 10, no. 2, pp. 1085–1097, 1995. 5

[29] S. Khanchi and V. K. Garg, "Unified power flow controller (facts device): A review," *system*, vol. 5, p. 6, 2013. 5

[30] C. Fuerte-Esquivel, E. Acha, and H. Ambriz-Perez, "A thyristor controlled series compensator model for the power flow solution of practical power networks," *IEEE transactions on power systems*, vol. 15, no. 1, pp. 58–64, 2000. 6

[31] Y. Amrane and N. E. Y. Kouba, "Chapter 1 - a multiobjective optimal var dispatch using facts devices considering voltage stability and contingency analysis," in *Predictive Modelling for Energy Management and Power Systems Engineering*, R. Deo, P. Samui, and S. S. Roy, Eds. Elsevier, 2021, pp. 1–26. [Online]. Available: https://www.sciencedirect.com/science/article/pii/B978012817772300001X 6, 7

[32] A. Singh, S. Bhowmick, and K. Shukla, "Load compensation with dstatcom and bess," in *2012 IEEE 5th India international conference on power electronics (IICPE)*. IEEE, 2012, pp. 1–6. 7

[33] B. Singh and J. Solanki, "A comparison of control algorithms for dstatcom," *IEEE Transactions on Industrial Electronics*, vol. 56, no. 7, pp. 2738–2745, 2009. 7

[34] A. Ram, P. R. Sharma, and R. K. Ahuja, "Power quality improvement using fuzzy-pi controlled d-statcom," in *2018 2nd IEEE International Conference on Power Electronics, Intelligent Control and Energy Systems (ICPEICES)*, 2018, pp. 414–419. 7, 8

[35] Y. Wang, J. Tang, and X. Qiu, "Analysis and control of d-statcom under unbalanced voltage condition," in *2011 International Conference on*

Mechatronic Science, Electric Engineering and Computer (MEC), 2011, pp. 1623–1625. 7

[36] A. R. Gupta, "Effect of optimal allocation of multiple dg and d-statcom in radial distribution system for minimizing losses and thd," in *2017 7th International Symposium on Embedded Computing and System Design (ISED)*, 2017, pp. 1–5. 8

[37] S. Zheng, J. Wang, F. Yang, F. Wang, L. M. Tolbert, and D. J. Costinett, "A dc controller for continuous variable series reactors (cvsrs)," in *2015 IEEE Energy Conversion Congress and Exposition (ECCE)*, 2015, pp. 5786–5793. 8, 47

[38] "Ieee guide for the application, specification, and testing of phase-shifting transformers - redline," *IEEE Std C57.135-2011 (Revision of IEEE Std C57.135-2001) - Redline*, pp. 1–71, 2011. 10

[39] T. Ding, R. Bo, Z. Bie, and X. Wang, "Optimal selection of phase shifting transformer adjustment in optimal power flow," *IEEE Transactions on Power Systems*, vol. 32, no. 3, pp. 2464–2465, 2017. 10

[40] T. J. Morrell and J. G. Eggebraaten, "Applications for phase-shifting transformers in rural power systems," in *2019 IEEE Rural Electric Power Conference (REPC)*, 2019, pp. 70–74. 10

[41] A. Baczyńska and W. Niewiadomski, "The impact of the phase-shifting transformers on the power flow in the transmission grid," in *2018 15th International Conference on the European Energy Market (EEM)*, 2018, pp. 1–5. 10

[42] T. Srikwamcharoen and K. Kveeyarn, "Load alleviation in transmission system by using phase shifting transformer," in *2018 International Electrical Engineering Congress (iEECON)*, 2018, pp. 1–4. 10

[43] R. Dakhare and V. K. Chandrakar, "Congestion management by phase shifting transformer using fuzzy logic control," in *2021 6th International Conference for Convergence in Technology (I2CT)*, 2021, pp. 1–4. 10, 12

[44] M. Begovic, A. Pregelj, A. Rohatgi, and D. Novosel, "Impact of renewable distributed generation on power systems," in *Proceedings of the 34th Annual Hawaii International Conference on System Sciences*, 2001, pp. 654–663. 12

[45] K. Sedghisigarchi, "Power flow control of inverter based distributed generators in lv microgrids," in *2011 IEEE Power and Energy Society General Meeting*, 2011, pp. 1–6. 12

[46] T. Zhong-zheng and S. Yang-zi, "Study on unbalanced power flow in distribution network with distributed generators of power grid," in *2016 China International Conference on Electricity Distribution (CICED)*, 2016, pp. 1–4. 12

[47] Z. Wang, B. Cui, and J. Wang, "A necessary condition for power flow insolvability in power distribution systems with distributed generators," *IEEE Transactions on Power Systems*, vol. 32, no. 2, pp. 1440–1450, 2017. 12

[48] M. Mosbah, R. Zine, S. Arif, R. D. Mohammedi, and S. Bacha, "Optimal power flow for transmission system with photovoltaic based dg using biogeography-based optimization," in *2018 International Conference on Electrical Sciences and Technologies in Maghreb (CISTEM)*, 2018, pp. 1–6. 12

[49] H. Yibo, R. DongHong, Q. Tao, and C. HongWei, "Power grid optimization planning based on dg acceptance capability evaluation of hybrid ac/dc transmission system," in *The 16th IET International Conference on AC and DC Power Transmission (ACDC 2020)*, vol. 2020, 2020, pp. 404–411. 12

[50] B. Papari, C. S. Edrington, M. Ghadamyari, M. Ansari, G. Ozkan, P. R. Badr, and B. H. Chowdhury, "Metrics analysis framework of control and management

system for resilient connected community microgrids," *IEEE Transactions on Sustainable Energy*, 2021. 12

[51] M. E. Baran and F. F. Wu, "Network reconfiguration in distribution systems for loss reduction and load balancing," *IEEE Power Engineering Review*, vol. 9, no. 4, pp. 101–102, 1989. 13

[52] X. Li and Q. Xia, "Stochastic optimal power flow with network reconfiguration: Congestion management and facilitating grid integration of renewables," in *2020 IEEE/PES Transmission and Distribution Conference and Exposition (T D)*, 2020, pp. 1–5. 13

[53] Y. Wu, J. Wang, and D. Li, "A network reconfiguration method for three-phase distribution network using simplified power flow model," in *2018 International Conference on Power System Technology (POWERCON)*, 2018, pp. 1573–1578. 13

[54] P. Meneses de Quevedo, J. Contreras, M. J. Rider, and J. Allahdadian, "Contingency assessment and network reconfiguration in distribution grids including wind power and energy storage," *IEEE Transactions on Sustainable Energy*, vol. 6, no. 4, pp. 1524–1533, 2015. 13

[55] N. I. Yusoff, A. A. M. Zin, and A. Bin Khairuddin, "Congestion management in power system: A review," in *2017 3rd International Conference on Power Generation Systems and Renewable Energy Technologies (PGSRET)*, 2017, pp. 22–27. 15

[56] H. Javaheri and R. Goldoost-Soloot, "Locating and sizing of series facts devices using line outage sensitivity factors and harmony search algorithm," *Energy Procedia*, vol. 14, pp. 1445–1450, 2012. 15

[57] K. Singh, V. K. Yadav, and A. Dhingra, "Congestion management using optimal placement of tcsc in deregulated power system," *International Journal on Electrical Engineering and Informatics*, vol. 4, no. 4, p. 620, 2012. 15

[58] G. Granelli, M. Montagna, F. Zanellini, P. Bresesti, R. Vailati, and M. Innorta, "Optimal network reconfiguration for congestion management by deterministic and genetic algorithms," *Electric power systems research*, vol. 76, no. 6-7, pp. 549–556, 2006. 15

[59] K. Singh, V. K. Yadav, N. P. Padhy, and J. Sharma, "Congestion management considering optimal placement of distributed generator in deregulated power system networks," *Electric power components and systems*, vol. 42, no. 1, pp. 13–22, 2014. 15

[60] B. Chong, X.-P. Zhang, K. Godfrey, L. Yao, and M. Bazargan, "Optimal location of unified power flow controller for congestion management," *European transactions on electrical power*, vol. 20, no. 5, pp. 600–610, 2010. 15

[61] R. Hemmati, H. Saboori, and M. A. Jirdehi, "Stochastic planning and scheduling of energy storage systems for congestion management in electric power systems including renewable energy resources," *Energy*, vol. 133, pp. 380–387, 2017. 15

[62] C. Yuan, C. Hu, and T. Li, "Review of congestion management methods for power systems," in *IOP Conference Series: Earth and Environmental Science*, vol. 233, no. 3. IOP Publishing, 2019, p. 032025. 16

[63] R. Gramlich, "Transmission congestion costs in the u.s. rtos," Nov 2020. [Online]. Available: https://gridstrategiesllc.com/2019/09/17/transmission-congestion-costs-in-the-u-s-rtos/ 16

[64] "2020 national electric transmission congestion study." [Online]. Available: https://www.energy.gov/oe/downloads/2020-national-electric-transmission-congestion-study 16

[65] P. Staudt, "Transmission congestion management in electricity grids-designing markets and mechanisms," Ph.D. dissertation, KIT-Bibliothek, 2019. 16

[66] N. E. Chang, "Locating shunt capacitors on primary feeder for voltage control and loss reduction," *IEEE Transactions on Power Apparatus and Systems*, no. 10, pp. 1574–1577, 1969. 18

[67] M. Saravanan, S. M. R. Slochanal, P. Venkatesh, and J. P. S. Abraham, "Application of particle swarm optimization technique for optimal location of facts devices considering cost of installation and system loadability," *Electric power systems research*, vol. 77, no. 3-4, pp. 276–283, 2007. 18

[68] S. Singh and A. David, "Optimal location of facts devices for congestion management," *Electric Power Systems Research*, vol. 58, no. 2, pp. 71–79, 2001. 18

[69] D. Gautam and N. Mithulananthan, "Optimal dg placement in deregulated electricity market," *Electric Power Systems Research*, vol. 77, no. 12, pp. 1627–1636, 2007. 18, 23

[70] M. Albadi, A. Al-Hinai, N. Al-Abri, Y. Al-Busafi, and R. Al-Sadairi, "Optimal allocation of renewable-based dg resources in rural areas using genetic algorithms," in *2012 Asia-Pacific Power and Energy Engineering Conference*. IEEE, 2012, pp. 1–4. 18

[71] M. Yosef, M. Sayed, and H. K. Youssef, "Allocation and sizing of distribution transformers and feeders for optimal planning of mv/lv distribution networks using optimal integrated biogeography based optimization method," *Electric Power Systems Research*, vol. 128, pp. 100–112, 2015. 18

[72] Y. Liao, "Fault location observability analysis and optimal meter placement based on voltage measurements," *Electric Power Systems Research*, vol. 79, no. 7, pp. 1062–1068, 2009. 18

[73] M. Mouwafi, R. A. El-Sehiemy, A. Abou El-Ela, and A. Kinawy, "Optimal placement of phasor measurement units with minimum availability of measuring channels in smart power systems," *Electric Power Systems Research*, vol. 141, pp. 421–431, 2016. 19

[74] N. J. Marand, R. M. Chabanloo, and M. Fallah, "Optimal placement of voltage measurements for wide area fault location observability considering the uncertainty of network parameters," *Electric Power Systems Research*, vol. 164, pp. 79–88, 2018. 19

[75] Y. Zheng, D. J. Hill, Y. Song, J. Zhao, and S. Y. R. Hui, "Optimal electric spring allocation for risk-limiting voltage regulation in distribution systems," *IEEE Transactions on Power Systems*, vol. 35, no. 1, pp. 273–283, 2019. 19

[76] G. Levitin, S. Mazal-Tov, and D. Elmakis, "Optimal sectionalizer allocation in electric distribution systems by genetic algorithm," *Electric Power Systems Research*, vol. 31, no. 2, pp. 97–102, 1994. 19

[77] S. Javadian and M.-R. Haghifam, "Optimal placement of protective devices in distribution networks based on risk analysis," in *2010 IEEE/PES Transmission and Distribution Conference and Exposition: Latin America (T&D-LA)*. IEEE, 2010, pp. 147–154. 19

[78] A. Moradi and M. Fotuhi-Firuzabad, "Optimal switch placement in distribution systems using trinary particle swarm optimization algorithm," *IEEE Transactions on power delivery*, vol. 23, no. 1, pp. 271–279, 2007. 19

[79] T. Ghanbari and E. Farjah, "A multiagent-based fault-current limiting scheme for the microgrids," *IEEE transactions on power delivery*, vol. 29, no. 2, pp. 525–533, 2013. 19

[80] A. V. Pombo, J. Murta-Pina, and V. F. Pires, "Multiobjective formulation of the integration of storage systems within distribution networks for improving reliability," *Electric Power Systems Research*, vol. 148, pp. 87–96, 2017. 19

[81] N. Jayasekara, M. A. Masoum, and P. J. Wolfs, "Optimal operation of distributed energy storage systems to improve distribution network load and generation hosting capability," *IEEE Transactions on Sustainable Energy*, vol. 7, no. 1, pp. 250–261, 2015. 20, 22

[82] M. Nick, R. Cherkaoui, and M. Paolone, "Optimal allocation of dispersed energy storage systems in active distribution networks for energy balance and grid support," *IEEE Transactions on Power Systems*, vol. 29, no. 5, pp. 2300–2310, 2014. 22

[83] S. Ghosh, S. P. Ghoshal, and S. Ghosh, "Optimal sizing and placement of distributed generation in a network system," *International Journal of Electrical Power & Energy Systems*, vol. 32, no. 8, pp. 849–856, 2010. 22, 23

[84] J. J. Grainger, *Power system analysis*. McGraw-Hill, 1999. 22, 54

[85] R. Billinton and R. N. Allan, *Reliability evaluation of engineering systems*. Springer, 1992, vol. 792. 22

[86] N. S. Rau and Y.-h. Wan, "Optimum location of resources in distributed planning," *IEEE Transactions on Power systems*, vol. 9, no. 4, pp. 2014–2020, 1994. 23

[87] G. Harrison and A. Wallace, "Optimal power flow evaluation of distribution network capacity for the connection of distributed generation," *IEE*

Proceedings-Generation, Transmission and Distribution, vol. 152, no. 1, pp. 115–122, 2005. 23

[88] Y. M. Atwa and E. El-Saadany, "Optimal allocation of ess in distribution systems with a high penetration of wind energy," *IEEE Transactions on Power Systems*, vol. 25, no. 4, pp. 1815–1822, 2010. 23, 24

[89] V. Chvatal, *Linear programming*. Macmillan, 1983. 23

[90] L. A. Wolsey, "Mixed integer programming," *Wiley Encyclopedia of Computer Science and Engineering*, pp. 1–10, 2007. 23

[91] F. Alizadeh and D. Goldfarb, "Second-order cone programming," *Mathematical programming*, vol. 95, no. 1, pp. 3–51, 2003. 23

[92] A. Prékopa, *Stochastic programming*. Springer Science & Business Media, 2013, vol. 324. 23

[93] A. Ben-Tal, L. El Ghaoui, and A. Nemirovski, *Robust optimization*. Princeton university press, 2009, vol. 28. 23

[94] D. P. Bertsekas, "Nonlinear programming," *Journal of the Operational Research Society*, vol. 48, no. 3, pp. 334–334, 1997. 23

[95] A. Arya, S. S. Verma, S. Mehroliya, S. Tomar, and C. Rajeshwari, "Optimal placement of distributed generators in power system using sensitivity analysis," in *Advances in Energy Technology: Select Proceedings of EMSME 2020*. Springer, 2022, pp. 749–759. 24

[96] M. Delfanti, G. P. Granelli, P. Marannino, and M. Montagna, "Optimal capacitor placement using deterministic and genetic algorithms," in *Proceedings of the 21st International Conference on Power Industry Computer Applications. Connecting Utilities. PICA 99. To the Millennium and Beyond (Cat. No. 99CH36351)*. IEEE, 1999, pp. 331–336. 24

[97] F. G. Lima, F. D. Galiana, I. Kockar, and J. Munoz, "Phase shifter placement in large-scale systems via mixed integer linear programming," *IEEE Transactions on Power Systems*, vol. 18, no. 3, pp. 1029–1034, 2003. 24

[98] L. A. Gallego, J. M. López-Lezama, and O. G. Carmona, "A mixed-integer linear programming model for simultaneous optimal reconfiguration and optimal placement of capacitor banks in distribution networks," *IEEE Access*, vol. 10, pp. 52 655–52 673, 2022. 24

[99] M. Heleno, S. Mashayekh, M. Stadler, G. Cardoso, and R. De Luís, "Optimal sizing and placement of distributed generation: Milp vs pso comparison in a real microgrid application," in *19th International Conference on Intelligent System Application to Power Systems*, 2017. 24

[100] M. Farrokhifar, F. H. Aghdam, A. Alahyari, A. Monavari, and A. Safari, "Optimal energy management and sizing of renewable energy and battery systems in residential sectors via a stochastic milp model," *Electric Power Systems Research*, vol. 187, p. 106483, 2020. 24

[101] A. Karimi, F. Aminifar, A. Fereidunian, and H. Lesani, "Energy storage allocation in wind integrated distribution networks: An milp-based approach," *Renewable energy*, vol. 134, pp. 1042–1055, 2019. 24

[102] A. C. Rueda-Medina, J. F. Franco, M. J. Rider, A. Padilha-Feltrin, and R. Romero, "A mixed-integer linear programming approach for optimal type, size and allocation of distributed generation in radial distribution systems," *Electric power systems research*, vol. 97, pp. 133–143, 2013. 24

[103] A. L. Ara, A. Kazemi, and S. N. Niaki, "Multiobjective optimal location of facts shunt-series controllers for power system operation planning," *IEEE Transactions on Power Delivery*, vol. 27, no. 2, pp. 481–490, 2011. 24

[104] S. Kaur, G. Kumbhar, and J. Sharma, "A minlp technique for optimal placement of multiple dg units in distribution systems," *International Journal of Electrical Power & Energy Systems*, vol. 63, pp. 609–617, 2014. 24

[105] D. R. Prabha, T. Jayabarathi, R. Umamageswari, and S. Saranya, "Optimal location and sizing of distributed generation unit using intelligent water drop algorithm," *Sustainable Energy Technologies and Assessments*, vol. 11, pp. 106–113, 2015. 24

[106] M. E. Baran and F. F. Wu, "Optimal capacitor placement on radial distribution systems," *IEEE Transactions on power Delivery*, vol. 4, no. 1, pp. 725–734, 1989. 26, 27

[107] F. Qian, G. Tang, and Z. He, "Optimal location and capability of facts devices in a power system by means of sensitivity analysis and eeac," in *2008 Third International Conference on Electric Utility Deregulation and Restructuring and Power Technologies*. IEEE, 2008, pp. 2100–2104. 26

[108] I. Ullah, W. Gawlik, and P. Palensky, "Analysis of power network for line reactance variation to improve total transmission capacity," *Energies*, vol. 9, no. 11, p. 936, 2016. 26

[109] V. S. Rao and R. S. Rao, "Optimal placement of statcom using two stage algorithm for enhancing power system static security," *Energy Procedia*, vol. 117, pp. 575–582, 2017. 26

[110] W. M. da Rosa, P. Rossoni, J. C. Teixeira, and E. A. Belati, "Insertion of wind generators in electrical power systems aimed at active losses reduction using sensitivity analysis," *International Journal of Electrical Power & Energy Systems*, vol. 80, pp. 306–311, 2016. 27

[111] D. Bharti and M. De, "A centrality index based approach for selection of optimal location of static reactive power compensator," *Electric Power Components and Systems*, vol. 46, no. 8, pp. 886–899, 2018. 27

[112] M. Saleh, Y. Esa, and A. Mohamed, "Applications of complex network analysis in electric power systems," *Energies*, vol. 11, no. 6, p. 1381, 2018. 27

[113] S. Mondal and M. De, "Optimal capacitor placement for unbalanced distribution system using graph theory," *IETE Journal of Research*, pp. 1–8, 2021. 27

[114] Y. Ding, Q. Wang, Z. Tian, Y. Lyu, F. Li, Z. Yan, and X. Xia, "A graph-theory-based dynamic programming planning method for distributed energy system planning: Campus area as a case study," *Applied Energy*, vol. 329, p. 120258, 2023. 29

[115] W. Liu and Z. Han, "Distribution system reconfiguration based on time interval," *Automation of Electric Power Systems*, vol. 30, no. 10, pp. 33–38, 2006. 29

[116] E. W. Dijkstra, "A note on two problems in connexion with graphs," in *Edsger Wybe Dijkstra: His Life, Work, and Legacy*, 2022, pp. 287–290. 29

[117] R. W. Floyd, "Algorithm 97: shortest path," *Communications of the ACM*, vol. 5, no. 6, p. 345, 1962. 29

[118] R. Benabid, M. Boudour, and M. Abido, "Optimal placement of facts devices for multi-objective voltage stability problem," in *2009 IEEE/PES Power Systems Conference and Exposition*. IEEE, 2009, pp. 1–11. 30

[119] V. Ajjarapu and C. Christy, "The continuation power flow: a tool for steady state voltage stability analysis," *IEEE transactions on Power Systems*, vol. 7, no. 1, pp. 416–423, 1992. 30

[120] B. Gao, G. Morison, and P. Kundur, "Voltage stability evaluation using modal analysis," *IEEE transactions on power systems*, vol. 7, no. 4, pp. 1529–1542, 1992. 30

[121] S. do Nascimento and M. M. Gouvêa Jr, "Voltage stability enhancement in power systems with automatic facts device allocation," *Energy Procedia*, vol. 107, pp. 60–67, 2017. 30

[122] S. M. Sajjadi, M.-R. Haghifam, and J. Salehi, "Simultaneous placement of distributed generation and capacitors in distribution networks considering voltage stability index," *International Journal of Electrical Power & Energy Systems*, vol. 46, pp. 366–375, 2013. 30

[123] N. Metropolis and S. Ulam, "The monte carlo method," *Journal of the American statistical association*, vol. 44, no. 247, pp. 335–341, 1949. 31

[124] G. Marmidis, S. Lazarou, and E. Pyrgioti, "Optimal placement of wind turbines in a wind park using monte carlo simulation," *Renewable energy*, vol. 33, no. 7, pp. 1455–1460, 2008. 31

[125] C. B. Donadel, J. F. Fardin, and L. F. Encarnação, "Optimal placement of distributed generation units in a distribution system with uncertain topologies using monte carlo simulation," *International Journal of Emerging Electric Power Systems*, vol. 16, no. 5, pp. 431–441, 2015. 31

[126] S. Galloway, I. Elders, G. Burt, and B. Sookananta, "Optimal flexible alternative current transmission system device allocation under system fluctuations due to demand and renewable generation," *IET generation, transmission & distribution*, vol. 4, no. 6, pp. 725–735, 2010. 31

[127] S. Lin and B. W. Kernighan, "An effective heuristic algorithm for the traveling-salesman problem," *Operations research*, vol. 21, no. 2, pp. 498–516, 1973. 32

[128] X.-S. Yang, *Nature-inspired metaheuristic algorithms*. Luniver press, 2010. 32

[129] K. Nara, Y. Hayashi, K. Ikeda, and T. Ashizawa, "Application of tabu search to optimal placement of distributed generators," in *2001 IEEE power engineering society winter meeting. Conference proceedings (Cat. No. 01CH37194)*, vol. 2. IEEE, 2001, pp. 918–923. 33

[130] K. Dharageshwari and C. Nayanatara, "Multiobjective optimal placement of multiple distributed generations in ieee 33 bus radial system using simulated annealing," in *2015 International conference on circuits, power and computing technologies [ICCPCT-2015]*. IEEE, 2015, pp. 1–7. 33

[131] M. Nazari-Heris and B. Mohammadi-Ivatloo, "Optimal placement of phasor measurement units to attain power system observability utilizing an upgraded binary harmony search algorithm," *Energy Systems*, vol. 6, pp. 201–220, 2015. 33

[132] D. E. Golberg, "Genetic algorithms in search, optimization, and machine learning," *Addion wesley*, vol. 1989, no. 102, p. 36, 1989. 34

[133] S. Gerbex, R. Cherkaoui, and A. J. Germond, "Optimal location of multi-type facts devices in a power system by means of genetic algorithms," *IEEE transactions on power systems*, vol. 16, no. 3, pp. 537–544, 2001. 34

[134] S. Lohia, O. P. Mahela, and S. R. Ola, "Optimal capacitor placement in distribution system using genetic algorithm," in *2016 IEEE 7th Power India International Conference (PIICON)*. IEEE, 2016, pp. 1–6. 34

[135] A. Alhamali, M. E. Farrag, G. Bevan, and D. M. Hepburn, "Determination of optimal site and capacity of dg systems in distribution network based on genetic algorithm," in *2017 52nd International Universities Power Engineering Conference (UPEC)*. IEEE, 2017, pp. 1–6. 34

[136] J. Kennedy and R. Eberhart, "Particle swarm optimization," in *Proceedings of ICNN'95-international conference on neural networks*, vol. 4. IEEE, 1995, pp. 1942–1948. 34

[137] A. A. Shehata, A. Refaat, M. K. Ahmed, and N. V. Korovkin, "Optimal placement and sizing of facts devices based on autonomous groups particle swarm optimization technique," *Archives of Electrical Engineering*, vol. 70, no. 1, pp. 161–172, 2021. 34

[138] A. Ameli, S. Bahrami, F. Khazaeli, and M.-R. Haghifam, "A multiobjective particle swarm optimization for sizing and placement of dgs from dg owner's and distribution company's viewpoints," *IEEE Transactions on power delivery*, vol. 29, no. 4, pp. 1831–1840, 2014. 34

[139] S. K. Singh and K. S. Swarup, "Optimal placement of phase shifting transformer for power flow control using linear search approach," in *2023 IEEE PES Conference on Innovative Smart Grid Technologies-Middle East (ISGT Middle East)*. IEEE, 2023, pp. 1–5. 34

[140] M. Dorigo, M. Birattari, and T. Stutzle, "Ant colony optimization," *IEEE computational intelligence magazine*, vol. 1, no. 4, pp. 28–39, 2006. 34

[141] A. A. A. El-Ela, M. T. Mouwafi, and A. A. Elbaset, "Optimal capacitor placement for power loss reduction and voltage profile improvement," in *Modern Optimization Techniques for Smart Grids*. Springer, 2022, pp. 107–139. 34

[142] M. Kefayat, A. L. Ara, and S. N. Niaki, "A hybrid of ant colony optimization and artificial bee colony algorithm for probabilistic optimal placement and sizing of distributed energy resources," *Energy Conversion and Management*, vol. 92, pp. 149–161, 2015. 34

[143] A. K. Jain, J. Mao, and K. M. Mohiuddin, "Artificial neural networks: A tutorial," *Computer*, vol. 29, no. 3, pp. 31–44, 1996. 35

[144] M. A. Al-Shaher, M. M. Sabry, and A. S. Saleh, "Fault location in multi-ring distribution network using artificial neural network," *Electric Power Systems Research*, vol. 64, no. 2, pp. 87–92, 2003. 35

[145] B. Das and P. K. Verma, "Artificial neural network-based optimal capacitor switching in a distribution system," *Electric Power Systems Research*, vol. 60, no. 2, pp. 55–62, 2001. 35

[146] P. Kayal and C. K. Chanda, "A simple and fast approach for allocation and size evaluation of distributed generation," *International Journal of Energy and Environmental Engineering*, vol. 4, pp. 1–9, 2013. 35

[147] G. Klir and B. Yuan, *Fuzzy sets and fuzzy logic*. Prentice hall New Jersey, 1995, vol. 4. 35

[148] S. Mekhamer, S. Soliman, M. Moustafa, and M. El-Hawary, "Application of fuzzy logic for reactive-power compensation of radial distribution feeders," *IEEE transactions on power systems*, vol. 18, no. 1, pp. 206–213, 2003. 36

[149] R. B. Magadum and D. Kulkarni, "Power loss reduction by optimal location of dg using fuzzy logic," in *2015 International Conference on Smart Technologies and Management for Computing, Communication, Controls, Energy and Materials (ICSTM)*. IEEE, 2015, pp. 338–343. 36

[150] A. Á. Téllez, G. López, I. Isaac, and J. González, "Optimal reactive power compensation in electrical distribution systems with distributed resources. review," *Heliyon*, vol. 4, no. 8, p. e00746, 2018. 36

[151] I. Oladeji, R. Zamora, and T. T. Lie, "Optimal placement of renewable energy sources distributed generation in an unbalanced network for modern grid operations," in *2021 International Conference on Smart Energy Systems and Technologies (SEST)*. IEEE, 2021, pp. 1–6. 36

[152] A. N. Abdalla, H. Tao, M. S. Nazir, Y. Ju, and R. B. Ishak, "Hybrid ant colony optimisation-random forest regression-based optimised framework of an intelligent active distribution network," in *Journal of Physics: Conference Series*, vol. 2467, no. 1. IOP Publishing, 2023, p. 012020. 36

[153] J. Liang, T. Jing, H. Niu, and J. Wang, "Two-terminal fault location method of distribution network based on adaptive convolution neural network," *IEEE Access*, vol. 8, pp. 54 035–54 043, 2020. 36

[154] H. Richter, "Combined light and power systems for ac. secondary networks," *Transactions of the American Institute of Electrical Engineers*, vol. 46, pp. 216–239, 1927. 37

[155] R. P. Fogarty, "Network vault design for high-rise and other commercial buildings," *IEEE Transactions on Industry and General Applications*, no. 4, pp. 544–552, 1971. 37

[156] D. Roop and N. Vidonic, "Arcing fault protection on vepco's 480y/277 volt secondary spot networks," *IEEE Transactions on Power Apparatus and Systems*, no. 2, pp. 364–372, 1983. 37

[157] R. J. Landman and B. Louie, "Fiberoptic scada system safeguards underground distribution network," *IEEE computer applications in power*, vol. 5, no. 2, pp. 39–44, 1992. 37

[158] W. A. Geyger, *Magnetic-amplifier Circuits: Basic Principles, Characteristics, and Applications*. McGraw-Hill, 1954. 46

[159] A. Boyajian, "Theory of dc. excited iron-core reactors and regulators," *Transactions of the American Institute of Electrical Engineers*, vol. 43, pp. 919–936, 1924. 46

[160] H. Kirschbaum and E. Harder, "A balanced amplifier using biased saturable core reactors," *Transactions of the American Institute of Electrical Engineers*, vol. 66, no. 1, pp. 273–278, 1947. 46

[161] R. A. Ramey, "On the mechanics of magnetic amplifier operation," *Transactions of the American Institute of Electrical Engineers*, vol. 70, no. 2, pp. 1214–1223, 1951. 46

[162] J. Manley and E. Peterson, "Negative resistance effects in saturable reactor circuits," *Electrical Engineering*, vol. 65, no. 12, pp. 870–881, 1946. 46

[163] J. Suozzi and E. Hooper, "An all-magnetic audio amplifier system," *Transactions of the American Institute of Electrical Engineers, Part I: Communication and Electronics*, vol. 74, no. 3, pp. 297–301, 1955. 46

[164] J. Jin, S. Dou, H. Liu, C. Grantham, Z. Zeng, Z. Liu, T. Blackburn, X. Li, H. Liu, and J. Liu, "Electrical application of high t/sub c/superconducting saturable magnetic core fault current limiter," *IEEE Transactions on Applied Superconductivity*, vol. 7, no. 2, pp. 1009–1012, 1997. 46

[165] J. Tate, "Improved multiple core transformer inverter with trc regulation via external variable volt-second saturable reactor," *IEEE Transactions on Magnetics*, vol. 2, no. 3, pp. 625–628, 1966. 46

[166] S. Zheng, J. Wang, F. Wang, and L. M. Tolbert, "Dc-saturated continuously variable series reactors (cvsrs) for power flow control in power transmission systems," *IEEE Transactions on Power Delivery*, 2021. 48

[167] MATLAB, *9.7.0.1190202 (R2019b)*. Natick, Massachusetts: The MathWorks Inc., 2018. 61

[168] R. C. Dugan, "Reference guide: The open distribution system simulator (opendss)," *Electric Power Research Institute, Inc*, vol. 7, p. 29, 2012. 61

[169] S. H. Cameron, "Piece-wise linear approximations," IIT RESEARCH INST CHICAGO IL COMPUTER SCIENCES DIV, Tech. Rep., 1966. 64

[170] J. Lofberg, "Yalmip: A toolbox for modeling and optimization in matlab," in *2004 IEEE international conference on robotics and automation (IEEE Cat. No. 04CH37508)*. IEEE, 2004, pp. 284–289. 65

[171] I. I. C. O. Studio, "12.10." 65

Vita

Okan Ciftci was born in Konya, Turkey in 1992. He received his B.S. degree in Electrical and Electronics Engineering at KTO Karatay University, and M.Sc. in Electrical Engineering at Louisiana State University 2014 and 2018, respectively. In 2015, he awarded Turkish Government Scholarship for M.Sc. and Ph.D. Education in the USA. He is currently pursuing his Ph.D. in Electrical Engineering at University of Tennessee and working as graduate research and teaching assistant with EECS at University of Tennessee. He has been author/co-author on multiple papers in power systems.